

“The role of vacuolar processing enzymes in programmed cell death in maternal tissues of the developing barley grain”

Dissertation

zur Erlangung des akademischen Grades

doctor rerum naturalium (Dr. rer. nat.)

an der Naturwissenschaftliche Fakultät I - Biowissenschaften

der

Martin-Luther-Universität Halle-Wittenberg

vorgelegt von

Frau M.Sc Tran, Thi Thuy Van

geb. am: 15.02.1975

in Vinh Stadt, Nghe An, Vietnam

Gutachter /in:

1. Prof. Dr. Thomas Altmann
2. Prof. Dr. Ulrike Zentgraf
3. Prof. Dr. Ralf-Bernd Klösgen

Halle (Saale): 28.04.2016

Verteidigungsdatum: 16. 01.2017

Table of contents

List of abbreviations	4
1. Introduction and Literature Review	6
1.1 Barley grain development	6
1.2 Programmed cell death in plants	7
1.2.1 Developmental PCD in plants	8
1.2.2 Cell death during seed development and germination of barley	10
1.2.3 PCD in the interaction between plants and environment.....	14
1.2.4 Morphological classification of plant PCD	14
1.2.6 PCD-related genes in the developing barley grains	21
1.2.7 Regulation of PCD in plants	22
1.3 Aim of the dissertation	24
2. Material and methods	26
2.1 Material	26
2.1.1 Plant material	26
2.1.2 Bacterial strains and plasmids	26
2.1.3 Oligonucleotides.....	27
2.1.4 Enzymes, reaction kits and chemicals	27
2.1.5 Special instruments	28
2.1.6 Bacterial media.....	29
2.1.7 Protein extraction buffer for caspase assay	29
2.1.8 Antibiotics.....	29
2.1.9 Antibodies used for Western blot and ELISA.....	29
2.1.10 Buffers for Western blot and ELISA	30
2.1.11 Buffers for starch, sugar and storage protein measurements	30
2.2 Methods	31
2.2.1 Plant cultivation conditions and tissue preparation	31
2.2.2 Tissue preparation for laser micro-dissection and pressure catapulting.....	31
2.2.3 Sequence isolation and identification of genes	31
2.2.4 Basic cloning methods.....	33
2.2.5 Genomic DNA extraction	33
2.2.6 RNA isolation	33
2.2.7. Southern and Northern blot hybridization analyses	34
2.2.8 Polymerase chain reaction (PCR).....	35

2.2.9 Quantitative reverse transcription-polymerase chain reaction	36
2.2.10 Protein extraction for caspase-like assays	36
2.2.11 Caspase-like assay	37
2.2.12 Histological studies	37
2.2.13 TUNEL assay	38
2.2.14 Preparation of VPE4i and VPE2i constructs for plant transformation	38
2.2.15 Stable transformation of barley plants	40
2.2.16 Extraction and determination of soluble sugars, starch, storage proteins, total carbon and nitrogen	40
2.2.15 Production of the recombinant MADS29 protein	41
2.2.16 Western blot analysis	42
2.2.17 Analysis of the CARG cis-elements present in the Jekyll and VPE2a promoters by ELISA	42
2.2.18 <i>In silico</i> analysis of promoter sequences	43
2.2.19 Computational analyses	43
3.1 PCD in maternal tissues of developing barley grains	44
3.1.1 Detection of PCD in developing tissues of barley grains by TUNEL assay	44
3.1.2 Caspase-like activities in pericarp and endosperm fractions	47
3.1.3 Expression analysis of genes encoding vacuolar processing enzymes 2a-2d (VPE2a- 2d) by qRT-PCR	49
3.2 Analysis of the role of <i>VPE4</i> on pericarp development by RNAi-mediated suppression	50
3.2.1 Analysis of the VPE4i primary transformed plants and preparation of homozygous lines	50
3.2.2 Phenotypic changes in VPE4i-repressed mature seeds	54
3.2.3. Accumulation of fresh weight during seed development	55
3.2.4 Pericarp degradation is delayed in developing VPE4-RNAi grains	57
3.2.5 Caspase-like activities in the pericarp of VPE4i-repressed barley grains	58
3.2.6 Storage compounds in mature transgenic grains as compared to the wild type	60
3.2.7 Accumulation of metabolites in the VPE4-repressed pericarp during grain development	60
3.3 Analysis of the role of vacuolar processing enzymes on development of nucellar tissues	62
3.3.1 Cloning of the full-length VPE2a cDNA	63
3.3.2 Repression of VPE activity in nucellar tissues	64
3.3.3 Analysis of the VPE2i primary transformed plants and preparation of homozygous lines	65
3.3.4 Analysis of expression of VPE2a to VPE2d genes in the homozygous VPE2i-transgenic plants	67

3.3.5 Growth characteristics of VPE2i transgenic plants.....	68
3.3.7 Impact of down-regulation of nucellar-specific VPEs on seed germination	71
3.3.8 Caspase-like activities in the endosperm fraction of VPE2i-repressed barley grains	72
3.4 Interaction of the MADS29 transcription factor with promoter sequences of <i>VPE2a</i> and <i>Jekyll</i> genes, both involved in PCD of nucellar tissues.....	73
3.4.1 Cloning and phylogenetic analysis of gene MADS29 from barley.....	73
3.4.2 MADS29 is expressed in the reproductive organs of barley	75
3.4.3 HvMADS29 binds to <i>Jekyll</i> and <i>VPE2a</i> gene promoter regions.....	76
3.4.5 Binding of MADS29 protein to the CArG motifs of the <i>VPE2a</i> promoter.....	78
3.4.6 Binding of MADS29 protein to the CArG motifs of the <i>Jekyll</i> promoter	79
3.4.7 Multiple copies of CArG cis-elements are present in the promoter sequences of genes transcriptionally active in the nucellar tissues.....	80
4. Discussion	85
4.1 Caspase-like activities is associated with PCD events in developing barley grains.....	85
4.2 VPE4 is required for cell death of the pericarp in developing barley grains	89
4.3 Nucellar PCD, mediated by VPE activity, is required for proper assimilate transfer to the endosperm	93
4.4 The barley MADS29 transcription factor regulates expression of genes involved in PCD in nucellar tissue of the developing barley grain	96
4.5 Concluding remarks.....	99
5. Summary.....	102
6. Zusammenfassung	104
7. References	106
8. Publications and Presentations (during PhD study)	119
8.1 Publications	119
8.2 Presentations at meetings and conferences	119
9. Acknowledgements	120
10. Curriculum Vitae	121
11. Declarations	122
Appendix	123
Supplemental Tables	123
Supplemental Figures.....	126

List of abbreviations

Ala / A	Alanine
Arg / R	Arginine
Asn / N	Asparagine
Asp / D	Aspartic acid
bp	Base pair(s)
BSA	Bovine serum albumin
CARG	Box DNA sequence: CC(AT) ₆ GG
Caspase	Cysteine-aspartic proteases or cysteine-dependent aspartate-directed proteases
cDNA	Complementary DNA
CHAPS	3-[(3-Cholamidopropyl) dimethylammonio]-1-propanesulfonate
C-terminal	Carboxy-terminus
Cys / C	Cysteine
DAF	Day after flowering
ddH ₂ O	Dideionized water
DMSO	Dimethylsulfoxide
DNA	Deoxyribonucleic acid
DNase	Deoxyribonuclease
dry wt	Dry weight
DTT	Dithiothreitol
ELISA	Enzyme-linked immunosorbent assay
ER	Endoplasmic reticulum
EST	Expressed sequence tag
Gln / Q	Glutamine
Glu / E	Glutamic acid
Gly / G	Glycine
h	hour (s)
HEPES	4-(2-hydroxyethyl)-1-piperazineethanesulfonic acid
His / H	Histidine
<i>hpt</i>	<i>Hygromycin phosphotransferase gene</i>
Ile / I	Isoleucine
kDa	KiloDalton(s)
LB	Left border
Leu / L	Leucine
LMPC	Laser micro-dissection and pressure catapulting
Lys / K	Lysine
M	molar (mol/l)
Met / M	Methionine

min	Minute(s)
Ni-NTA	Nickel-nitrilotriacetic acid
NP	Nucellar projection
N-terminal	Amino-terminus
OD	Optical density
ORF	Open-reading frame
PAGE	Polyacrylamide gel electrophoresis
PBS	Phosphate-buffered saline
PCD	Programmed cell death
PCR	Polymerase chain reaction
PGI	Phosphoglucose Isomerase
Phe / F	Phenylalanine
pNPP	p-Nitrophenyl phosphate
Pro / P	Proline
Pubi	Ubiquitin 1 gene promoter from maize
qRT-PCR	Quantitative real time polymerase chain reaction
RB	Right border
RNA	Ribonucleic acid
RNase	Ribonuclease
RT	Room temperature
SAG	Senescence-associated genes
SD	Standard deviation
SDS	Sodium dodecyl sulfate
Sec	Second
Ser / S	Serine
Spec ^r	Spectinomycin resistance
T ₀	Primary transgenic plant
T35S	Terminator of the <i>CaMV 35S</i> gene
TF	Transcription factor
TGW	Thousand grain weight
Thr / T	Threonine
Tnos	Nopaline synthase gene terminator
Tris	Tris-(hydroxymethyl)-aminomethane
Trp / W	Tryptophan
TUNEL	Deoxynucleotidil transferase dUTP end labelling
Tyr / Y	Tyrosine
Val / V	Valine
VPE	Vacuolar processing enzyme
WT	Wild type (<i>Hordeum vulgare</i> cv. Golden Promise)

1. Introduction and Literature Review

1.1 Barley grain development

Barley (*Hordeum vulgare* L.) belongs to the *Poaceae* (*Gramineae*) family of monocotyledonous flowering plants. Barley is grown for its seeds and as such it is one of the major cereal crops grown in temperate climates with fourth rank position among the most important cereals (as for 2003, The World Bank). Therefore, understanding of barley seed development is important for improving grain yield. Barley is also widely used as a model organism for cereal genetics and genomics (Sreenivasulu *et al.*, 2008).

Seeds are complex structures aided for reproduction and spread of higher plants. They consist of three genetically distinct constituents: seed coat (or testa), embryo and endosperm. The diploid seed coat is entirely maternal in origin (Radchuk and Borisjuk, 2014). The embryo and endosperm (both filial tissues) originate from double fertilization, the most distinctive characteristic of the angiosperms. The diploid embryo results from the fusion between an egg cell and a sperm nucleus, while the endosperm develops after fusion between the two central cell nuclei and a second sperm nucleus to produce (in diploid species) a triploid structure. The enclosure of the developing embryo and endosperm into maternal tissues affords their protection and thereby enhances the chance to reach maturity and establish the subsequent generation (Radchuk and Borisjuk, 2014). Both maternal and filial organs undergo rapid changes during seed development.

The mature barley grain consists of the surrounding husks and the caryopsis, a fruit characterized by a fusion between pericarp and seed coat. From anthesis to maturity, caryopsis development can be divided into four stages based on morphological, physiological and molecular-biological data (Figure 1.1) (Wobus *et al.*, 2004; Sreenivasulu *et al.*, 2008). The first stage lasts between anthesis and around 6 days after flowering (DAF) and is characterized by cell divisions and morphogenesis (pre-storage phase). This stage is followed by a transition phase (between 6 to 8-10 DAF), where massive transcriptional rearrangements take place (Sreenivasulu *et al.*, 2006). Accumulation of starch and storage proteins in starchy endosperm and lipids in embryo and aleurone layer occurs during storage accumulation stage (between 8-10 and around 20 DAF). The last stage is characterized by seed maturation and water loss (desiccation phase).

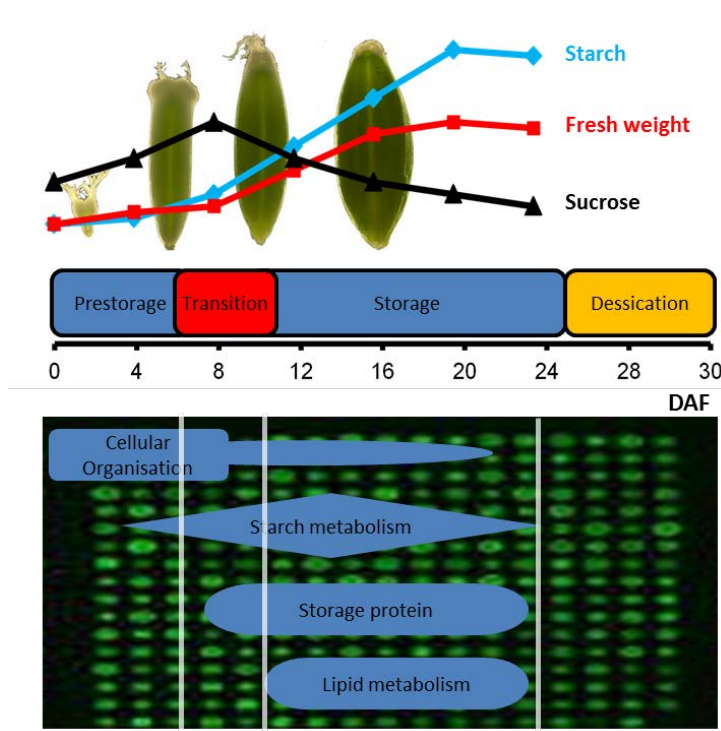


Figure 1.1 General scheme of barley seed development. Developmental and biochemical parameters (shown below) lead to the widely accepted definition of four main stages (pre-storage, transition, storage and desiccation phase) of barley seed development (modified from Wobus *et al.*, 2004).

The development of cereal seeds including barley depends on tightly interconnected processes of tissue proliferation, functionalization and controlled degradation *via* programmed cell death. At maturity, the cereal grain consists of the living tiny embryo and aleurone layer while the bulk of seed is dead.

1.2 Programmed cell death in plants

Programmed cell death (PCD) is a genetically regulated cellular suicide process essential for development, integrity, response to the environment and survival of all eukaryotic organisms (Gechev *et al.*, 2006; Lam, 2004). Activation of PCD pathways results in a highly controlled and coordinated set of reactions leading to degradation of cellular contents which is accompanied by characteristic morphological and biochemical changes. In plants, PCD accompanies the whole life cycle, from formation of embryo until death of the whole plant (Van Hautegeem *et al.*, 2015; Wu and Cheung 2000; Beers, 1997; Pennell and Lamb, 1997). Coordination between cell death and proliferation, growth, and differentiation is of fundamental importance for the maintenance of tissue and organ homeostasis in both animal and plant organisms. There are at least two broad categories of PCD in plants: developmentally regulated and environmentally induced PCD (Van Hautegeem *et al.*, 2015; Gunawardena *et al.*, 2004). These two categories of PCD may require different molecular

mechanisms for initiation and execution as derived from recent results that indicate that the transcriptional signatures of developmentally controlled cell death are largely distinct from those associated with environmentally induced cell death (Olvera-Carrillo *et al.*, 2015).

1.2.1 Developmental PCD in plants

Developmental PCD is a terminal stage of plant cell differentiation. PCD is involved in many aspects of vegetative and reproductive development starting from formation of embryos until death of the whole plant (Van Hautegeem *et al.*, 2015; Thomas and Franklin-Tong, 2004). During vegetative growth, PCD is a part of formation of xylem tracheary elements (Escamez and Tuominen, 2014), shedding of root caps (Wang *et al.*, 1996), emergence of lateral and adventitious roots and aerenchyma (Orman-Ligeza *et al.*, 2013; Drew *et al.*, 2000), leaf shaping (Gunawardena, 2008) as well as abscission and senescence processes (Bar-Dror *et al.*, 2011; Masclaux-Daubresse *et al.*, 2008).

Tracheary element differentiation includes several steps such as cell specification, secondary wall formation and lignification, PCD and clearance of cellular content (Courtois-Moreau *et al.*, 2009; Fukuda, 1996) and is shown to be controlled by several hormones and transcription factors (TF) (Milhinhos and Miguel, 2013; Kubo *et al.*, 2005). It was also shown that genes encoding Zinnia endonuclease 1 (ZEN1) and the Arabidopsis xylem cysteine protease 1 (XCP1), XCP2 and metacaspase 9 are involved in xylem PCD; however, functional evidence for these and other hydrolases is still lacking (Escamez and Tuominen, 2014).

The root cap has important functions in root growth; gravity sensing and protection of stem cells of the root tip (Arnaud *et al.*, 2010). The cells of root cap are constantly removed during root growth by coordinated PCD process. Bifunctional nuclease 1 (BFN1) and plant aspartic protease A3 (PASPA3), which play also a role in tracheary element formation (Escamez and Tuominen, 2014), were found as markers of PCD in the root cap (Fendrych *et al.*, 2014). PCD in root cap is characterized by effective cell corpse elimination (Fendrych *et al.*, 2014). Cortex and epidermal PCD have been observed to promote lateral and adventitious root emergence in cereals (Orman-Ligeza *et al.*, 2013). ROS production and a localized mechanical force by the emerging adventitious roots have been implicated in epidermal PCD signaling together with ethylene and gibberellin in rice (Steffens *et al.*, 2012). Large intercellular lacunae for gas

exchange and transport in aerenchyma are also generated by PCD (Drew *et al.*, 2000). Again, ROS and ethylene are necessary for cell death during aerenchyma formation.

The production of complex leaf shape during leaf morphogenesis at least in some plant species from Araceae (*Monstera* spp) and distantly related Aponogetonaceae families (*Aponogeton madagascariensis*) requires controlled cell death (Gunawardena, 2008). Although the order of cellular events occurring during leaf perforation is well characterized, the molecular network that governs these processes is still largely unknown; however ethylene has been recently shown to play a significant role (Rantong *et al.*, 2015).

Tissue separation processes fulfil vital functions during plant development, including leaf shedding, floral and fruit abscission as well as release of pollen and seeds by anther and fruit dehiscence. Abscission and dehiscence involve the differentiation a specialized margin cell types for which PCD processes having been suggested (Bar-Dror *et al.*, 2011). Expression of PCD-associated hydrolases was found to be induced by ethylene in the abscission zone of tomato leaves and flowers (Bar-Dror *et al.*, 2011). In *Arabidopsis*, BFN1 expression has been observed in the abscission zone of stamens, petals and sepals (Farage-Barhom *et al.*, 2008), suggesting similar PCD processes during abscission and root cap shedding.

Plant senescence is a genetically encoded program of the death of single plant organ or the entire plant (Thomas, 2013). In contrast to the above described PCD types, where only defined cells undergo cell disintegration, senescence-induced cell death occurs in all cell types of an organ or a plant. Leaf senescence and ensuring PCD are controlled by ethylene in a complex cross-talk with other hormones and TFs. Hormones affect leaf senescence differentially: senescence is delayed by cytokinins and gibberellic acids and accelerated by abscisic acid and jasmonates (Jibrán *et al.*, 2013). Developmental aging and senescence involves chlorophyll degradation by PAO, specific proteases and N transporters (Kohl *et al.*, 2015). Specific members of the NAC and WRKY TF family are co-regulated with senescence-associated genes (Christiansen and Gregersen, 2014) and frequently involved in senescence signalling (Christiansen and Gregersen, 2014; Breeze *et al.*, 2011; Zentgraf *et al.*, 2010).

Developmentally regulated PCD plays an important role in gametophyte establishment, during fertilization and subsequent seed development being a crucial determinant of successful sexual reproduction. The plant life cycle alternates between haploid gametophyte and diploid sporophyte generations. During establishment of female gametophyte, only the functional megaspore is selected for further development, whereas the three non-functional

megaspores degenerate by developmentally controlled processes (Friedman and Ryerson, 2009), similarly to animal oogenesis. The antipodal cells of mature embryo sac undergo PCD around fertilization, which is possibly influenced by still unknown central cell-derived factors (Heydlauff and Cross-Hardt, 2014). Contrary to this, controlled death of synergid cells is well studied in respect with co-ordinately happened pollination and fertilization processes (Heydlauff and Cross-Hardt, 2014). These data implicate that PCD in the female gametophyte not only disposes redundant cells, but is also crucial for successful plant sexual reproduction (Heydlauff and Cross-Hardt, 2014). Contrary to the megaspore in female gametophyte, all microspore cells develop into mature pollen inside of anthers. However, pollen development and release is depended on function and degradation of the tapetum (Solis *et al.*, 2014; Plackett *et al.*, 2011). Numerous mutants producing aborted or unfertile pollen helped to discover the mechanisms of tapetal cell degradation (Zhu *et al.*, 2011; Parish and Li, 2010). In barley, the expression of Jekyll gene in the tapetum is required for both successful pollen development and tapetal cell degeneration that is a prerequisite for effective pollen release (Radchuk *et al.*, 2012). In maize, sex determination involves the selective killing of the female reproductive primordia in order to develop the male floral structures (the stamens) in the tassel (Greenberg, 1996). Developmental PCD is an important part of a self-incompatibility mechanism used by many angiosperms to prevent self-fertilization and inbreeding (Wilkins *et al.*, 2014). Alterations of cytoskeleton, caspase-like proteases activities and mitogen-activated protein kinase signalling have been shown to be necessary to execute PCD during pollen incompatibility.

1.2.2 Cell death during seed development and germination of barley

Cell disintegration during grain development in cereals, including barley, represents a typical case of developmental PCD in plants. After double fertilization, the diploid zygote together with the triploid initial endosperm cell, the antipodal cells and the synergids are surrounded by the maternal nucellus and embedded into the embryo sac demarcated by the inner and outer integuments (Fig. 1.2) (Radchuk and Borisjuk, 2014). During early grain development, maternal seed parts (style, pericarp and nucellus) represent the bulk of the establishing seed. The antipodal and synergid cells degenerate soon after fertilization. They, however, belongs to the embryo sac but not to the seed itself. The nucellus, a tissue of maternal

origin, is located between the integuments and the embryo sac. At early stages of barley seed development, the nucellus is among the first degenerating tissues. Nucellar cells undergo a process of PCD, which has been well characterized at the morphological and biochemical levels (Radchuk *et al.*, 2011; Dominguez *et al.*, 2001). In a transcriptome study, high expressed transcripts of the aspartic protease nucellin (Chen and Foolad, 1997), a cathepsin B-like protease (Dominguez and Cejudo, 1998) and the vacuolar processing enzyme nucellain (Linnestad *et al.*, 1998) clustered together during early development. The respective enzymes are possibly involved in nucellar PCD process (Sreenivasulu *et al.*, 2006). Numerous starch granules are already detectable in nucellar cells at anthesis. They undergo rapid degradation, as suggested from accumulation of transcripts for α -amylase AMY4 in the nucellus at 2 DAF (Radchuk *et al.*, 2009). It has been proposed that PCD of the nucellus serves for remobilization of its cellular contents, which are needed for the nourishment of the growing endosperm. The nucellus degenerates till 4 DAF except that part adjacent to the main vascular bundle, where it forms the nucellar projection, which functions as a transfer tissues supplying assimilates to the endosperm (Radchuk and Borisjuk, 2014). There is evidence that nucellar projection and assimilate transfer involve PCD (Radchuk *et al.*, 2006; Thiel *et al.*, 2009). The nucellar projection cells form a complex tissue consisting of roundish meristematic cells close to the pigment strand and adjacent to the vascular tissue, the middle zone with elongated cells, transfer cells with peculiar cell wall invaginations and autolyzing cells adjacent to the endosperm cavity (Thiel *et al.*, 2009). First degrading nuclei in the nucellar projection are visible by TUNEL assay already at 5-6 DAF in the cells adjacent the endosperm cavity (Radchuk *et al.*, 2011; Dominguez *et al.*, 2001). Progressive cell turnover occurs in the nucellar projection with continuously dividing cells in the meristematic zone and dying cells facing the endosperm transfer cells. This turnover is likely important for assimilate transfer via the nucellar projection (Melkus *et al.*, 2011). However, direct evidence for the role of PCD in the assimilate transfer through the nucellar projection and therefore for the seed filling has not been provided yet.

In parallel to the nucellus, style volume scales rapidly down soon after anthesis (Gubatz and Weschke, 2014) and pericarp starts to expand in most of its parts mainly by cell elongations. The pericarp of barley grains originates from the gynoeceum and represents a major part of early fruit consisting of the outer epidermis, several layers of parenchyma cells, a three-cell-layered chlorenchyma, and the inner epidermis (Cochrane and Duffus, 1980). As seen from

transcriptional activity, cell divisions in pericarp cease already after 2 DAF (Radchuk *et al.*, 2011). A decrease in cell divisions is accompanied by strong increase in cell expansion and cell wall synthesis indicating that pericarp grows predominantly by cell elongations. During development, the number of cell rows in the pericarp decrease starting from 3 DAF first in dorsal and later in lateral regions suggesting that PCD occurs there (Radchuk *et al.*, 2011). Indeed, fragmentation and degradation of nuclear DNA in pericarp cells increase with aging of the tissue (Radchuk *et al.*, 2011). The first cellular symptoms of pericarp degeneration appear at 4 DAF in the innermost cell layers closed to endosperm (Radchuk *et al.*, 2011; Dominguez *et al.*, 2001). Then, PCD events are extended to the whole tissue during the period of 6–10 DAF (Radchuk *et al.*, 2011). Starch transiently accumulates around the two lateral vascular bundles and, later on, also adjacent to main vascular bundle (Radchuk *et al.*, 2009; Weschke *et al.*, 2000). This starch becomes remobilized as PCD is initiated in these areas (Radchuk *et al.*, 2009). In addition, transcription of specific proteins, potentially associated with PCD, is activated such as specific C1 cysteine proteases (SAG12, Cys-EP, RD19A), cathepsin, serine proteases, F-box COI1 and FBL3 proteases (Sreenivasulu *et al.*, 2006) as well as vacuolar processing enzyme 4 (VPE4; Radchuk *et al.*, 2011) (see also below).

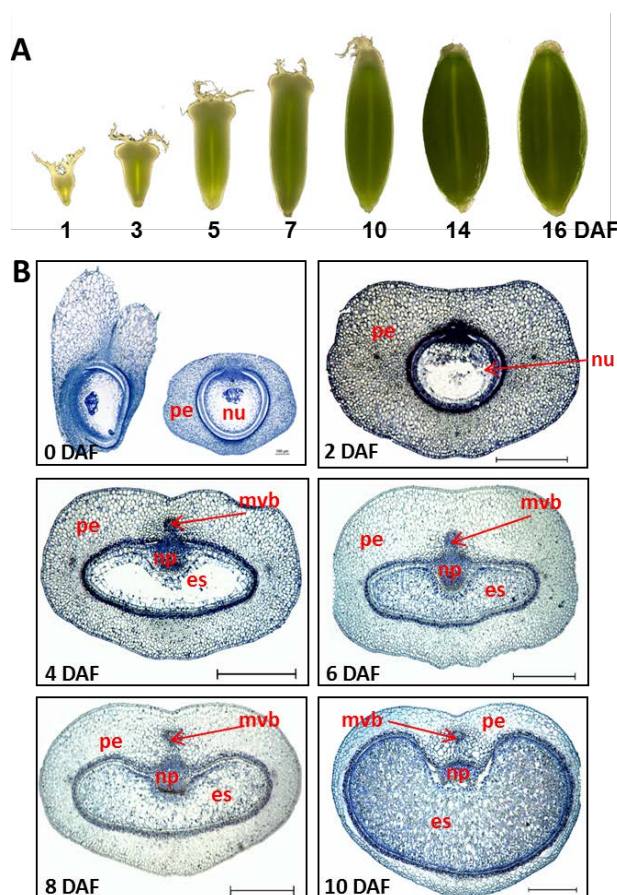


Figure 1.2 The developing barley grain. (A) Barley grains at different developmental stages. Glumes and awn were removed before taking photographs. (B) Median transverse sections of barley grains at different developmental stages. Bars, 500 μ m. DAF, days after flowering; es, endosperm; mvp, main vascular bundle; np, nucellar projection; nu, nucellus; pe, pericarp.

The pericarp serves as a transient storage tissue during early grain development (Radchuk *et al.*, 2009) besides being protective tissue for endosperm/embryo against harmful environmental influences (Radchuk and Borisjuk, 2014). Furthermore, PCD of pericarp is required for providing space for the expanding endosperm and for nutrient remobilization (Radchuk *et al.*, 2009; 2011). However, this assumption requires experimental confirmation. During late development, the pericarp is completely disintegrated and its remnants become part of the protective hull.

PCD is also an integral part of endosperm and embryo development. In endosperm, however, PCD occurs as terminal stage of tissue differentiation following proliferation, differentiation and storage compound accumulation stages. After double fertilization, the endosperm nucleus suffers many rounds of divisions in the absence of cell wall formation to form an endosperm coenocyte (Olsen, 2004). Cellularization of the endosperm coenocyte starts around 3 DAF with cells opposite to the nucellar projection to form endosperm transfer cells. The process of endosperm cellularization spreads into lateral as well as central parts and is finished several days later. Starting around 8 DAF, the outer endosperm cell layers differentiate into aleurone/subaleurone layers which accumulate predominantly storage proteins and lipids. Aleurone layer persists throughout whole grain development, remains one of two live organs (second is the embryo) in dry seeds and degrades at the onset of germination (Becraft and Gutierrez-Marcos, 2012). The cells of starchy endosperm accumulate large amounts of starch but also a variety of storage proteins (prolamins, α -globulins and 11S legumin; Weber *et al.*, 2010) and eventually undergo PCD during maturation (Olsen, 2004). From 10 DAF onward, caryopsis volume increases mainly by thickening of the starchy endosperm. The onset of PCD is promoted by a rise of ethylene production at mid to late endosperm development (Young *et al.*, 1997). DNA fragmentation is evident during endosperm PCD but the digestion of most cellular contents does not occur until germination. The molecular mechanisms that trigger PCD in endosperm remain to be explored.

PCD is also a part of embryo patterning (Bozhkov *et al.*, 2005) and is known to be involved in deleting of embryo suspensor (Huang *et al.*, 2016; Lombardi *et al.*, 2007). In barley, suspensor consists of only two cells, which degenerate during early embryo development by a still not known mechanism.

1.2.3 PCD in the interaction between plants and environment

Environmentally induced PCD occurs in response to external abiotic stimuli such, for example, as heat (Lord and Gunawardena, 2011), ultraviolet light (Nawkar *et al.*, 2013), hydrogen peroxidase (Gechev *et al.*, 2006) and pathogen attack (Greenberg, 1997). PCD is also connected with plant immunity to biotrophic pathogens. In all these examples, PCD is essential or beneficial for plants. However, necrotrophic pathogens can cause disease by triggering PCD in healthy tissues (Coffeen and Wolpert, 2004; Navarre and Wolpert, 1999; Wang *et al.*, 1996). Unwanted PCD can also be instigated by many abiotic factors like extreme temperatures, salinity, and pollutants (Koukalova *et al.*, 1997; Overmyer *et al.*, 2000; Swidzinski *et al.*, 2002). Plants are continuously challenged by a wide variety of pathogens, such as viruses, bacteria, fungi, and oomycetes. The spread of disease is limited by plant immune responses, including the hypersensitive response (HR), which is characterized by a rapid and localized PCD known as hypersensitive cell death (Greenberg, 1997). The HR is controlled by multiple signal transduction pathways that are initiated upon the recognition of a pathogen avirulence factor by a plant resistance gene product (Dangl and Jones, 2001; Jones and Dangl, 2006). Caspase peptide inhibitors suppress the HR in response to infection with an avirulent *Pseudomonas syringae* pv. *phaseolicola* strain (del Pozo and Lam, 1998). In *Arabidopsis thaliana*, the genetic control of the HR is beginning to be elucidated. Mutants of *Arabidopsis* called *acd2* (accelerated cell death 2) and *lsd* (lesions simulating disease) activate the HR and multiple defenses in the absence of any pathogen (Greenberg *et al.*, 1994; Delaney, 1994). Since some of these mutations are recessive, one model is that the *ACD2* and some *LSD* genes negatively regulate the HR and multiple defense function. In addition, caspase-like activity was detected in tobacco plants in response to tobacco mosaic virus (del Pozo and Lam, 1998). Nuclear DNA cleavage has been observed before the vacuole collapse during the HR (Mittler *et al.*, 1997).

1.2.4 Morphological classification of plant PCD

PCD has been extensively studied in animals and numerous molecular regulators have been identified. In animals, cell death can be divided into three main categories based on morphological characteristics: apoptosis, autophagy and necrosis or non-lysosomal PCD (Kroemer *et al.*, 2009). To define these three major classes, only two simple criteria were used: the presence of apoptotic bodies or cell protrusions and engulfment of these by other

cells to specify the apoptotic pathway; presence of autophagosomes and derived vesicles are characteristic for autophagy. The third class of animal PCD, necrosis, includes all types of PCD which do not fit into the first two criteria (Kroemer *et al.*, 2009). A number of morphological, biochemical and cytological features of PCD in plants share similarities to those of animals suggesting a high evolutionary conservation among Eukaryotes (van Doorn, 2011; Williams and Dickman, 2008, Della Mea *et al.*, 2007). Therefore, early publication often used animal-based PCD categories to describe plant PCD processes (Reape and McCabe, 2010; 2008; Love *et al.*, 2008) leading to confusion and misinterpretations (van Doorn *et al.*, 2011; van Doorn, 2011). The long evolutionary distance and, especially, distinct cellular architecture between the two kingdoms lead for the differences in the mechanisms of plant and animal PCD. At first, plants do not exhibit classic apoptosis (van Doorn *et al.*, 2011). Apoptosis in animals is characterized by formation of apoptotic bodies and is often associated with chromatin condensation, cell shrinkage, plasma membrane blebbing, internucleosomal DNA cleavage and degradation in phagocytic lysosomes by adjacent cells (Hofius *et al.*, 2007). In plants, formation of apoptotic bodies is precluded by rigid cell walls and the phagocytic cells are absent (van Doorn *et al.*, 2011). Therefore, a new classification system for plant PCD was proposed recently (van Doorn *et al.*, 2011) and included three classes: vacuolar, necrotic and mixed or atypical plant PCD. However, van Doorn (2011) has further shown that the class of atypical PCD is arbitrary and therefore ambiguous. Based on last definitions (van Doorn, 2011), only two classes of PCD in plants are described: autolytic or vacuolar and non-autolytic or necrotic. Vacuolar or autolytic PCD occurs mainly during normal plant development and during physiological abiotic stress, while necrotic or non-autolytic PCD takes place mainly during plant-pathogen interactions and during non-physiological levels of abiotic stress (van Doorn, 2011).

1.2.4.1 Autolytic or vacuolar plant PCD

Plants have elaborated an extensive vacuolar system that, among others, also includes lytic vacuoles that are used to recycle parts of cells during normal development and stress response, similarly to the roles of lysosomes in animals (Müntz, 2007). These lytic vacuoles acquire a central role in one major class of plant cell death termed vacuolar PCD (van Doorn

et al., 2011). Because this PCD type is characterized by rapid clearance of cytoplasm after tonoplast rupture, this class is also termed as autolytic PCD (van Doorn, 2011).

In this type of plant PCD, death is preceded by the appearance of small lytic vacuoles in cytoplasm, which eventually merge. Considerable amounts of cytoplasmic structures, in particular, plastids, ribosomes, membranes of endoplasmic reticulum disappear during this process. Engulfment of the cytoplasm by lytic vacuoles with subsequent cargo degradation is a major mechanism of cell dismantling during vacuolar PCD (van Doorn *et al.*, 2011). The final step is rupture of the tonoplast and a massive release of vacuolar hydrolases, which becomes activated and help to degrade cytoplasm (Senatore *et al.*, 2009) rapidly destroying entire protoplast or even whole cell including cell wall. The remobilization of macromolecules is often associated with autolytic cell death. Extensive degradation of DNA, RNA, lipids, proteins and complex carbohydrates has been observed in senescent leaves and petals (van Doorn, 2004; Gregensen *et al.*, 2008) as well as during seed germination (Young and Gallie, 2000). The autolytic cell death often includes processes as increase in Ca²⁺ ion concentration in cytosol (Bosch *et al.*, 2008), cytosol acidification, changes in microtubule and actin cytoskeletons (Smertenko *et al.*, 2003; Bosch *et al.*, 2008), chromatin aggregation and nucleus condensation and breakdown (Yamada *et al.*, 2003; 2006a; 2006b; Kladnik *et al.*, 2004).

During normal plant development, vacuolar cell death accompanies the remodeling and senescence of various organs, including cotyledons, leaves, petals and roots (Gunawardena, 2008; Rubinstein, 2000), tapetum degeneration in anthers (Hanamata *et al.*, 2014), the formation of xylem conduits (Fukuda, 1996) and development and germination of seeds (Lopez-Fernandez and Maldonado, 2015; Young and Gallie, 2000). Vacuolar PCD is involved in the induction of aerenchyma in waterlogged roots (Drew *et al.*, 2000) and precocious leaf yellowing because of stress conditions (Gepstein and Glick, 2013). Normally, execution of vacuolar PCD takes several days from PCD initiation till rupture of tonoplast and protoplast clearance (van Doorn and Woltering, 2005; Filonova *et al.*, 2000). The cell wall can be largely degraded, as for example, during aerenchyma formation, leaf reshaping or petal senescence (Gunawardena, 2008; Drew *et al.*, 2000; Rubinstein, 2000) or can remain intact, as in case of xylem differentiation (Courtois-Moreau *et al.*, 2009; Fukuda, 1996).

1.2.4.2 Necrotic or non-autolytic PCD in plants

This type of PCD is characterized by absence of rapid clearance of the cytoplasm due to early rupture of the plasma membrane and loss of intracellular content (van Doorn, 2011; van Doorn *et al.*, 2011). Non-autolytic cell death often includes mitochondrial swelling (Scott and Logan, 2008; Jones, 2000), the absence of growing lytic vacuoles and early rupture of the plasma membrane leading to shrinkage of the protoplast. The corps of necrotic cells remains largely unprocessed because of absence of lytic vacuoles. Necrotic PCD is induced by successful recognition of a pathogen during the hypersensitive response (Heath, 2000). It is also found in tissues challenged by necrotrophic pathogens (Kuroyanagi *et al.*, 2005). Necrosis or non-lytic PCD is typically an acute cell death response that develops within minutes (response to toxic treatments) or within a day (hypersensitive response).

1.2.5 Molecular mechanisms of initiation and execution of PCD in plants

PCD is an active process that requires “*de novo*” protein synthesis for specific genetic control and cellular activities. Apoptosis in animals can be initiated by one of two pathways. In the intrinsic pathway, the cell kills itself because it senses internal cell stress, while in the extrinsic pathway the cell kills itself because of signals from other cells (Jin and El-Deiry, 2005). Both pathways induce cell death by activating caspases, a group of ubiquitously expressed cysteine-dependent aspartate-specific proteases. They possess characteristic cysteines in the catalytic domain and cleave target proteins after aspartate residues (Hengartner, 2000). Caspase activation occurs via a proteolytic cascade, started by initiator caspases (e.g. caspases-2, -8, -9 and -10 in human) that activate executor caspases (e.g. caspases-3, -6 and -7 in human), which in turn activate other proteases and nucleases to degrade a plethora of vital proteins (Boatright and Salvesen, 2003; Hengartner, 2000). The initiation of this cascade reaction is regulated by caspase activators and inhibitors (Ekert *et al.*, 1999). To conclude, main players in animal PCD are ubiquitously expressed caspases, which activities are predominantly regulated at the post-translational level.

Since the first report about proteolytic activity towards a synthetic caspase substrate in tobacco (del Pozo and Lam, 1998), caspase-like activities have been observed in plants during different processes and often associated with PCD events (Woltering *et al.*, 2002). In tobacco, the capsase-1-like activity was required for bacterially induced PCD (del Pozo and

Lam, 1998), and this caspase-like activity could be inhibited with specific inhibitors but not by caspase-unrelated protease inhibitors. Caspase-1, caspase-3 and caspase-6-like activities were detected in the degenerating nucellus of *Sechium edule* (Lombardi *et al.*, 2007). Cytosolic extracts from barley embryonic suspension cells exhibited both caspase-1-like and caspase-3-like activities (Korthout *et al.*, 2000). In the developing barley grains, caspase-1, caspase-3, caspase-6, caspase-8 and caspase-9-like activities were measured at 10 and 30 days after flowering (Boren *et al.*, 2006). However, taking into account that diverse and often contradictory processes happen simultaneously in the barley grain (i.g., degeneration of pericarp coincides with endosperm expansion), measurements of caspase activities in distinct tissues over whole development are necessary to distinguish specific PCD processes in the developing grain. Caspase-2 and caspase-4-like activities have not been reported in plants so far (Cai *et al.*, 2014).

It took a long period of time to identify plant proteases responsible for caspase-like activities. Despite of some cellular similarity in PCD between plants and animals, no sequences for functional homologs of animal caspases have been identified in plant genomes (Xu and Zhang, 2009). The metacaspases, proteases with weak similarity to animal caspases, are found only in eukaryotes lacking true caspases such as plants and fungi (Vercammen *et al.*, 2007). They are unable to cleave caspase substrates and have arginine or lysine specificity instead of aspartate (Bonneau *et al.*, 2008; Vercammen *et al.*, 2007) and therefore cannot be responsible for caspase-like activities in plants. Nevertheless, metacaspase activity has been implicated in different plant PCD processes including PCD induced by abiotic (He *et al.*, 2008) and biotic stresses (Fagundes *et al.*, 2015), development of embryo patterning (Bozhkov *et al.*, 2005; Suarez *et al.*, 2004) and xylem (Escamez *et al.*, 2016).

Caspase-like activities in plants must therefore originate from proteases unrelated to animal caspases. Current investigations have shown that such proteases as phytaspase (Chichkova *et al.*, 2010), saspase (Coffeen and Wolpert, 2004), a protease from the 26S proteasome complex (Han *et al.*, 2012) and a vacuolar processing enzyme (VPE) (Hara-Nishimura *et al.*, 2005) are responsible for certain types of caspase-like activities in plants. Plant proteases with caspase-like activities identified so far fall into two broad groups: subtilisin family serine endopeptidases (saspase, phytaspase) and legumain family cysteine endopeptidases (VPE) (Rantong and Gunawardena, 2014).

A phytaspase has been found to exhibit caspase-6 activity in tobacco and rice in response to pathogen attack (Chichkova *et al.*, 2010). The phytaspase is synthesized as preproenzyme that further is able to autocatalytic activation (Vartapetian *et al.*, 2011). The active phytaspase is localized in the apoplast until PCD is induced suggesting that it might be playing a protective role within the apoplast against pathogens (Vartapetian *et al.*, 2011). Purified saspase proteins from *Avena sativa*, which are very similar to phytaspase, exhibit enzymatic activities predominantly against caspase-6 substrate but also weakly against caspase-8 substrate (Coffeen and Wolpert, 2004). The saspase is synthesized as a precursor comprising a signal peptide, a prodomain and a peptidase domain (Coffeen and Wolpert, 2004). In *A. sativa*, saspase is thought to be responsible for caspase-like activity involved in victorin-induced PCD (Coffeen and Wolpert, 2004).

The 20S proteasome, composed of many α and β subunits, executes caspase-3-like activity during xylem development (Han *et al.*, 2012) and in response to biotic stress (Hatsugai *et al.*, 2009). It has been also shown that the β 1 subunit and, possibly, the β 2 subunit provide caspase-3-like activity whereas the β 5 subunit of the 20S proteasome does not (Han *et al.*, 2012). It has also been reported recently that subtilisin-like protease StSBTc-3, isolated from potato (*Solanum tuberosum*) leaves infected with *Phytophthora infestans*, exhibits caspase-3-like activity (Fernandez *et al.*, 2015). The purified StSBTc-3 protein was able to induce cytoplasm shrinkage in vitro and to cause cell death (Fernandez *et al.*, 2015).

VPE (sometimes also called as legumain, Julian *et al.*, 2013) was originally described as a vacuole-localized cysteine proteinase responsible for the maturation and activation of vacuolar proteins, which are synthesized in the endoplasmic reticulum (ER) as a proprotein precursor and then transported to vacuoles (Hara-Nishimura, 1987; Hara-Nishimura *et al.*, 1991). VPE was the first identified enzyme with caspase-like activity in plants possessing activity against caspase-1 substrate (Hatsugai *et al.*, 2015). VPE proteins share some conserved structural properties to mammalian apoptotic caspase-1 whilst sequence similarity is lacking (Hara-Nishimura *et al.*, 2005). Similarly to caspase-1, VPEs are cysteine proteases which cleave peptide bonds on the C-terminal side of aspartate and asparagine residues. VPEs contain also conserved essential amino acid residues comprising two cysteine and two histidine residues of which Cys-215 and His-172 represent the catalytic residues (Hara-Nishimura *et al.*, 2005). VPE proteins from diverse plants are able to digest the synthetic peptide YVAD, which is specific for caspase-1 activity (Hara-Nishimura *et al.*, 2005),

indicating that VPE may be responsible for caspase-1-like activity in plants. Caspase-specific inhibitors but not general protease inhibitors are able to suppress this reaction (Hara-Nishimura *et al.*, 2005). In VPE-silenced tobacco plants, the reduced VPE activity parallels the reduction of caspase-1-like activity (Hatsugai *et al.*, 2004). Four VPE genes, α VPE, β VPE, γ VPE, and δ VPE, are encoded by the Arabidopsis genome (Nakaune *et al.*, 2005). Quadruple knockout mutants of Arabidopsis lack both VPE activity and any caspase-1-like activity, indicating that VPEs are responsible for the activity in plants and no other proteases perform this activity (Kuroyanagi *et al.*, 2005). These data support that VPE is the only plant protease with caspase-1-like activity.

VPE gene products are predicted to be classic pre-pro-peptides which are processed at both C- and N-terminals to produce the mature and active enzyme. The precursor protein is self-catalytically converted into the active mature form at low pH during delivery to the vacuole and no other factors are necessary for VPE activation (Kuroyanagi *et al.*, 2005; Hiraiwa *et al.*, 1999). However, both mature and intermediate VPEs have been shown to exhibit proteolytic activities in plant cells (Kuroyanagi *et al.*, 2002; Rojo *et al.*, 2004). The papaver VPE is apparently not processed and only the full length protein displayed caspase activity (Bosch *et al.*, 2010). Besides YVAD (caspase-1-like activity), poppy VPE can cleave also DEVD (caspase-3-like) and IETD (caspase-8-like) activities (Bosch *et al.* 2008) albeit at lower efficiencies. This difference may be either isoform or species-dependent.

VPEs have been shown to be involved in PCD during both disease resistance and developmental processes (Hatsugai *et al.*, 2015; Hatsugai *et al.*, 2006; Nakune *et al.*, 2005). Arabidopsis α VPE and γ VPE, predominantly expressed in vegetative tissues, are involved in PCD during leaf senescence, lateral root formation and diverse stresses (Hara-Nishimura and Maeshima, 2000; Kinoshita *et al.*, 1999). A VPE gene of tobacco (*Nicotiana tabacum*) exhibits caspase-1-like activity and is involved in Tobacco mosaic virus-induced hypersensitive cell death (Hatsugai *et al.*, 2004). The β VPE gene is expressed during later seed development and is essential for processing of storage proteins in cotyledons (Shimada *et al.*, 2003). However, transcriptional repression of Arabidopsis β VPE by specific antisense RNA in transgenic tobacco seeds has no strong effect on 11S pro-globulin processing (Müntz and Shutov, 2002) indicating additional β VPE functions during late seed development. The seed specific δ VPE is expressed in two inner cell layers of the early seed coat of Arabidopsis (Nakaune *et al.*, 2005). This tissue undergoes developmental PCD at early stages, thereby reducing its

thickness by >50%. In a δ -type deficient mutant, PCD is delayed and the seed coat remains thick throughout development (Nakaune *et al.*, 2005) showing that δ VPE is responsible for PCD in Arabidopsis seed coats. The interspecific F1 hybrid of *Nicotiana glauca* and *N. glauca* exhibits hybrid lethality at the seedling stage by vacuolar collapse (Mino *et al.*, 2007). The vacuolar collapse and cell death were suppressed by the inhibition of VPE activity indicating for involvement of VPE in hybrid lethality.

1.2.6 PCD-related genes in the developing barley grains

Genes encoding proteases with the respective caspase-like activity have not been described so far in barley except VPE genes (Radchuk *et al.*, 2011). Eight VPE homologs have been identified in barley, and some may be involved in PCD during the development of maternal seed tissues, including the nucellus and pericarp (Julian *et al.*, 2013; Radchuk *et al.*, 2011; Linnestad *et al.*, 1998). VPE4, which is weakly similar to Arabidopsis δ VPE, is exclusively expressed in the deteriorating pericarp associated with specific DNA degradation. This correlative evidence suggested that VPE4 is involved in the PCD of the pericarp (Radchuk *et al.*, 2011); however, direct confirmation of this is missing. The VPE2a gene, also known as nucellain (Linnestad *et al.*, 1998), encodes a cysteine proteinase with predicted caspase-1-like activity that is exclusively expressed in the nucellus and nucellar projection of the developing grains (Linnestad *et al.*, 1998). However, the full-length cDNA of the VPE2a gene was not published (Radchuk *et al.*, 2011; Linnestad *et al.*, 1998). Three additional cDNAs (VPE2b, VPE2c and VPE2d) share high homology with the known VPE2a sequence (Radchuk *et al.*, 2011). Nucellus-specific expression was also supposed for these genes (Radchuk *et al.*, 2011). All these genes are predicted to be involved in PCD of nucellus and nucellar projection. Again, as in case of the barley VPE4 gene, the direct role of VPE2a, VPE2b, VPE2c and VPE2d genes in nucellar PCD was not provided. Besides a predicted role during grain development, VPE2b (HvLeg2) gene is highly expressed during germination (Julian *et al.*, 2013) where its molecular function is also still unknown.

Cereal seed development depends on the intimate interaction of filial and maternal tissues, ensuring nourishment of the new generation. The gene Jekyll, which was identified in barley, is localized and preferentially expressed during sexual reproduction of barley being active in the developing anthers and gynoecium (Radchuk *et al.*, 2012) as well as in developing grains

(Radchuk *et al.*, 2006). In the developing caryopsis, Jekyll is expressed exclusively in the nucellus and nucellar projection tissues. Jekyll is upregulated in cells destined for autolysis. Down-regulation of Jekyll transcription in barley grains leads to drastic reduction of PCD in the nucellar tissues, and decelerates autolysis and cell differentiation within the nurse tissues. Flower development and seed filling are thereby extended, and the nucellar projection no longer functions as part of the main transport route for assimilate. Diminished assimilate transfer results in slowing down the proliferation of endosperm nuclei, and a severely impaired ability to accumulate storage products in the endosperm leads to the formation of irregular and small-sized seeds at maturity. Jekyll plays a decisive role in the differentiation of the nucellar projection and drives the programmed cell death necessary for its proper function (Radchuk *et al.*, 2006).

1.2.7 Regulation of PCD in plants

Animal caspases are ubiquitously expressed genes. Therefore, their activation or repression occurs mostly post-translationally and involves Bcl-2/Bcl-2-like proteins, defender against apoptotic cell death (DAD1) and Bax inhibitor 1 (BI1) (Jin and El-Deiry, 2005). All plant proteases with caspase-like activities known so far show very specific temporal, developmental and spatial patterns of expression (Christoff *et al.*, 2014; Julian *et al.*, 2013; Radchuk *et al.*, 2011; Hara-Nishimura *et al.*, 2005) indicating that transcriptional regulation may have higher impact on regulation of PCD in plants than in animals. However, as shown by numerous experiments, post-translation regulation of PCD takes place also in plants. Furthermore, plants possess unique regulators in forms of hormones, in this context especially jasmonic acid and ethylene.

1.2.7.1 Regulation of plant PCD by a transcription factor

The MADS box TFs are critical regulators of plant reproductive development. Being the main members of the ABC model, they are the most important regulators of floral organ development (Yamaguchi and Hirano, 2006; Lohmann and Weigel, 2002). Some MADS-box genes were also predicted to play roles in regulation of seed development in rice (Arora *et al.*, 2007). Genes of the Bsister clade are the closest relatives of B genes (Becker *et al.*, 2002) and are important regulators of sexual plant reproduction including seed development. The

Arabidopsis thaliana TRANSPARENT TESTA 16 (TT16) is required for protoantocyanidin accumulation and inner integument development of the seed coat (Nesi *et al.*, 2002). GORDITA, another *Arabidopsis* Bister clade member, has a role in maintaining cell size of the outer integument in seed coat and in fruit development (Prasad *et al.*, 2010). Recently, a nucellus-expressed MCM1/AGAMOUS/DEFISIENS/SRF (MADS) box TF in rice, OsMADS29, has been shown to directly regulate several PCD-associated genes in rice (Yin and Xue, 2012). OsMADS29 is exclusively expressed in generative organs such as anthers, ovules and developing seeds. Especially high mRNA and protein accumulation was detected in the nucellus and nucellar projection of early developing grains (Yang *et al.*, 2012; Yin and Xue, 2012), but OsMADS29 transcripts and protein were also detected in maternal pericarp and vasculature (Nayar *et al.*, 2013; Yang *et al.*, 2012) and even in the outer layer (aleurone) of the developing endosperm (Nayar *et al.*, 2013). Besides, OsMADS29 is expressed in the developing embryo (Yang *et al.*, 2012; Yin and Xue, 2012). Functional analysis, by using of RNAi-mediated gene down-regulation, revealed the role of OsMADS29 in transcriptional regulation of PCD in maternal tissue of the developing grains that affect nutrient transport and thereby endosperm development and starch accumulation (Yang *et al.*, 2012; Yin and Xue, 2012). In this respect, the phenotype of rice grains with suppressed OsMADS29 expression resembles those of barley grains with down-regulated Jekyll expression (Radchuk *et al.*, 2006). OsMADS29 protein binds directly to the promoter regions of genes that encode a Cys protease and the nucleotide binding site-Leu-rich repeat protein, both potentially involved in PCD (Yin and Xue, 2012). However, the importance of these proteins for PCD has been still not shown. Another study, based on MADS29 gain-in-function and knock-down models, implicated the MADS29 role in multiple aspects of seed development, including plastid biogenesis, cell division and differentiation, and starch biosynthesis by controlling cytokinin and auxin homeostasis (Nayar *et al.*, 2013). Dimerization of MADS29 with its own monomer or another MADS protein is required for MADS29 translocation into the nucleus (Nayar *et al.*, 2014). The MADS29 TF was proposed to play a relevant function in the control of nucellus and nucellar projection cells degeneration (Yin and Xue, 2012; Yang *et al.*, 2012). The barley homolog of OsMADS29 has still not been described. It is also not known, whether other PCD-related genes are transcriptionally regulated by MADS29. Yang *et al.* (2012) found that expression of the OsVPE1 gene (a homolog of barley VPE2a gene) was strongly down-regulated in OsMADS29-deficient grains while the expression of the VDAC and PBZ1 genes,

both involved in PCD induced by abiotic stress (Kim *et al.*, 2011; Varda *et al.*, 2008), was not changed. These data indicate that MADS29 may be a transcriptional regulator of VPE genes.

1.3 Aim of the dissertation

Barley grain development depends on both, growth and cellular disintegration. One of the major players in cellular disintegration is programmed cell death (PCD). PCD is known to play a role in cellular degeneration of the starchy endosperm and in germination, but the molecular events driving PCD in maternal grain tissues are barely understood.

Developing barley grains exhibit different caspase-like activities. Vacuolar processing enzymes (VPEs) have been shown to exhibit enzymatic properties similar to caspase-1 that mediate PCD pathway in animals. However, the genes encoding proteases with the respective caspase-like activity have not been described so far in barley, and there are many other components involved in the plant PCD model that are still less understood.

Barley *VPE4* is probably involved in PCD of the barley pericarp. *VPE4* is weakly similar to *Arabidopsis* *δVPE*, which is exclusively expressed in the deteriorating pericarp and associated with apoptotic DNA degradation. *HvVPE2α*, which is also known as nucellain, is localized in the nucellar projection that degenerates in developing barley grains. Less information at the genetic, molecular and biochemical level is presented for the two genes/enzymes. Regulatory mechanism and physiology studies associating expression and activity of the enzymes with developmental processes in the maternal part of developing barley grains are missing so far.

The general aim of this study is a detailed analysis of seed-specific barley VPEs to elucidate their role in PCD in maternal tissues of the developing barley grain.

The detailed objectives of this study are as follows:

1. Study on temporal and spatial PCD patterns during whole barley grain development and analysis of caspase-like activities in the developing barley seed. Confirmation of the supposed caspase-like activity of the barley VPEs.
2. Generation of transgenic barley plants using RNAi-mediated down-regulation of *VPE4* and *VPE2α* expression in pericarp and nucellus tissue, respectively, of developing barley grains.
3. Analysis of phenotypic changes in transgenic seeds.

4. Proof of tissue-specific VPE repression and investigation of differentiation and storage product accumulation in maternal and endosperm tissue of developing barley grains.
5. Analysis of interactions between DNA and recombinant proteins in binding studies of the barley B_{sister} clade TF MADS29 with promoter regions of the genes required for PCD in nucellar tissues of developing barley grains.

2. Material and methods

2.1 Material

2.1.1 Plant material

Two-rowed spring cultivars Barke and Golden Promise of barley (*Hordeum vulgare* L.) were obtained from Genebank department (IPK, Gatersleben, Germany) and used throughout this study as wild types. Golden Promise was used for plant transformation and all transgenic plants were produced in this background.

2.1.2 Bacterial strains and plasmids

Cells of *Escherichia coli* strain DH5 α were used for general molecular biological cloning procedures. *E. coli* BL21 cells were used for recombinant protein production. *Agrobacterium tumefaciens* cells of the strain EHA105 were used for plant transformation. Descriptions of the bacterial strains are given in Table 1.

Table 2.1. Bacterial strains.

Strain	Genotype description	Task	Reference or source
<i>Escherichia coli</i> DH5 α	F ⁻ ϕ 80 <i>lacZ</i> Δ M15 Δ (<i>lacZYA-argF</i>)U169 <i>recA1 endA1 hsdR17</i> (r _k ⁻ m _k ⁺) <i>phoA supE44, thi-1 gyrA96 relA1</i> λ -	General DNA (sub)-cloning	Grant <i>et al.</i> , 1990
<i>Escherichia coli</i> BL21(DE3)	<i>fhuA2 [lon] ompT gal</i> (λ DE3) [<i>dcm</i>] Δ <i>hsdS</i> λ DE3= λ <i>sBamHlo</i> Δ <i>EcoRI-B int::(lacI:: PlacUV5::T7 gene1) i21</i> Δ <i>nin5</i>	protein expression	Novagen, Germany
<i>Agrobacterium tumefaciens</i> EHA105	C58 pTiBo542; T-region:: <i>aph</i> , A281 Km ^(S)	plant transformation	Hood <i>et al.</i> , 1993

Table 2.2. Basic plasmids and vectors.

pGEM [®] -T easy	Amp ^r (Promega, USA)
pET32a(+)	Amp ^r (Novogen, Australia)
pAXi (pNOS-AB-M)	Intermediated vector, Amp ^r (DNA cloning service, Germany)
p6U	Binary vector, Spec ^r (DNA cloning service, Germany)

2.1.3 Oligonucleotides

The oligonucleotides for PCR and qRT-PCR were designed using PrimerSelect software (DNASTar Lasergen12 Core Suite) and Primer3 software (v0.4.0; <http://frodo.wi.mit.edu/primer3>). Oligonucleotides were purchased from Metabion (Munich, Germany). Oligonucleotide sequences are listed in the Supplemental Tables S1-S3.

2.1.4 Enzymes, reaction kits and chemicals

Amersham, Germany	[γ 32P]dCTP, nylon membrane Hybond-N+
Applied Biosystems	SYBR-Green-PCR master mix
Bio-Rad, Germany	Bio-Rad protein assay reagent
BioRad, USA	Bradford assay
Enzo Life Science GmbH, Germany	Caspase substrates: caspase-1 substrate (Ac-YVAD-AMC), caspase-3 substrate (Ac-DEVD-AMC); caspase-4 substrate (Ac-LEVD-AMD); caspase-6 substrate (Ac-VEID-AMC); caspase-8 substrate (Ac-IETD-AMD); caspase-9 substrate (Ac-LEHD-AMC) Protease inhibitors: Ac-YVAD-CHO to suppress caspase-1 activity; Ac-DEVD-CHO to suppress caspase-3 activity; Ac-LEVD-CHO to suppress caspase-4 activity; Ac-VEID-CHO to suppress caspase-6 activity; Ac-IETD-CHO to suppress caspase-8 activity and Ac-LEHD-CHO to suppress caspase-9 activity
Fermentas, Lithuania	GeneRuler™ DNA Ladder, PageRuler™ pre-stained protein ladder mix, Rapid DNA Ligation Kit, restriction enzymes, dNTPs
GE Healthcare Life Science, UK	Amersham Rediprime III DNA Labeling System, ECL™ Western blotting detection reagents
Gibco BRL, Germany	Coomassie Brilliant Blue
Invitrogen, Germany	Superscript III, TA-cloning kit
Machery-Nagel GmbH, Germany	NucleoSpin® Gel and PCR Clean-up
Merck, Germany	Ethidium bromide, benzamidine, DTT, formamide, iodine, magnesium chloride, MOPS, potassium iodide, sodium acetate, sodium chloride, sodium hydroxide, sodium hypochloride, sodium phosphate, sucrose, Tris, imidazol

Promega, USA	Go Tag® DNA Polymerase
Qiagen, Germany	Plasmid Isolation Kit, QIAquick PCR Purification Kit, RNA Isolation Kit, RNase-free DNase Set, Ni-NTA-agarose
Roche, Germany	Tag DNA polymerase, glucose-6-phosphate-dehydro-genase, hexokinase, phosphoglucose isomerase, NAD and adenosine-5'-triphosphate disodium salt (ATP), amyloglucosidase
Roth, Germany	Acetic acid, ethanol, chloroform, phenol, isopropanol, glycine, glycerol, acetone, formaldehyde (37%), HCl2, and other chemicals
Serva, Germany	Albumin fraction V (BSA), Tween 20, EDTA
Sigma-Aldrich, USA	4-Nitrophenyl phosphate disodium salt hexahydrate, IPTG, DMSO, 3-[(3-Cholamidopropyl) dimethylammonio]-1-propanol sulfonate hydrate, HEPES, invertase from baker's yeast
ThermoFisher Scientific, USA	Trizol® Reagent, Nunc streptavidin plate C8 transparent, F16 black maxisorp fluoronunc cert plate

2.1.5 Special instruments

Agilent, USA	Bioanalyzer
Applied Biosystems, USA	ABI Prism 7900HT Sequence Detection System
Bio-Rad Laboratories, USA	Mini PROTEAN II™ for protein gel electrophoresis; Mini Tran-Blot® electrophoresis transfer cell
Eppendorf, Germany	PCR Thermocycler for PCR amplification of DNA
Goebel Instrumentelle Analytic, Germany	Spectrophotometer UVIKON
GTA Sensorik GmbH	Marvin for seed weight and size analysis
Infinite M200 PRO TECAN, Austria	Binding study in ELISA
Molecular Devices, USA	Spectra Max Gemini spectrofluorometer for enzyme assay
Peqlab, Germany	Nanodrop for measurement DNA, RNA and protein concentrations

2.1.6 Bacterial media

LB: 10 g NaCl, 5 g tryptone, 5 g yeast extract for 1 L (pH 7.4 – 8.0)

SOC: 0.58 g NaCl, 0.186 g KCl, 10 mM MgCl₂, 20 g tryptone, 5 g yeast extract, 20 mM glucose for 1L (pH 7.4-8.0)

The solidified media contain 1.5% Difco-agar.

2.1.7 Protein extraction buffer for caspase assay

2x Protein extraction buffer (2xCASPB):

100 mM HEPES (4-(2-hydroxyethyl)-1-piperazineethanesulfonic acid); 0.2% CHAPS (3-[(3-Cholamidopropyl) dimethylammonio]-1-propanesulfonate); 10 mM DTT; pH 7.0

2.1.8 Antibiotics

All antibiotics were prepared in deionized H₂O and sterilized using a syringe filter (0.20 µm CA membrane, Heinemann Labortechnik GmbH, Germany). Concentrations of stock and working solutions are listed in Table 3.

Table 2.3. List of antibiotics

Antibiotics	Stock concentration	Working concentration	Company
Ampicillin (Amp)	50 g l ⁻¹	100 mg l ⁻¹	Duchefa, The Netherland
Spectinomycin (Spec)	50 g l ⁻¹	500 mg l ⁻¹	Duchefa, The Netherland

2.1.9 Antibodies used for Western blot and ELISA

Table 2.4. List of Antibodies and producers

Antibody	Characteristics and Origin
Mouse monoclonal anti-polyHistidine antibody	Monoclonal primary antibodies, Sigma-Aldrich, USA
Rabbit anti-mouse IgG (whole molecule)-peroxidase antibody	Secondary antibodies, Sigma-Aldrich, USA
Rabbit anti-mouse IgG alkaline phosphatase conjugate	Polyclonal secondary antibodies, Sigma-Aldrich, USA

2.1.10 Buffers for Western blot and ELISA

4x Marvel buffer (4x TBS buffer):

80 mM Tris-HCl, 720 mM NaCl, adjusted to pH 7.8

Transfer buffer:

10% methanol (v/v), 24 mM Tris, 194 mM Glycine

SDS-PAGE running buffer:

125 mM Tris-HCl, 960 mM Glycine, 0.5% SDS, adjusted to pH 8.3

2x SDS sample buffer:

100 mM Tris-HCl, 4% SDS, 0.2% (w/v) Bromophenolblue, 20% (v/v) Glycerol, adjusted to pH 8.3

0.1 M PBS buffer:

0.22 g/l NaH_2PO_4 , 1.33 g/l Na_2HPO_4 , 8.5 g/l NaCl, adjusted to pH 7.4

TES buffer:

10 mM Tris-HCl pH 7.4, 300 mM NaCl

TBS buffer:

20 mM Tris pH 7.4, 150 mM NaCl

TBS-Tween buffer:

TBS+0.1% Tween20, 1% BSA-TBS-Tween20

Diethanolamine-HCl buffer:

97 ml Diethanolamine, 0.1 g MgCl_2 , 0.2 g/ NaN_3 , adjusted to pH 9.8

2.1.11 Buffers for starch, sugar and storage protein measurements

Extraction buffer for starch and sugars:

80 % Ethanol

Sugar measurement buffer:

100 mM Imidazol pH 6.9, 5 mM $\text{MgCl}_2 \cdot 6\text{H}_2\text{O}$, 2 mM NAD, 1 mM ATP

Storage protein extraction buffer:

Buffer 1: 400 mM NaCl, 60 mM KH_2PO_4

Buffer 2: 400 mM NaCl, 65 mM $\text{Na}_2\text{HPO}_4 \cdot 2\text{H}_2\text{O}$

Storage protein measurement buffer:

BCA-assay (Pierce) kit, 25 ml reagent A, 500 μl reagent B

2.2 Methods

2.2.1 Plant cultivation conditions and tissue preparation

Plants were grown in pots under standard greenhouse conditions at 18°C with 16/8 h of light/dark regime. Determination of developmental stages for developing barley seeds and tissue isolation were performed as described (Weschke *et al.*, 2000). Days after flowering (DAF) were defined by determining anthesis on a spikelet in the center of the spikes. Only five grains from each row corresponding to this region were used in all the studies presented. Grain tissue samples were collected based on grain development stages in two or four-day interval. If necessary, caryopses were manually separated into the pericarp and endosperm fractions under a microscope and snap-frozen in liquid nitrogen.

2.2.2 Tissue preparation for laser micro-dissection and pressure catapulting

For laser micro-dissection and pressure catapulting (LMPC) of tissues, frozen caryopses were transferred to a cryostat and kept at -20°C. Using a razor blade, the middle part of the caryopsis was cut out and glued onto the sample plate by using OCT compound. Sections of 20 µm thickness were cut and immediately mounted on PEN membrane slides (Zeiss, Germany). PEN membrane slides were stored for 7 days in the cryostat at -20°C until complete dryness. Prior to laser-assisted micro-dissection, dry cryo-sections were adapted to room temperature (RT) for several minutes. LMPC procedure for isolation of specific grain tissues using the PALMH MicroBeam laser system (Zeiss, Germany) has been performed as previously described (Thiel *et al.*, 2008).

2.2.3 Sequence isolation and identification of genes

The full-length *VPE4* (Genbank accession number FR696366) and partial *VPE2a* (Genbank accession number FR696361) cDNA sequences used in the study were described earlier (Radchuk *et al.*, 2011). The corresponding cDNA clones were introduced into pGEM-T easy plasmid (Promega, USA), re-sequenced and used in the present work as sources for DNA fragments for Southern and Northern blots as well as for preparation of genetic constructs. To identify full-length genome sequences of both *VPE4* and *VPE2a* genes together with their promoter regions, cDNA sequences of either *VPE4* or *VPE2a* were blasted using BLASTN

against the barley genome sequence (International Barley Genome Sequencing Consortium, 2012). The screening with *VPE4* cDNA resulted in the genome clone Morex_cn60679 that comprised whole exon-intron fragments as well as the putative promoter region 5' upstream of ATG start codon. The screening of barley full genome sequence with partial *VPE2a* cDNA resulted in two partially overlapping clones: HVVMRXALLhA0751I05_v23_c3 and morex_cn245248.

Because the full-length cDNA of the *VPE2a* gene was not fully cloned, the genomic *VPE2a* fragment was used to predict the putative start codon and the potential 5' untranslated region in order to clone the full-length *VPE2a* cDNA. To perform this, the HVVMRXALLhA0751I05_v23_c3 and morex_cn245248 genome sequences were aligned with full-length cDNAs of *VPE2b*, *VPE2c* and *VPE2d* genes. The described fragment of *VPE2a* cDNA shares among 83.4% and 95.0% identity to the *VPE2b*-*VPE2d* cDNAs. The resulting alignment defined the potential transcriptional start for *VPE2a* cDNA. The primers in 5' and 3' untranslated regions of the deducted *VPE2a* cDNA were designed (primers are listed in the Supplemental Table S1) and the corresponding cDNA for the *VPE2a* gene was PCR amplified from the reverse-transcribed mRNA derived from young barley caryopses. The amplified fragment was cloned into pGEM-T easy vector and sequenced. The resulting cDNA sequence was fully identical to the sequence predicted from the full length genome sequence.

To clone the barley *MADS29* gene, a BLAST search based on the *OsMADS29* (LOC_Os02g07430) sequence as query was used to identify the *MADS29* cDNA from a barley full length cDNA library (Matsumoto *et al.*, 2011) and its related genomic sequence from the barley genome sequence (International Barley Genome Sequencing Consortium, 2012). The primer pair in the 5' and 3' untranslated region of the *MADS29* cDNA was designed (primers are listed in the Supplemental Table S1) and the corresponding *MADS29* cDNA was amplified from the reverse-transcribed mRNA derived from young barley caryopses. The resulting DNA fragment was cloned into pGEM-T easy vector and sequenced.

All sequence data were processed using Lasergene software (DNASTar, USA), and phylogenies were constructed using ClustalW software (DNASTar, USA). Exon-intron structure of the genes was determined manually by aligning of the cDNA sequence to the corresponding genome fragment and taking into account GT/AG intron boarding nucleotides.

2.2.4 Basic cloning methods

The basic molecular cloning methods such as DNA fragment amplifications, DNA enzymatic digestions and DNA electrophoreses were performed according to the standard protocols (Sambrook and Russell, 2001). DNA fragments were isolated and purified from agarose gel by NucleoSpin® Gel and PCR clean-up kits. Plasmid extractions were done using Qiagen Plasmid kit according to the manufactures' protocol. Transformation of *E. coli* cells was performed using heat-shock procedure (Cohen *et al.*, 1972).

2.2.5 Genomic DNA extraction

The genomic barley DNA was extracted following the protocol as previously described (Palotta *et al.* 2000). Leaf tissue (100-200 mg) was collected, homogenized in liquid N₂, incubated with 800 µl of extraction buffer (100 mM Tris-HCl, 10 mM EDTA, 100 mM NaCl and 1% N-lauroylsarcosin, pH 8.0) for 5 min at RT. Subsequently, 800 µl of Phenol/Chloroform/Isoamylalcohol (25:24:1) mix was added and the sample was vortexed for 2 min. The sample was centrifuged at 5,300 g for 3 min at RT. The obtained supernatant (approx. 700 µl) was transferred to fresh Eppendorf tube and incubated on ice for 15 min after addition of one volume of isopropanol (700 µl) and 1/10 (70 µl) volume of 3 M sodium acetate, pH 5.2. DNA was precipitated by centrifugation at 13,000 g for 10 min at 4°C. The DNA pellet was washed in 70% ethanol and centrifuged at 8,000 g for 10 min at 4°C. The pellet was air-dried to remove any traces of alcohol, re-suspended in 50 µl of water and kept overnight in refrigerator at 4°C. RNA was removed by adding 2 µl of RNase (40 µg/ml) and incubating for 30 min at 37°C. DNA was then quantified using Nanodrop.

2.2.6 RNA isolation

Total RNA was isolated either from whole caryopses or separated tissues using Trizol® reagent and cleaned by RNeasy® Plant Mini kit columns (Qiagen, Germany) as follows. The sample (~100 mg) was grinded in liquid nitrogen to a homogenous powder. 1 ml Trizol was added, incubated at 60°C for 5 min, centrifuged at 13,000 g for 10 min at 4°C and the supernatant was transferred to a new tube. 200 µl of chloroform was added and the probe was incubated at room temperature for 2–3 min. The sample was centrifuged at 13,000 g for 10 min at 4°C. The aqueous phase (600 µl) was transferred to a new Eppendorf tube. For

precipitation, 360 μ l of isopropanol and 60 μ l of 3 M sodium acetate (pH 5.2) were added, mixed well with the aqueous phase and incubated for 5 min at RT. The sample was again centrifuged as described above. The pellet was washed with 1 ml of 70% cold ethanol and centrifuged at 13,000 g for 5 min at 4⁰C and briefly dried for 5 min. The pellet containing total RNA was dissolved in 50 μ l of deionized water. For RNA cleaning, 350 μ l of RLT buffer (Qiagen, Germany) with 0.01% β -mercaptoethanol and 250 μ l of absolute ethanol were added to the dissolved RNA, mixed well, transferred into the RNeasy[®] Plant Mini columns (Qiagen, Germany) and centrifuged for 30 sec at 13,000 g. DNase digestion was done in-column using RNase-free DNase set (Qiagen, Germany) following the manufacturer's protocol. After DNA digestion, columns were washed three times with washing buffers from RNeasy[®] Plant Mini kit (Qiagen, Germany) and total RNA was eluted by 50 μ l of RNase-free deionized water. RNA concentration was measured using the NanoDrop photometer according to the manufacturer's instructions.

Total RNA from micro-dissected tissues was isolated essentially as previously described (Thiel *et al.* 2008). Shortly, for each sample RNA was extracted from 30 to 50 sections of isolated tissues (see subchapter 2.2.2) using the Absolutely RNA Nanoprep Kit (Invitrogen, USA). Total RNA was amplified by one round of T7-based mRNA amplification using the MessageAmp aRNA Kit (Ambion, USA) to generate tissue-specific antisense RNA (aRNA). After quality assessment of aRNA populations, first strand of cDNA was synthesized using SuperScript III (Invitrogen, USA) with random priming according to the manufacturer's instructions.

2.2.7. Southern and Northern blot hybridization analyses

For Southern blot hybridization, genomic DNA (10 μ g) was digested overnight at 37°C with appropriate restriction enzyme(s) (100 U) in 40 μ l reaction volume consisting of 1x restriction buffer (4 μ l of 10x buffer) and 4 μ l of 40 mM spermidin. The digested DNA was separated by gel electrophoresis for 4 h (90 V) in 1 x TAE buffer supplemented with 1% agarose. After electrophoresis, the gel was treated with 0.25 M HCl solution for 5 min, incubated with 1.5 M NaCl/0.5 M NaOH solution two times for 15 min on a shaker and washed with 0.5 M Tris-HCl/3 M NaCl solution two times for 15 min. The DNA was transferred from the treated gel to Hybond N+ membrane by capillary transfer in presence of 0.4 M NaOH, dried, treated

with UV light for 3 min and hybridized with radioactively P³²-dCTP labeled cDNA fragments. Labelling was performed by using the RediPrime™ II Labeling System (GE Healthcare, UK). The hybridization was carried out in Church buffer (250 mM sodium phosphate, 7% SDS, 1% BSA) (Church and Gilbert, 1984) at 65⁰C according to the procedure described by Sambrook and Russel (2001).

For Northern blot hybridization analysis, 10 µg of total RNA was separated on 1% formaldehyde-agarose gel in 1x MOPS buffer (0.02 M MOPS, 5 mM sodium acetate, 1 mM EDTA, pH 7.0). The gel was washed twice in 1x SSPE buffer (0.36 M NaCl, 20 mM sodium phosphate, 2 mM EDTA, and pH 7.7) for 15 min each time and RNA was blotted on nylon membrane Hybond N+ using 20x SSPE buffer. The hybridization was done exactly as described for Southern blotting.

2.2.8 Polymerase chain reaction (PCR)

All PCR reactions were done in a Thermocycler machine (Eppendorf, Germany). PCR products were separated on 0.8-1.5% agarose gels by electrophoresis (30-45 min at 100 V) in 1x TAE buffer (40 mM Tris, 20 mM acetic acid, 2 mM EDTA, pH 8.0). Gels were stained with ethidium bromide (0.0015 mg/ml), and DNA was visualized with an UV transilluminator (PEQLAB Biotechnology GmbH, Germany).

The standard PCR reactions were carried out in a volume of 25 µl and contained:

5.0 µl of GoTaq polymerase buffer (5x), 2 mM MgCl₂, 250 µM dNTPs, 1 µl of each primer (10 pM), 2.5 U of Taq polymerase, 100-200 ng of genomic DNA, add ddH₂O

For the PCR a reaction following protocol was used:

	Cycles	Time	Temp
Initial Denaturation	1	3 minutes	95°C
Denaturation	35	30 seconds	95°C
Annealing		40 seconds	56 - 60°C
Elongation		0.5 - 1 minute	72°C
Final Elongation	1	7 minutes	72°C
Cooling	indefinitely		4°C

2.2.9 Quantitative reverse transcription-polymerase chain reaction

Quantitative reverse transcription-polymerase chain reaction (qRT-PCR) was used to quantify gene expression in micro-dissected tissues. The reverse transcription was performed from RNA of micro-dissected tissues (subchapter 2.2.6) using the SuperScript III (Invitrogen, USA). 5 µg of total RNA, 1 µl of 50 µM oligo-dT primer and 1 µl of 10 mM dNTP mix and water were added to each tube to obtain a total volume of 10 µl and the reaction mixture was incubated at 65°C for 5 min, and then rapidly cooled on ice. 10 µl of cDNA master mix consisting of 2 µl of 10x RT buffer, 4 µl of 25 mM MgCl₂, 2 µl of 0.1 M DTT, 1 µl of RNase OUT (40 units/µl) and SuperScript III reverse transcriptase (200 units/µl) were added and incubated for 50 min at 50°C. The reaction was terminated by incubation at 85°C for 5 min and chilled on ice. 1 µl of RNase H was added to each reaction tube and incubated for 20 min at 37°C to remove RNA. The synthesized cDNA was stored at -20°C for further use. Power SYBR Green PCR master mix (ThermoFisher Scientific, USA) was used to perform reactions in an ABI7900HT Real-Time PCR system (Applied Biosystems, USA). Data were analyzed using SDS2.2.1 software (Applied Biosystems, USA). Three replications were conducted for each transcript. The *actin* cDNA of *Hordeum vulgare* (Genbank acc. nr. AY145451) was used as an internal standard. The data were analyzed by ANOVA followed by a posthoc-test using Microsoft Excel with Daniel's XL toolbox version 6.10 by Kraus (2014). The highest relative expression in the group of genes was taken to 100% and expression of the other genes and stages was recalculated to that value. Primers used for qRT-PCR are listed in Supplemental Table S2.

2.2.10 Protein extraction for caspase-like assays

The whole caryopses or hand-separated pericarp and endosperm tissues of wild type and transgenic plants were finely ground in liquid nitrogen and 200 mg of tissues were re-suspended in 2x CASPB buffer (100 mM HEPES, 0.1% CHAPS, 1 M DTT, pH 7.0) at 4°C. Cell debris was separated by centrifugation at 13,000 g for 10 min at 4°C and the supernatant was used for the reactions or stored at -80°C. Protein concentrations were determined by Bradford assay (BioRad, USA) using a linear concentration range of bovine serum albumin as a standard.

2.2.11 Caspase-like assay

Caspase-like activities were measured in 150 µl reaction mixtures containing 25 µg of protein sample and 10 µM of caspase substrate. Caspase-like activities were detected using the following substrates: acetyl-Tyr-Val-Ala-Asp-7-amido-4-methyl coumarin (Ac-YVAD-AMC) for caspase-1 activity; acetyl-Asp-Glu-Val-Asp-7-amido-4-methyl coumarin (Ac-DEVD-AMC) for caspase-3 activity; acetyl-Leu-Glu-Val-Asp-7-amido-4-methyl coumarin (Ac-LEVD-AMD) for caspase-4 activity; acetyl-Val-Glu-Ile-Asp-7-amido-4-methyl coumarin (Ac-VEID-AMC) for caspase-6 activity; acetyl-Ile-Glu-Thr-Asp-7-amido-4-methyl coumarin (Ac-IETD-AMD) for caspase-8 activity; and acetyl-Leu-Glu-His-Asp-7-amido-4-methyl coumarin (Ac-LEHD-AMC) for caspase-9 activity. Emitted fluorescence was measured after 20 minutes or one hour incubation at RT with a 360 nm excitation wave length filter and 460 nm emission wave length filter in a spectrofluorometer (Spectra Max Gemini, Molecular Devices, USA). Four repetitions were performed for determination of each value and standard deviations were calculated. The system was calibrated with known amounts of AMC hydrolysis product in a standard reaction mixture. Blanks were used to account for the spontaneous breakdown of the substrates. The caspase fluorometric assay is based on the hydrolysis of the peptide substrate acetyl, resulting in the release of the fluorescent 7-amino-4-methylcoumarin (AMC) moiety. The data were analyzed by one-way analysis of variance (ANOVA) followed by a posthoc-test after Holm-Sidak using Microsoft Excel version 2010, with Daniel's XL toolbox version 6.10 and Student's *t* test. To check the specificity of the caspase assays, the specific protease inhibitors were used to suppress the respective caspase-like activity. The following inhibitors were used: Ac-YVAD-CHO to suppress caspase-1 activity, Ac-DEVD-CHO to suppress caspase-3 activity, Ac-LEVD-CHO to suppress caspase-4 activity, Ac-VEID-CHO to suppress caspase-6 activity, Ac-IETD-CHO to suppress caspase-8 activity and Ac-LEHD-CHO to suppress caspase-9 activity. All caspase substrate and inhibitors were purchased from Enzo Life Sciences (Germany). Assays were performed as described above with the addition of the respective inhibitors (20 µM) to the reaction mixture.

2.2.12 Histological studies

For histological studies, caryopses were fixed overnight in 4% paraformaldehyde, 10 mM dithiothreitol (DTT) in PBS or 0.025 M phosphate buffer, pH 7.0. After fixation, caryopses

were washed in PBS containing 10 mM DTT and dehydrated in an ethanol series containing 10 mM DTT. Samples were passed through a graded ethanol-methacrylate series as described in Baskin *et al.* (1992) and polymerised for at least 48 h in UV light at -20°C . Using a Leica RM 2165 microtome, the 3–5 μm sections were cut. The sections were stained with toluidine blue and examined in bright field using either a Zeiss Axioskop or a Nikon E 600 microscope.

2.2.13 TUNEL assay

In situ detection of DNA fragmentation was carried out with the TUNEL method following the protocol of the *In Situ* Cell Death Detection kit (Roche Diagnostics, Germany) essentially as described. Grain sections, prepared as above described, were de-waxed, rehydrated and treated with $2\ \mu\text{g ml}^{-1}$ proteinase K for 30 min at 37°C followed by incubation in a mixture of fluorescein labelled deoxynucleotides and TdT (TUNEL mix) for 60 min at 37°C . The fluorescein fluorescence of nuclei with fragmented DNA was observed using a microscope with blue light excitation.

For negative control, TdT was omitted in the reaction. For positive control of the reaction, the sections were treated with DNase ($1500\ \text{U ml}^{-1}$) prior to performing labelling with the TUNEL mix. Both negative and positive controls were performed only at 10 DAF.

2.2.14 Preparation of VPE4i and VPE2i constructs for plant transformation

The VPE4i construct was prepared in the shuttle pAXi vector. The pAXi vector is a modified form of pNos-AB-M plasmid that already contains 253 nucleotides of the first intron of potato (*Solanum tuberosum*) GA20 oxidase gene and the *nopaline synthase* (*nos*) terminator. First, the antisense fragment of VPE4 was amplified using PCR with primers introducing *Spe* I and *Xho* I restriction sites at one and the other end of the fragment (primer sequences are listed in the Supplemental Table S3). The amplified fragment was digested with the *Spe* I/*Xho* I restriction enzymes and cloned into the pAXi vector using the corresponding restriction sites to become pAX-as construct. Similarly, the sense VPE4 fragment was amplified with the primers introducing *Sal* I and *Bam* HI restriction sites at the flanking positions, digested with *Sal* I and *Bam* HI enzymes and cloned into the pAXi-as vector between the corresponding restriction sites to become pAX-sas vector. The VPE4 promoter was PCR-amplified using

primer introducing *Pst* I and *Stu* I at the end of the fragment, digested with these enzymes and cloned into the pAX-sas vector using the same restriction sites. Afterwards, the whole RNAi cassette of *VPE4* was introduced into the p6U binary vector (DNA cloning service, Hamburg, Germany) by digestion the shuttle vector with *Sfi* I restriction enzyme and cloning into the corresponding site of the binary vector p6U resulting in the vector for plant transformation called pVPE4i (Fig. 2.1). The VPE4i cassette was sequenced by Agowa (Germany) to prove the correctness of the sequences and DNA fragment orientation.

As in case of the pVPE4i construct, the shuttle pAXi vector has been used for preparation of pVPE2i construct. The antisense fragment of *VPE2a* was PCR-amplified using primers introducing *Spe* I and *Pst* I restriction sites at both ends of the fragment, digested with the *Spe* I/*Pst* I restriction enzymes and cloned into pAXi vector into the corresponding restriction sites. The sense *VPE2a* fragment was amplified with the primers introducing *Sal* I and *Bam* HI restriction sites at flanking positions, digested with *Sal* I and *Bam* HI enzymes, and cloned into pAXi-as vector between the corresponding restriction sites. The *VPE2a* promoter was PCR-amplified using primers introducing *Pst* I and *Stu* I at the end of the fragment, digested with these enzymes and cloned into pAX-sas vector using the same restriction sites. Afterwards, the whole VPE2i RNAi cassette was introduced into the p6U binary vector by restriction the shuttle vector with *Sfi* I restriction enzyme and cloned into the corresponding site to get the vector for plant transformation called pVPE2i (Fig. 2.2). Again, the VPE2i cassette was sequenced. Primer sequences used for amplification of fragments for VPE2i preparation are listed in the Supplemental Table S1. The pVPE4i and pVPE2i constructs were subsequently transformed into *Agrobacterium tumefaciens*, EHA105 strain, for barley plant transformation.

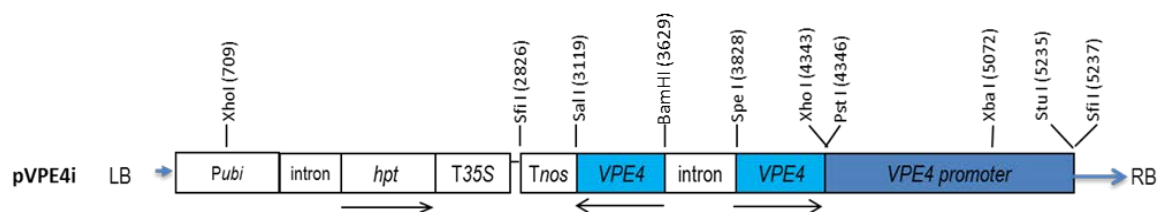


Figure 2.1 Scheme of the T-DNA region of the binary construct pVPE4i used for RNAi-mediated inhibition of VPE4 gene expression under control of the gene's own promoter. Abbreviations: *hpt*, hygromycin phosphotransferase gene; intron, the first intron of *GA20 oxidase* gene from potato (*Solanum tuberosum*); LB, left border; *Pubi*, ubiquitin 1 gene promoter from maize; T35S, terminator of the *CaMV 35S* gene, *Tnos*, *nopaline synthase* gene terminator, RB, right border.

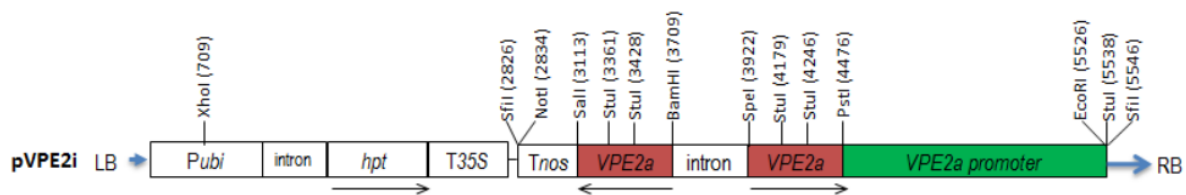


Figure 2.2. Schematic representation of T-DNA region of the construct pVPE2i used for RNAi-mediated inhibition of VPE2a-VPE2d gene expression under control of the VPE2a gene promoter. Abbreviations: *hpt*, *hygromycin phosphotransferase* gene; intron, the first intron of *GA20 oxidase* gene from potato (*Solanum tuberosum*); LB, left border; *Pubi*, ubiquitin 1 gene promoter from maize; T35S, terminator of the *CaMV 35S* gene, *Tnos*, *nopaline synthase* gene terminator, RB, right border.

2.2.15 Stable transformation of barley plants

The transformation of barley plants was done in the group Plant Reproductive Biology (IPK) using the method developed in that group (Hensel *et al.*, 2009).

2.2.16 Extraction and determination of soluble sugars, starch, storage proteins, total carbon and nitrogen

For measurements of starch, sugar, protein, total carbon (C) and total nitrogen (N), at least six biological replicates were analysed. Total carbon and nitrogen in dried barley flour were determined with the Vario EL Elementar analyzer (Elementar Analysensysteme GmbH, Germany). Starch was measured as described (Weschke *et al.*, 2000). NADH which generated during the conversion of glucose-6-phosphate to 6-phosphogluconate is used to measure starch and sugars in developing seeds. Around 10 to 20 mg of powdered seeds was incubated in 80% ethanol at 60°C for 30 min with continuous shaking at 500 rpm in thermomixer. The sample was centrifuged at 13,000 g for 10 min and the pellet was re-washed following the same protocol. The pellet was dissolved in 1.5 ml of 2 N HCl and incubated for 1 h at 95°C (Kozloski *et al.*, 1999). Supernatant obtained after centrifugation (13.000 g for 5 min) was used for glucose estimation and the hydrolyzed product of starch. Around 5-10 µl of supernatant was incubated with 750 µl imidazole buffer (2 mM NAD and 1 mM ATP, pH 6.9) and 2 µl of glucose-6-phosphate dehydrogenase (2 units) at RT and initial absorbance is recorded immediately at 340 nm to measure NADH. Absorbance at 340 nm is recorded after incubation with 10 µl of hexokinase (8 units) for 25 min. The difference in the

absorbance for the NADH is proportional to the total amount of glucose formed by the hydrolysis of starch.

For measurement of sucrose, 20 mg of dried and powdered seeds were incubated in 80% ethanol at 60°C for 30 min with continuous shaking at 500 rpm in thermomixer. The sample was centrifuged at 13,000 g for 10 min and the pellet was re-washed following the same protocol for at least two times. Residual ethanol was removed from the supernatant by centrifugation in a SpeedVac at RT. Then the supernatant was diluted in 500 µl of ddH₂O to measure sugar content. For sucrose measurement, 20 µl of obtained supernatant were incubated for 10 min with 750 µl of imidazole buffer (100 mM imidazole, pH 6.9; 5 mM MgCl₂ 6H₂O, 2 mM NAD and 1 mM ATP), 2 µl glucose-6-phosphate dehydrogenase and 5 µl hexokinase at RT. Afterward, the sample was mixed well with 10 µl of invertase, incubated for 30 min at RT and initial absorbance was recorded at 340 nm to measure sucrose by a spectrophotometer (Spectrophotometer UVIKON). Glucose and fructose were measured as follows: 20 µl of obtained sample were incubated with 750 µl imidazole buffer (2 mM NAD and 1 mM ATP, pH 6.9), 2 µl of glucose-6-phosphate dehydrogenase for 10 min at RT.

For measurement of storage proteins, albumin/globulin and gliadin fractions were sequentially extracted. Seeds were ground into fine powder and dried out overnight at 70°C. Then, 20 mg of the powder were mixed with 1.5 ml storage protein extraction buffer and shaken for 25 min. The samples were centrifuged for 15 min at 20°C and supernatant was collected. The initial absorbance of the supernatant was recorded immediately at 562 nm to measure gliadin fraction in a spectrophotometer (Spectrophotometer UVIKON). To measure albumin/globulin fraction, 50 µl supernatant were mixed with 1 ml storage protein measurement buffer and incubated for 30 min at 37°C in a thermomixer and then initial absorbance was recorded immediately at 562 nm.

2.2.15 Production of the recombinant MADS29 protein

The *MADS29* coding region was PCR-amplified from cDNA introducing the *Bam* HI and *Hind* III restriction sites at both ends of the coding sequence (Primers used are listed in Supplemental Table S3). The resulting amplicon was digested with *Bam* HI/*Hind* III enzymes and introduced into the pET-32a(+) vector (Novagen, USA). The derived construct was transferred into *E. coli* BL21 cells. The cell culture was grown overnight at 37°C. The bacterial

cells were disrupted by sonication and centrifuged at 10,000 g at 4°C for 30 min. The recombinant MADS29 protein was purified from the supernatant using Ni-NTA resin (Qiagen, Germany) by His-tag.

2.2.16 Western blot analysis

Isolated proteins from different fractions of the *E. coli* culture were separated by SDS-PAGE and transferred to nitrocellulose. Commercial anti poly-histidine and anti-mouse IgG peroxidase antibody conjugates (Sigma, USA) were used for the identification of the recombinant MADS29 protein.

2.2.17 Analysis of the CARG cis-elements present in the *Jekyll* and *VPE2a* promoters by ELISA

Putative CARG-like sequences harbored by the *Jekyll* and *VPE2a* promoters were identified in the regions 1,000 nt upstream from the start codon of each gene. Double-stranded oligonucleotide fragments of 32-42 nt in length, with and without a CARG-like motif, respectively, were then analyzed by an ELISA-type binding assay following the procedure published by Mönke *et al.* (2004). Pairs of base complementary single-stranded oligonucleotides were obtained from Metabion (Germany). The oligonucleotide sequences are given in Supplemental Table S2. The sense strands were labelled at the 5' end with biotin by manufacturer (Metabion, Germany). Double-stranded DNAs were generated by dissolving two complementary oligonucleotides (1 nM of each) in 10 mM Tris-HCl, 1 mM EDTA, 300 mM NaCl, holding the reaction at 95°C for 5 min followed by slowly cooling down to RT. A 100 µL aliquot of a 0.01 pmol µl⁻¹ solution of double-stranded biotinylated DNA fragment (dissolved in TBS-T) was introduced into a streptavidin-coated microwell plate (Nunc, USA) and incubated at 37°C for 1 h. Recombinant barley MADS29 protein (0.01 pmol µl⁻¹ in TBS-T buffer containing 0.1% BSA) was then added and incubated for 1 h at 25°C. Following five washes with TBS-T, rabbit anti-mouse IgG alkaline phosphatase conjugate (Novagen, USA), diluted 1:2,000 in TBS-BSA buffer was added and phosphatase activity was determined by introducing *p*-nitrophenyl phosphate dissolved in diethanolamine-HCl (pH 9.8). The absorbance signal was measured at 405 nm after 1 h incubation at 37°C. For the competition assay, purified recombinant HvMADS29 was mixed with non-labeled double-stranded DNA,

and the mixture was incubated overnight at 4⁰C. A standard ELISA was performed at the following day as described above. Various ratios of labeled and unlabeled DNA were compared. At least four repetitions were performed for each reaction. The highest value in each experiment was equated to 100% and relative values of the other measurements were calculated.

2.2.18 *In silico* analysis of promoter sequences

The 20 genes putatively implicated in PCD of the nucellus were selected from Tran *et al.* (2014) and from a sub-cluster 3_1 of genes published by Sreenivasulu *et al.* (2006). As a control set, 20 genes encoding enzymes active in starch synthesis and specifically transcribed in the late endosperm (Radchuk *et al.*, 2009) were chosen; these all belong to sub-cluster 5_3 (Sreenivasulu *et al.*, 2006). The corresponding ESTs of the selected genes were blasted against the full-length cDNA collection (Matsumoto *et al.*, 2011) in order to find the full-length cDNA and determine the ATG start codon. Then the open reading frame of the corresponding cDNA was blasted against the full-length barley genome sequence (International Barley Genome Sequencing Consortium, 2012) to select promoter sequences (1000 nt 5' upstream of the ATG start codon). These sequences were scanned manually for the presence of CArG-like motifs, based on the consensus CArG *cis*-element sequence derived from the *Jekyll* and *VPE2a* promoters.

2.2.19 Computational analyses

Sequence searches in the National Center for Biotechnology Information databases were performed with BLAST (<http://www.ncbi.nlm.nih.gov/BLAST/>). Alignments of nucleotide and amino acid sequences were performed using ClustalW (DNASTar, USA). Sequence data were analyzed using Lasergene software (DNASTar).

Search for promoter sequences was done using the <http://webblast.ipk-gatersleben.de/barley/viroblast.php> (Barley Genome Sequencing Initiative, 2012). EST search was done by the IPK Crop EST Database (CR-EST): <http://pgrc.ipk-gatersleben.de/est/>.

The data were analyzed by one-way analysis of variance (ANOVA) followed by a posthoc-test after Holm-Sidak using Microsoft Excel version 2010, with Daniel's XL toolbox version 6.10 (Kraus, 2014) and Sigma plot 10, version 2007 (<http://www.sigmaplot.com/>).

3. Results

3.1 PCD in maternal tissues of developing barley grains

3.1.1 Detection of PCD in developing tissues of barley grains by TUNEL assay

Degradation of DNA and disintegration of nuclei are common features of PCD that can be detected by the terminal deoxynucleotidyl transferase-mediated dUTP nick end labeling (TUNEL) of the 3'-OH groups (Gavireli *et al.*, 1992). Using this assay, the spatial distribution of degrading nuclei in the different tissues of developing barley grains was analyzed. Only nuclei of the nucellar cells facing the endosperm were TUNEL-labeled between anthesis and three days after flowering (DAF) (Fig. 3.1 B, C). This degeneration coincides with expansion of the endosperm (Radchuk *et al.*, 2011). The nucellus is completely degenerated around 4 DAF (Fig. 3.1 D), and further endosperm expansion occurs at the expense of the pericarp (Radchuk *et al.*, 2011). Coinciding with this, the first TUNEL-labeled nuclei were visible in the innermost cells of the lateral mesocarp region (Fig. 3.1 D, E; Radchuk *et al.*, 2011). The other tissues, including endosperm and nucellar projection, were free of label. Beginning at 6 DAF, the TUNEL-positive nuclei spread throughout the whole mesocarp layer being especially abundant in lateral and dorsal regions (Fig. 3.1 E, F). The chlorenchyma (endocarp) however did not show any labeled nuclei remaining alive till grain maturation (Fig. 3.1 E-G). Starting from 6 DAF, first labeled nuclei were also visible at margins of the nucellar projection facing endosperm transfer cells (Fig. 3.1 E). The early developing endosperm was completely free of label (Fig. 3.1 B-J). With ongoing caryopsis development, the dorsal region of the pericarp became largely disintegrated and only few labeled nuclei were visible (Fig. 3.1 H). On the contrary, the ventral region of the pericarp was filled with numerous TUNEL-positive nuclei indicating intensive disintegration process (Fig. 3.1 I). Disintegrating nuclei were also observed at the margins of the nucellar projection, but not in main vascular bundle, in chlorenchyma and in starchy endosperm (Fig. 3.1 G-J). At the late grain filling phase (16 DAF) TUNEL-positive nuclei were still detected in the nucellar projection and the ventral parts of the pericarp (Fig. 3.1 K). Numerous labeled nuclei were also visible in different regions of the starchy endosperm but not in the aleurone layer (Fig. 3.1 K, L). In addition, some nuclei of the transfer cell layer were TUNEL-positive at 16 DAF (Fig. 3.1 K). Two days later, labeling of nuclei spreads to almost all cells of the transfer cell layer (Fig. 3.1 M) and is also detectable in the starchy endosperm and nucellar projection.

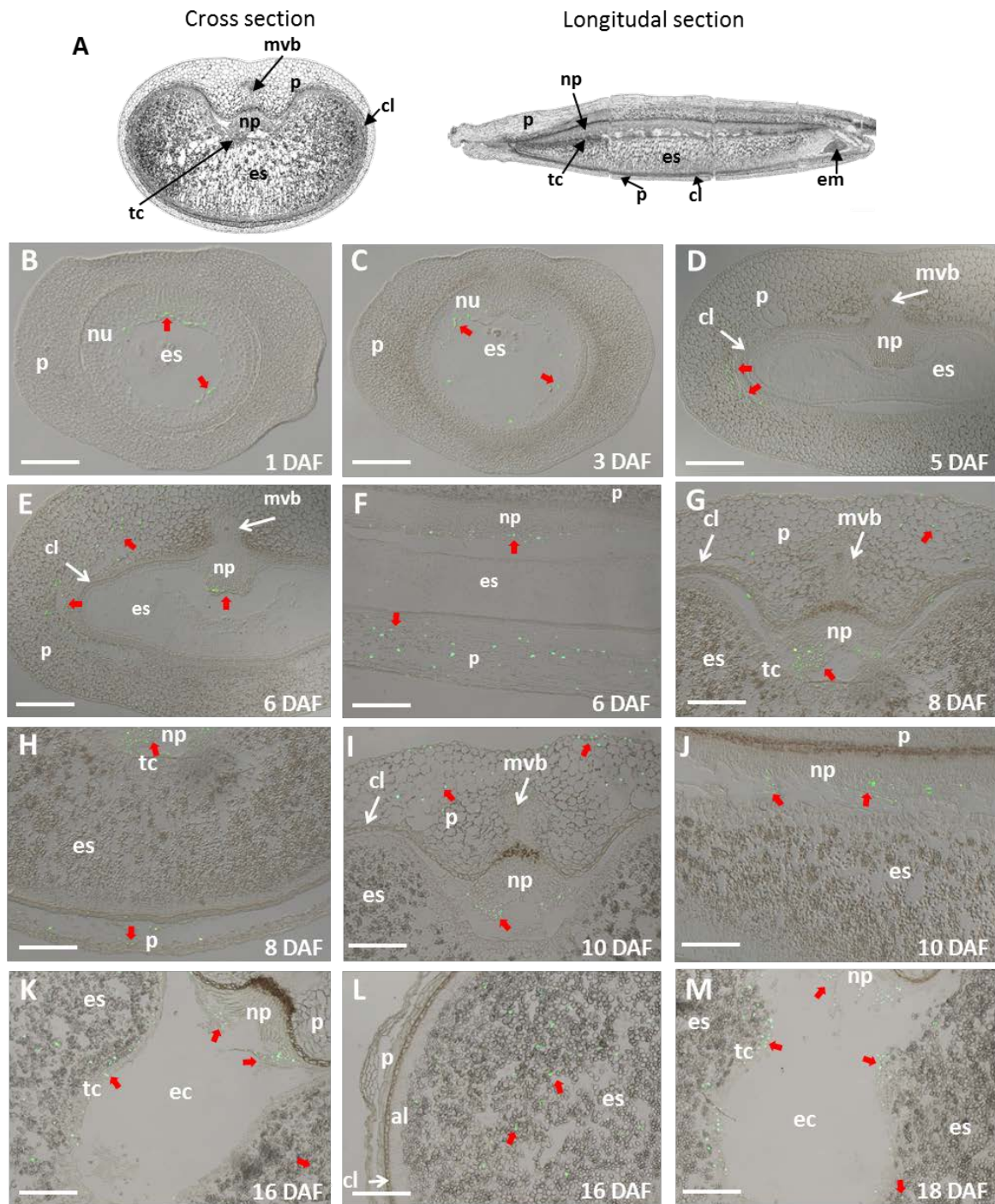


Figure 3.1 Localization of nuclear DNA fragmentation detected by the TUNEL assay during barley grain development. (A) Median transverse (left) and longitudinal section (right) of a barley grain at 7 DAF. The sections are taken from a 3-D model reconstructed from serial transverse sections. (B – M) Histological sections visualizing TUNEL-positive nuclei in distinct tissues of the developing grain. al, aleurone; cl, chlorenchyma, ec, endosperm cavern; em, embryo; es, endosperm; mvb, main vascular bundle; np, nucellar projection; p, pericarp, tc, transfer cells. TUNEL-positive nuclei are visualized as green signals and indicated by red arrows.

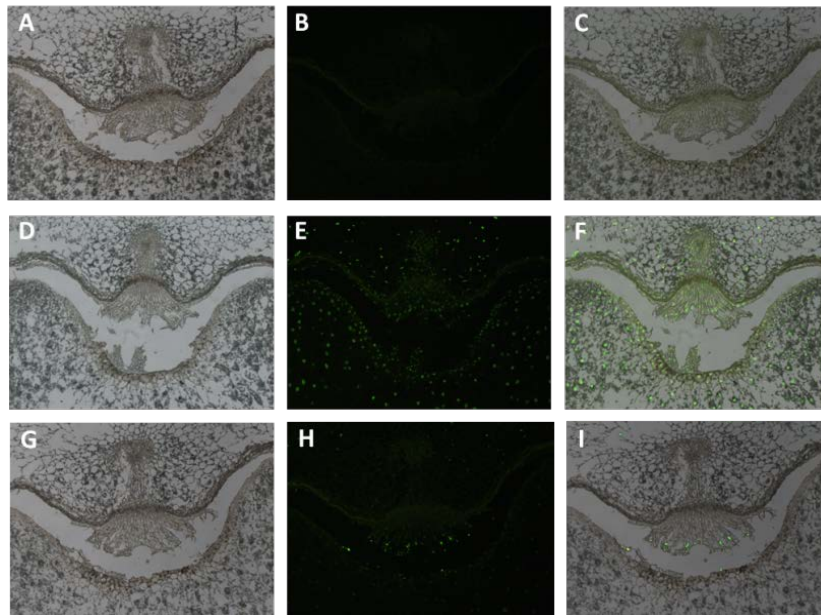


Figure 3.2. Negative and positive controls of TUNEL assay performed on sections of developing grains at 10 DAF. A-C: Negative control of TUNEL assay where TdT was omitted in the reaction. D-F: Positive control of TUNEL assay. The sections were treated with DNase (1500 U ml^{-1}) prior to labelling with the TUNEL mix. G-H: Localization of nuclear DNA fragmentation detected by the TUNEL assay at the same stage as in A-F.

No TUNEL labeling was detected in control sections when the TdT enzyme had been omitted (negative control, Fig. 3.2). Almost all nuclei were labeled in positive controls, treated with DNase prior to TUNEL assay, demonstrating the validity of the procedure (Fig. 3.2).

To conclude, the distribution of TUNEL-positive nuclei in the pericarp reveals that degradation of pericarp tissues starts around 4 DAF from inner mesocarp cells spreading to the outer pericarp layers during further grain development. The dorsal region of the pericarp disintegrates first while the ventral region around the main vascular bundle stays alive till early maturation quickly disintegrating later. The nucellus disintegrates soon after fertilization between 0 and 2 DAF besides the region in close proximity to main vascular bundle where the nucellar projection differentiates. The first TUNEL-positive nuclei are visible at margins of the nucellar projection starting from 5-6 DAF. Thereafter, TUNEL positive nuclei are detectable at margins of the nucellar projection until maturation indicating a continuous cell turnover in this region. Highly coordinated patterns of cell disintegration in maternal tissues suggest a timely and spatially regulated PCD processes.

3.1.2 Caspase-like activities in pericarp and endosperm fractions

Similar to animals, plant PCD has been shown to be associated with caspase-like activities (Woltering *et al.*, 2002). The profiles of YVADase (caspase-1-like), DEVDase (caspase-3-like), LEVDase (caspase-4-like), VEIDase (caspase-6-like), IETDase (caspase-8-like) and LEHDase (caspase-9-like) activities were investigated in pericarp and endosperm fractions of developing caryopses. In the pericarp, highest activity was detected with the caspase-6 substrate (Ac-VEID-AMC), followed by caspase-3 (Ac-DEVD-AMC), caspase-4 (Ac-LEVD-AMC), caspase-1 (Ac-YVAD-AMC), and caspase-8 (Ac-IETD-AMC) substrates (Fig. 3.3). Cleavage

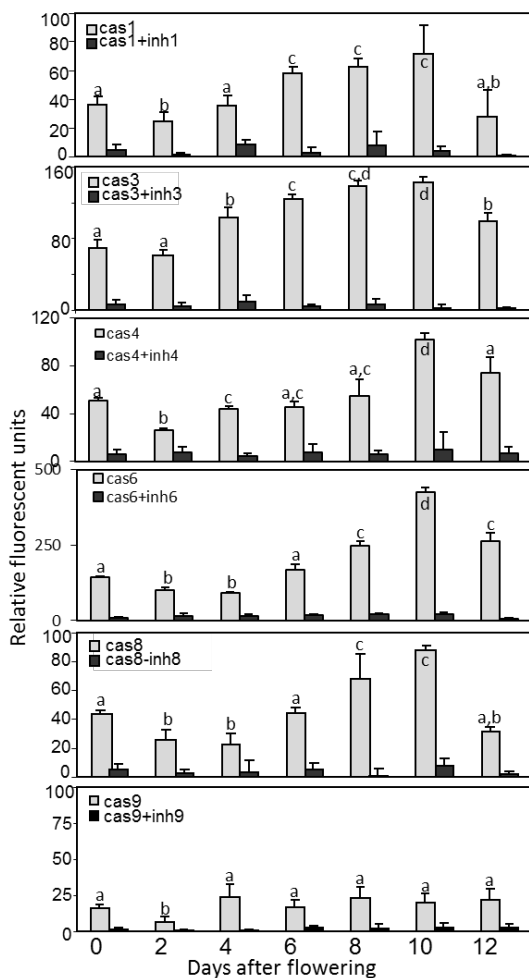


Figure 3.3 Caspase-like activities and effect of specific caspase inhibitors on the corresponding caspase-like activity in the barley pericarp. Data are means \pm SD, n = 4, values labeled by the same letter do not differ significantly at $p > 0.05$.

activities using all substrates generally increased with aging of the pericarp and all peaked at 10 DAF (Fig. 3.3). The caspase-9-like (Ac-LEHD-AMC substrate) activity was overall low in the pericarp and did not show any developmental pattern. Protease inhibitors, specific for each caspase, strongly inhibited the corresponding caspase-like activity validating the measured caspase-like activities in the developing pericarp (Fig. 3.3).

In the fraction representing the developing endosperm, two peaks of caspase-like activities were detected for caspase-1, caspase-3, caspase-4, caspase-6 and caspase-8 substrates. High activity was measured between anthesis and 12 DAF with quick decline thereafter. A second increase in activity was observed during grain maturation starting from 20–22 DAF (Fig. 3.4). This increase in caspase-1-like and caspase-6-like activities was not strongly pronounced (Fig. 3.4). The activities with the caspase-9 substrate were barely detectable in the

endosperm fraction throughout development except of grain maturation where a strong increase in activity was detected after 20 DAF (Fig. 3.3). The specific caspase inhibitors showed inhibitory effects to corresponding caspase-like activity in the endosperm fraction. To conclude, caspase-1-like, caspase-3-like, caspase-4-like, caspase-6-like and caspase-8-like activities were detected in the developing pericarp, all increasing towards 10 DAF. Two increases in caspase-like activities were measured in the endosperm fraction with the majority of caspase substrates. The increase in caspase-9-like activity was only detected during grain maturation.

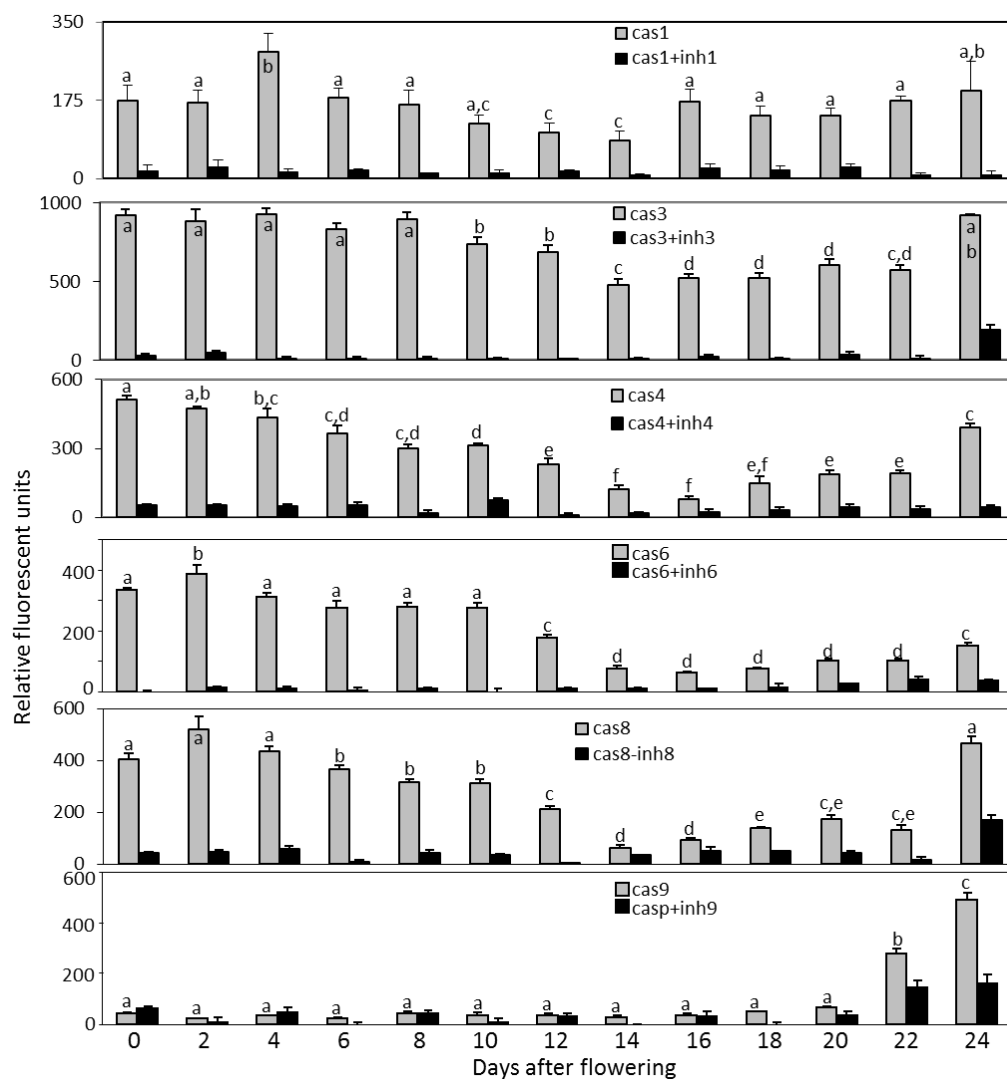


Figure 3.4 Caspase-like activities and effect of specific caspase inhibitors on corresponding caspase-like activity in the developing endosperm fraction. Data are means \pm SD, n = 4, values followed by the same letter do not differ significantly at $p > 0.05$.

3.1.3 Expression analysis of genes encoding vacuolar processing enzymes 2a-2d (VPE2a-2d) by qRT-PCR

Further work was concentrated on analysis of the role of gene products with caspase-1-like activities in development and PCD of maternal tissues.

VPEs display caspase-1-like activity *in vitro* as well as *in vivo* (Kuroyanagi *et al.*, 2005). The expression profile of the solely pericarp-specific *VPE4* gene was published (Radchuk *et al.*, 2011). Predominant localization of *VPE2a* to the nucellus and nucellar projection of the developing grains was shown early by *in situ* hybridization (Linnestad *et al.*, 1998). Expression of *VPE2a-VPE2b* and *VPE2d* genes was predicted in nucellar tissues (Radchuk *et al.*, 2011) but not experimentally proved due to the complex structure of hand-isolated endosperm fraction, which was used for analyses. Therefore, the detailed analysis of expression of *VPE2a-VPE2d* genes was performed from laser micro-dissected tissues of developing barley grains at 1, 3, 5, 7, 10 and 14 DAF (Fig. 3.5). Expression of the *VPE2a*, *VPE2b* and *VPE2d* genes was found exclusively in nucellus and nucellar projection with a maximum of transcript abundance between 7 and 10 DAF (Fig. 3.5). *VPE2b* gene activity was highest among all VPEs expressed in these tissues. The accumulation of *VPE2a* transcripts was two-fold lower than that of *VPE2b*. Transcript levels of *VPE2d* reached only one tenth of that of *VPE2b*. Expression of *VPE2c* was detected only at basal level (less than 1% of *VPE2b*) in all studied tissues (Fig. 3.5) confirming previous data (Radchuk *et al.*, 2011).

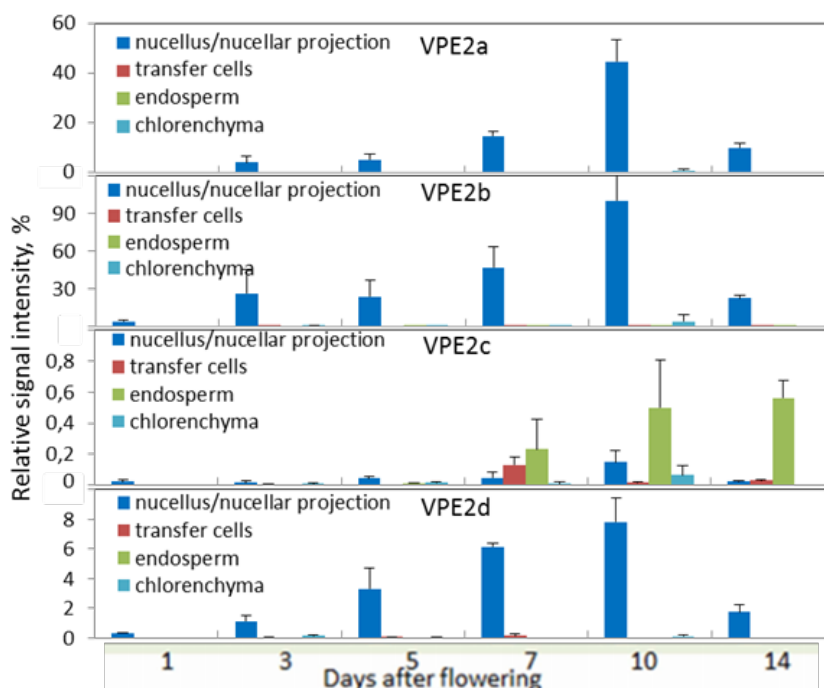


Figure 3.5. Expression profiles of genes for vacuolar processing enzymes VPE2a-VPE2d in different tissues micro-dissected from developing barley grains as analyzed by qRT-PCR.

To conclude, the transcripts of *VPE2a*, *VPE2b* and *VPE2d* genes were detected exclusively in nucellar tissues of the developing barley grains.

3.2 Analysis of the role of *VPE4* on pericarp development by RNAi-mediated suppression

To decrease the mRNA level of the pericarp-specific *VPE4* gene (Radchuk *et al.*, 2011), the RNA-interference (RNAi) approach was used expressing a *VPE4*-RNAi construct under control of the *VPE4* gene promoter to achieve precise temporal and spatial down-regulation of *VPE4* gene expression.

The full length sequence of the *VPE4* gene was depicted from the full-length barley genome sequence. The *VPE4* gene sequence consists of nine exons and eight introns (Fig. 3.6). The *VPE4* promoter fragment contained 932 nucleotides 5'-upstream of the ATG start codon. The region was amplified from barley genomic DNA using fragment-specific primers, cloned into pGEM-T easy vector, re-sequenced and used for p*VPE4i* construct preparation. The *VPE4i* construct contained sense and antisense fragments from the same coding region of *VPE4* cDNA separated by the first intron of GA oxidase of potato (Fig. 2.1). The construct contained also a gene for hygromycin resistance driven by the ubiquitin promoter for selection of transformed cells. The p*VPE4i* construct was transformed into *Agrobacterium tumefaciens* cells and used for barley plant transformation, which was performed in the Group Plant Reproduction (IPK).



Figure 3.6 Exon-intron structure of the *VPE4* gene. Exons are given by boxes, introns by lines.

3.2.1 Analysis of the *VPE4i* primary transformed plants and preparation of homozygous lines

Following transformation, 35 putatively transgenic plants were regenerated. All these plantlets were screened by PCR analysis for the presence of the transformed T-DNA by amplification of marker gene *hpt* encoding hygromycin phosphotransferase. PCR amplification was performed by using the genomic DNA isolated from 15-days old plants and revealed amplification signals in 33 regenerated plants (Fig. 3.7). No PCR product was observed in non-transgenic control plants (Fig. 3.7).

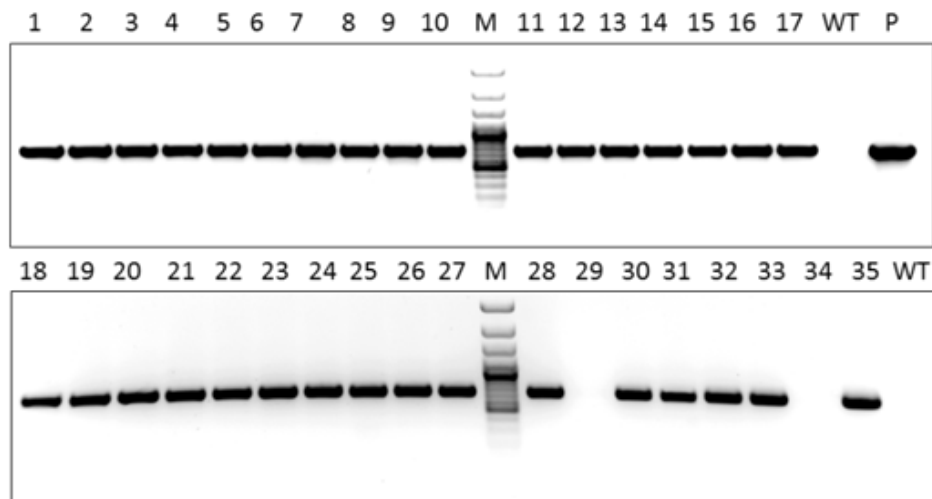


Figure 3.7 PCR analysis of primary regenerated plants transformed with pVPE4i amplifying an *hpt* gene fragment. M, 1 kb marker ladder; P, amplification of a relevant fragment from pVPE4i plasmid as a positive control; WT, amplification from non-transformed plant as a negative control; lanes 1-35, T₀ putatively transgenic plants.

All regenerated lines were further analysed to estimate the number of integrated transgene copies by Southern blot hybridizations using subsequently fragments of the *hpt* gene and the *VPE4* gene promoter as probes. 33 out of 35 regenerated plants showed hybridization signals using the *hpt* fragment as a probe (Fig. 3.8 A). The number of hybridization bands ranged between 1 and 6 (Fig. 3.8 A). One transgene copy was present in the genomes of 19 lines (54.3%). No signal was detected in the not transformed line. When the fragment of the *VPE4* gene promoter was used for hybridization, only 25 regenerated plants showed hybridizing bands (Fig. 3.8 B). One hybridization signal was found in the untransformed control that corresponds to the endogenous *VPE4* promoter sequence. A fragment of identical size was detected in all regenerated plants. A second band of different size indicates presence of the transgene. As in case of hybridization with *hpt* fragment, line 22 contains the highest number of the transgene insertions. 15 lines (or 42.9%) were detected carrying one transgene copy in the genome.

Transgenic plants carrying one T-DNA copy of the RNAi construct were analyzed for down-regulation of the *VPE4* transcript by Northern blot hybridization using a fragment of *VPE4* cDNA as a probe (Fig. 3.9). Total RNA was isolated from whole caryopses at 8 DAF from 15 transgenic plants and the non-transgenic wild type.

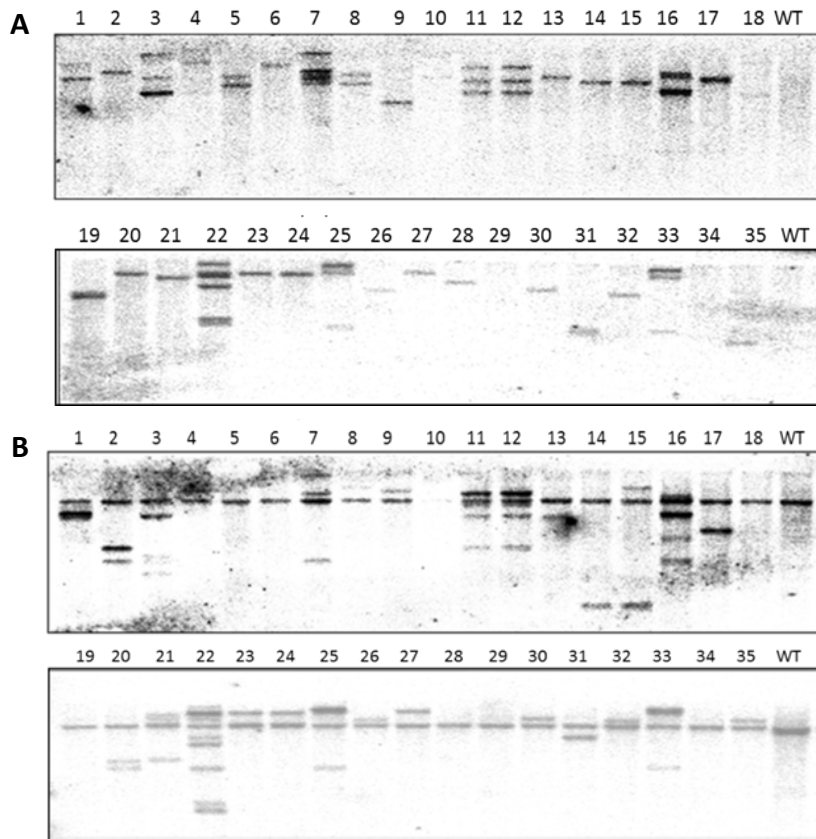


Figure 3.8 Southern blot hybridization of primary transgenic VPE4i plants using *hpt* (A) and *VPE4* gene promoter (B) fragments as probes. 1-35: regenerated T₀ plants; WT, untransformed plant.

Lines 6, 9, 19, 34 showed weak or no reduction of the *VPE4* transcripts, lines 11, 12, 13, 17 and 23 were characterized by very strong reduction of the *VPE4* transcript level (Fig. 3.9).

Three transgenic plant lines, VPE4i-13, VPE4i-17 and VPE4i-23, with one transgene copy (Fig. 3.8) and strong reduction of *VPE4* expression (Figure 3.9) were selected for further analyses.

Transgenic plants carrying one T-DNA copy of the

RNAi construct were analyzed for down-regulation of the *VPE4* transcript by Northern blot hybridization using a fragment of *VPE4* cDNA as a probe (Fig. 3.9). Total RNA was isolated from whole caryopses at 8 DAF from 15 transgenic plants and the non-transgenic wild type. Lines 6, 9, 19, 34 showed weak or no reduction of the *VPE4* transcripts, lines 11, 12, 13, 17 and 23 were characterized by very strong reduction of the *VPE4* transcript level (Fig. 3.9). Three transgenic plant lines, VPE4i-13, VPE4i-17 and VPE4i-23, with one transgene copy (Fig. 3.8) and strong reduction of *VPE4* expression (Figure 3.9) were selected for further analyses. The analysis of the *VPE4* gene function in developing seeds strongly depends on stable inheritance of the RNAi effect to the next generation(s). Stable integration of the transgene to the progenies of the lines VPE4i-13, VPE4i-17 and VPE4i-23 was shown by analyzing the T₂ generation. Segregation of the transgene was observed close to 3:1 as expected according the Mendelian laws (not shown). Non-transgenic plants were discarded. Homozygous lines were selected from seeds of the next generation resulting from self-pollination.

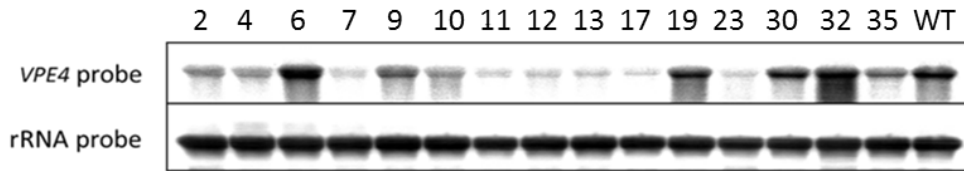


Figure 3.9 Northern blot analysis of selected primary VPE4i-transformed plants by hybridization with a *VPE4* gene fragment as a probe (upper panel). Hybridization with 25S rDNA was used as a loading control (lower panel). 2-35: independent transgenic lines; WT, non-transformed control grains.

Around 30 seeds of selected T₂ plants were sown and analyzed for presence of the transgene in the T₃ generation by Southern blot hybridizations using the *hpt* gene fragment as a probe. Lines with a hybridization band in all offspring plants were considered as homozygous (Fig. 3.10). Developing seeds from homozygous T₃ plants were further analyzed for the *VPE4* gene transcript level by Northern blot hybridization using the *VPE4* gene fragment as a probe. Total RNA was isolated from developing seeds of three VPE4-repressed transgenic lines and the untransformed control at 2, 4, 6, 8 and 10 DAF. The expression patterns of the *VPE4* gene in wild type caryopses were similar to that reported earlier (Radchuk *et al.*, 2011) with the maximum of expression at around 8 DAF (Fig. 3.11 A).

In the transgenic lines, *VPE4* transcript levels were moderately (line VPE4i-13) or strongly (lines VPE4i-17 and VPE4i-23) decreased compared to non-transgenic barley seeds (Fig. 3.11 A).

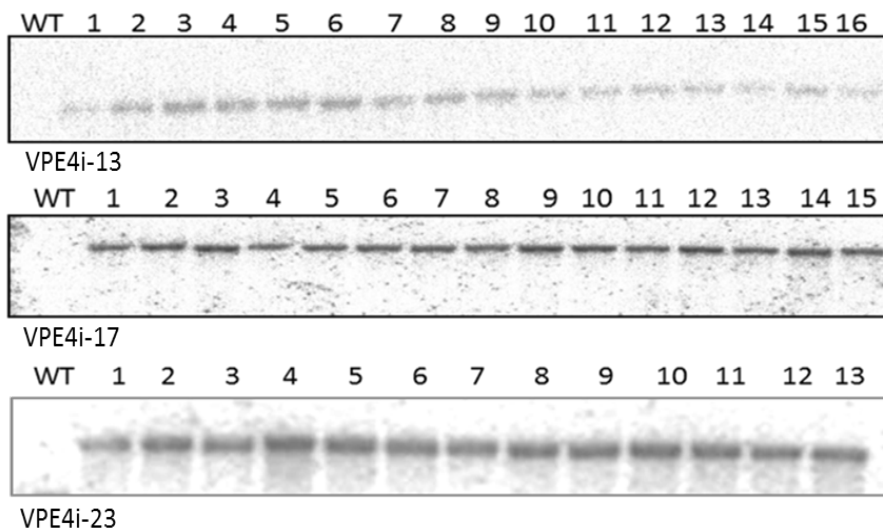


Figure 3.10 Southern blot analysis of selected lines demonstrating the homozygous state of T₃ grains of three independent transgenic VPE4i lines. 1-16, individual plants of the three independent lines; WT, non-transformed control plant.

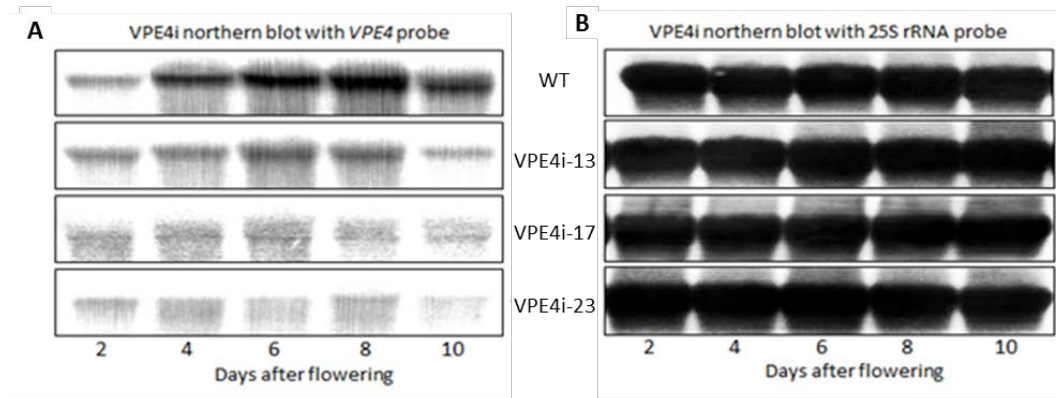


Figure 3.11 Northern blot analysis of *VPE4* gene expression in developing grains of the transgenic lines VPE4i-13, VPE4i-17 and VPE4i-23, and the untransformed control (WT) (A). Hybridization of the same filter with 25S rDNA used for loading control (B).

3.2.2 Phenotypic changes in VPE4i-repressed mature seeds

No differences in the phenotype were observed between VPE4i-transgenic and untransformed plants during vegetative growth. Also start of tillering and begin of flowering were not altered. However, the transgenic spikes remained longer green during maturation and showed a longer desiccation phase than the wild type spikes indicating delayed development of transgenic spikes and/or seeds. Whereas wild type plants start to turn gradually to yellow already after 20 DAF, transgenic spikes stay green at least till 25 DAF (Fig. 3.12 A).

Mature seeds of all three transgenic lines appeared smaller than non-transgenic seeds (Fig. 3.12 B). Indeed, the thousand grain weight of all VPE4i-repressed lines was significantly lower than that of non-transgenic grains (Fig. 3.13 A). The reduction of grains weight can be mainly addressed to the reduction of seed width (Fig. 3.13 B) and, possibly, seed thickness. Lines VPE4i-13 and VPE4i-23 showed strong reduction of seed width, but VPE4i-17 line did not. Because the latter line did also not show any significant increase in seed length (Fig. 3.13 C), it has been concluded that the decrease in grain weight of the VPE4i-17 line is achieved mainly by decrease in seed thickness.

Seeds of VPE4i-13 and VPE4i-23 lines were weakly but significantly longer than WT seeds (Fig. 3.13 C). However, increase in seed length of these lines does not compensate the reduction in total seed weight (Fig. 3.13 A). Based on this observation, it was assumed that seed thickness of the VPE4i-13 and VPE4i-23 transgenic lines was also strongly decreased.

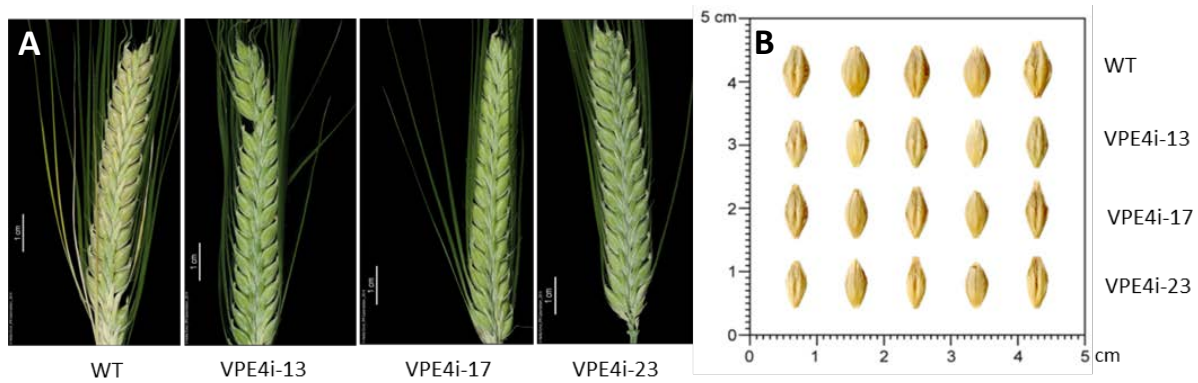


Figure 3.12 Phenotypic differences between untransformed (WT) and transgenic spikes (A) and seeds (B). At 25 DAF, spikes of all three transgenic lines stay green whereas WT spikes turn yellow (A). Transgenic seeds of all transgenic lines are smaller than WT seeds (B).

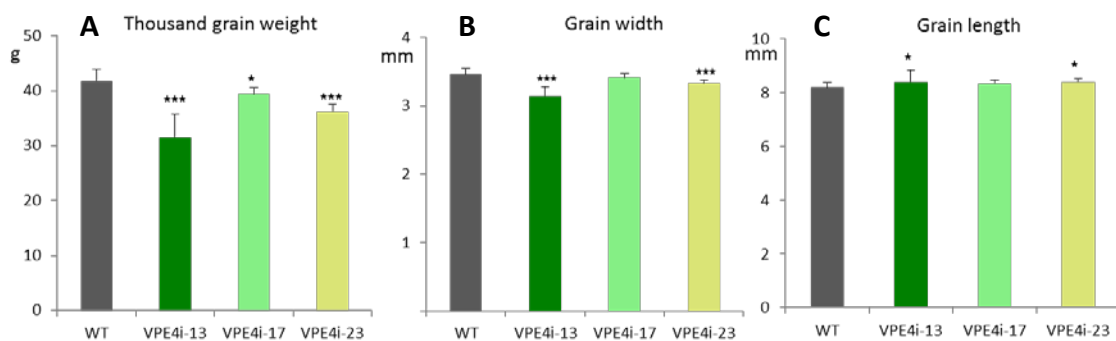


Figure 3.13 Thousand grain weight (A), width (B) and length of mature VPE4i-transgenic grains (C) as compared to wild type grains. Data are means \pm SD, $n = 10$ for (A) and $n = 100$ for (B-C), * t significant at $P < 0.05$, ** t significant at $P < 0.01$ and *** t significant at $P < 0.001$.

To conclude, repression of the pericarp-specific *VPE4* gene resulted in significantly lower grain weight due to lower seed width and, possibly, seed thickness. The reduction of seed weight could not be compensated either by prolonged development or by slightly increased seed length registered for transgenic lines.

3.2.3. Accumulation of fresh weight during seed development

Lower weight of the mature transgenic grains results from affected fresh weight accumulation during development. To compare fresh weight accumulation between transgenic lines and wild type, the average fresh weight of developing caryopses was determined using at least 50 caryopses for each line at each developmental stage (Fig. 3.14).

Fresh weight of developing seeds of all three VPE4i-transgenic lines was significantly lower than that of the wild type already at 4 DAF (Fig. 3.14, left panel). This difference increased towards 8 DAF. However, between 10 and 14 DAF, the fresh weight of the transgenic seeds was similar to that of the wild type. Second delay in fresh weight accumulation of transgenic grains was observed after 16 DAF and this delay was preserved until maturation (Fig. 3.14, right panel).

To conclude, down-regulation of the pericarp-specific *VPE4* gene resulted in a biphasic reduction of fresh weight accumulation during seed development. More slow accumulation of fresh weight during early development leveled up in all lines at middle stages of seed development with new delay in fresh weight accumulation in the transgenic seeds during late development and maturation. The strong reduction of fresh weight accumulation during storage phase and maturation of the transgenic grains is obviously responsible for the reduction in thousand grain weight. However, levelling of fresh weight accumulation during middle caryopsis development was unexpected and needs further explanation.

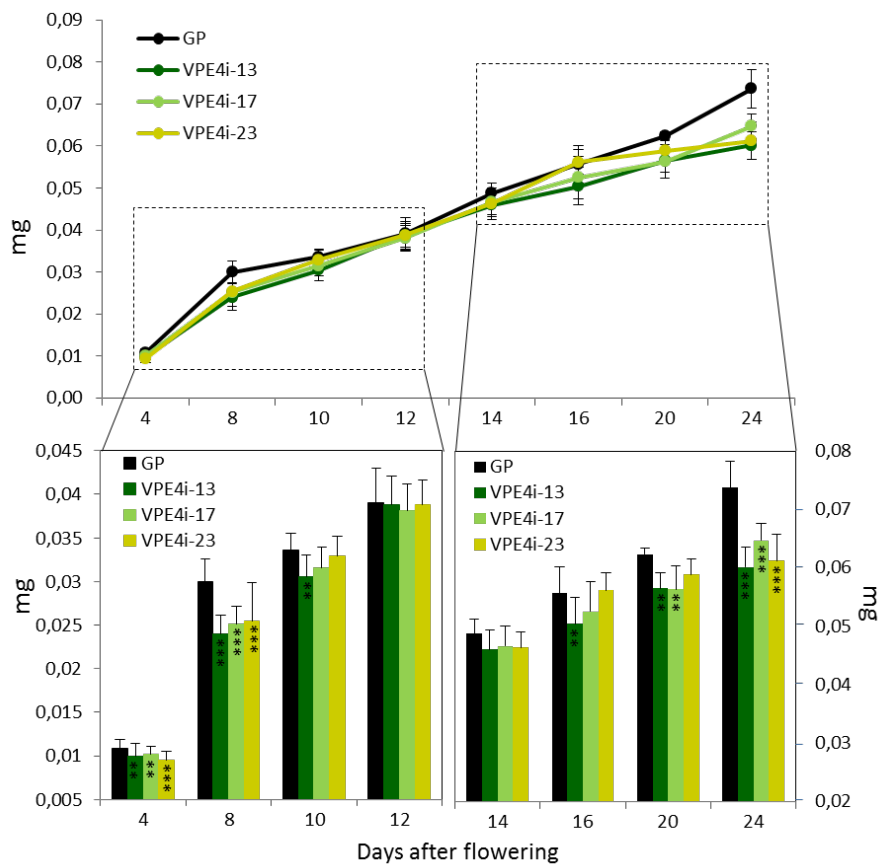


Figure 3.14 Accumulation of fresh weight of developing grains of VPE4i-transgenic and GP lines. Data are means \pm SD, $n \geq 50$, ***t* significant at $P < 0.01$ and ****t* significant at $P < 0.001$.

3.2.4 Pericarp degradation is delayed in developing VPE4-RNAi grains

To find an explanation for the biphasic reduction of fresh weight accumulation in transgenic barley grains (Fig. 3.14), a histological analysis was performed to visualize possible alteration in pericarp development at the cellular level (Fig. 3.15). Line VPE4i-23 with the strongest phenotype was selected for the analyses.

Pericarp thickness in ventral, lateral and dorsal regions of developing barley grains was determined using histological images of transgenic and untransformed control caryopses at 8 and 12 DAF. Dorsal and lateral pericarp regions in transgenic grains remained thicker than that of the non-transgenic control due to higher number of cell layers (Figure 3.15).

This effect is especially pronounced in the dorsal pericarp. These differences were statistically significant at both 8 and 12 DAF in the dorsal and lateral regions but not in the ventral part of the pericarp (Figure 3.16).

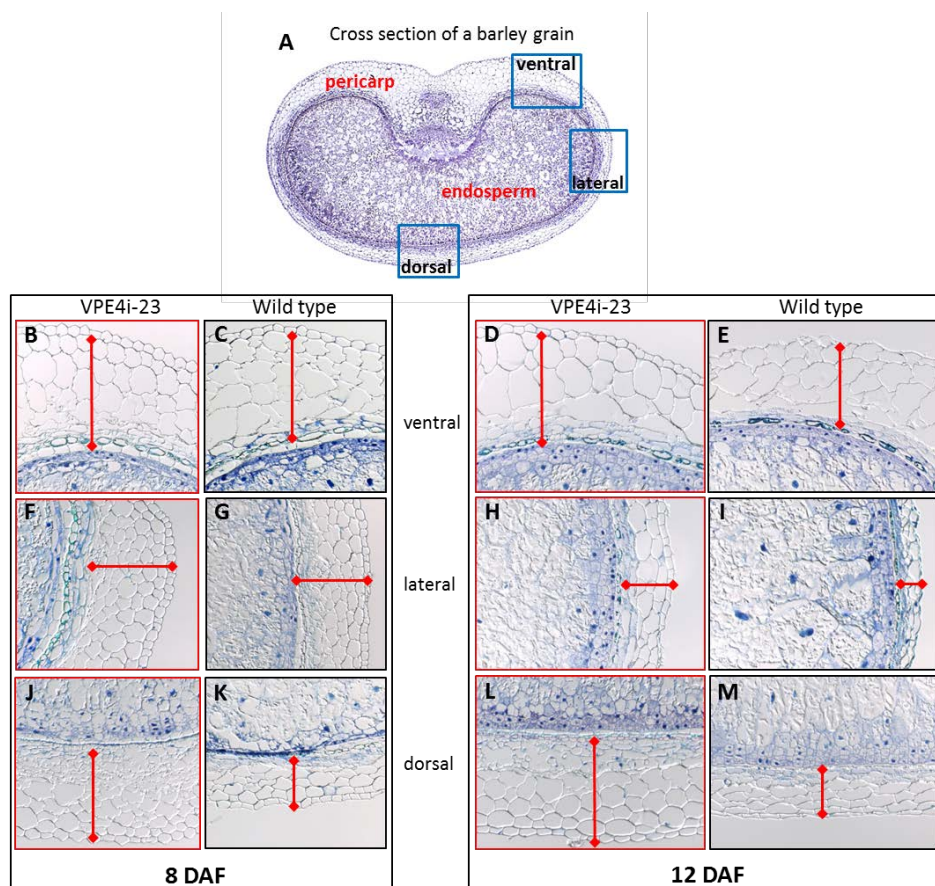


Figure 3.15 Alterations in pericarp structure of developing barley grains in VPE4-repressed (VPE4i-23) vs wild type grains. (A) A cross section of a barley grain. Positions of histological sections used for detailed analyses in (B-M) are boxed. Red frames denote seed sections of the VPE4i-23 transgenic line, black frames are used for wild type seed sections. Red bars show the thickness of the pericarp.

It is suggested that repression of *VPE4* gene expression delayed cell death in the pericarp tissue of transgenic grains resulting in a higher number of cells and thicker pericarp when compared to the non-transgenic wild type. The ventral part of pericarp remains alive till maturation. Therefore, the delay in PCD was not clearly detectable here at early and middle grain development. Histological analyses also revealed delayed cell disintegration of the late pericarp in *VPE4*-repressed grains compared to the wild type.

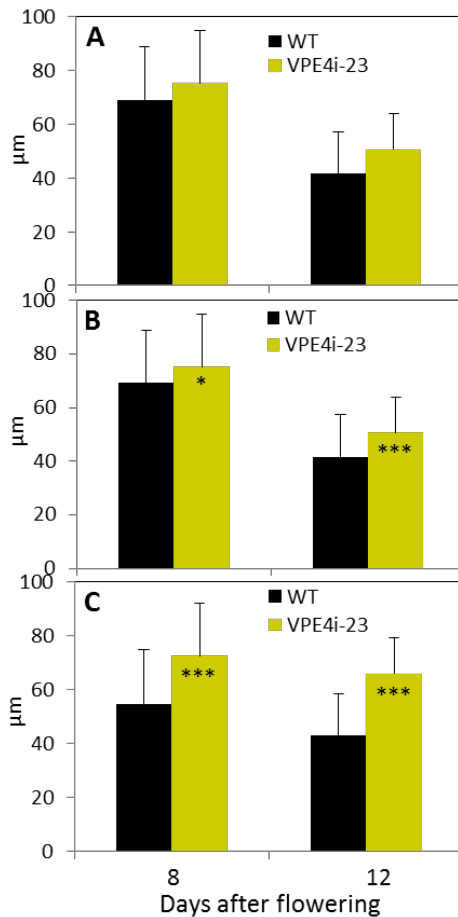


Figure 3.16 Quantification of pericarp thickness in ventral (A), lateral (B) and dorsal regions (C) of the VPE4i-23 transgenic grains and in the untransformed control (WT) at 8 and 12 DAF. Data are means \pm SD, $n = 20$, * t significant at $P < 0.05$ and *** t significant at $P < 0.001$.

3.2.5 Caspase-like activities in the pericarp of VPE4i-repressed barley grains

Because VPE displays caspase-1-like activity in plants (Kuroyanagi *et al.*, 2005), alterations in caspase-1-like activity were analyzed in the *VPE4*-repressed pericarp. Pericarp tissue was manually separated from the endosperm fraction of transgenic and non-transgenic control barley grains at 4 and 8 DAF and used for caspase assays. Caspase-1-like activity was decreased in all analysed transgenic lines compared to the wild type (Fig. 3.17 A). The decrease in activity correlates well with the repression of *VPE4* gene expression (Fig. 3.11). Decrease in caspase-1-like activity was weaker in line VPE4i-13 with moderate down-

regulation of *VPE4* expression than in *VPE4i-17* and *VPE4i-23* lines, both with strong *VPE4* gene down-regulation. Caspase-1-like activity was stronger decreased in older than younger transgenic pericarp (compare 8 DAF to 4 DAF) indicating that transcriptional repression leads to progressive down-regulation of caspase-1-like activity.

Caspase-3, -4, -6 and -8-like activities were measured in transgenic and non-transgenic pericarp tissues as well. Because caspase-9-like activity is low in the barley pericarp (Fig. 3.3), this activity was not analyzed. Surprisingly, all measured activities were significantly lower in the pericarp of all three transgenic lines compared to the activity in the wild type pericarp (Fig. 3.17 B-E). To conclude, down-regulation of *VPE4* gene expression resulted in decreased levels not only of caspase-1-like activity but also of caspase-3, -4, -6, and -8-like activities.

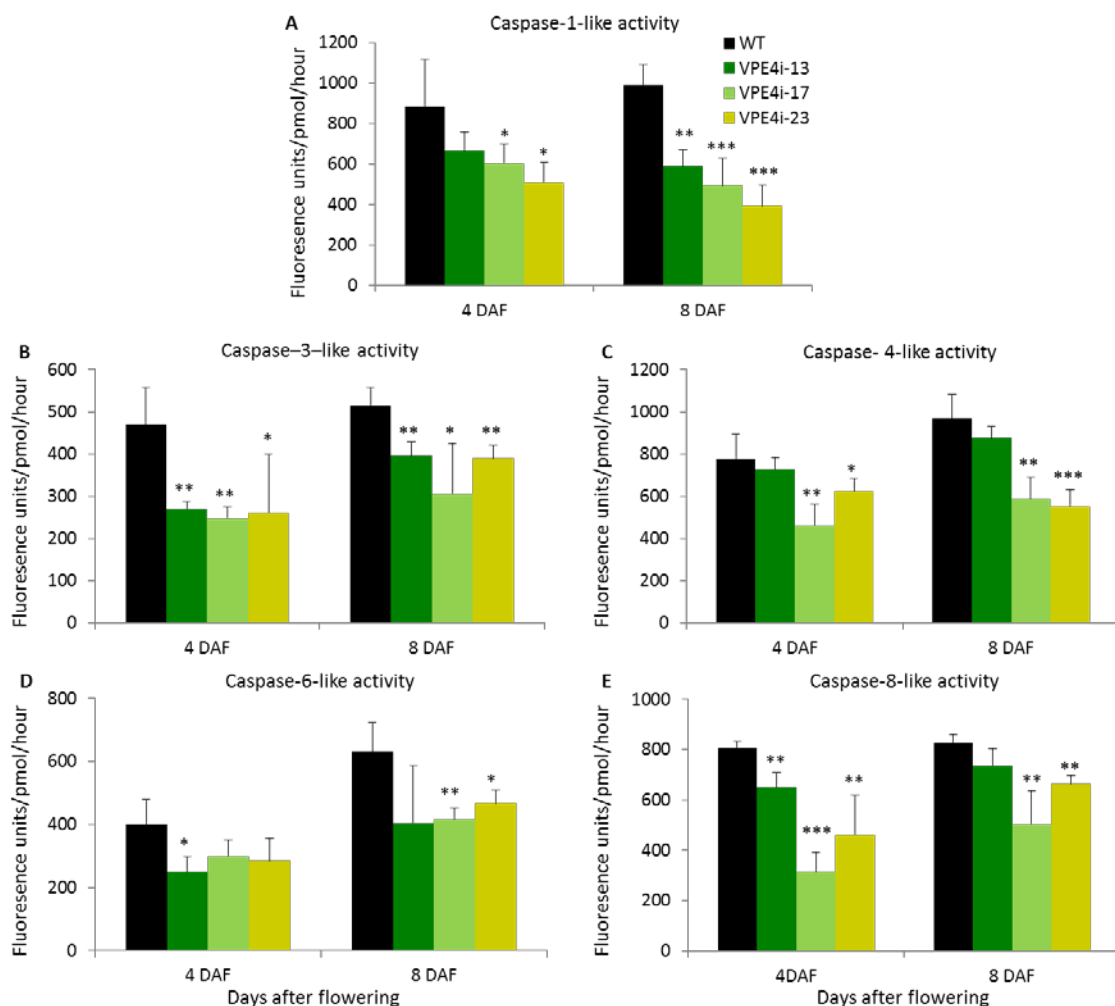


Figure 3.17 Caspase-1 (A), caspase-3 (B), caspase-4 (C), caspase-6 (D) and caspase-8-like activities (E) in developing grains at 4 and 8 DAF of wild type (GP) and three *VPE4i* transgenic lines. Data are means \pm SD, $n = 4$, * t significant at $P < 0.05$, ** t significant at $P < 0.01$ and *** t significant at $P < 0.001$.

3.2.6 Storage compounds in mature transgenic grains as compared to the wild type

Homozygous *VPE4*-repressed and non-transgenic control grains were harvested, and starch, sugar and protein content were analyzed. Starch content was significantly decreased in all *VPE4*-repressed transgenic seeds (Fig. 3.18 A). Sucrose content was not changed except line *VPE4i-13*, where it was increased (Fig. 3.18 B). Seed protein content was slightly increased in the transgenic grains, but a significant difference was found of both albumin/globulin and gliadin fraction only in grains of line *VPE4i-23* (Fig. 3.18 C, D). Furthermore, in *VPE4i-17* grains the gliadins content was significantly increased (Fig. 3.18 D). The most obvious finding was the reduction of starch accumulation in *VPE4*-repressed lines.

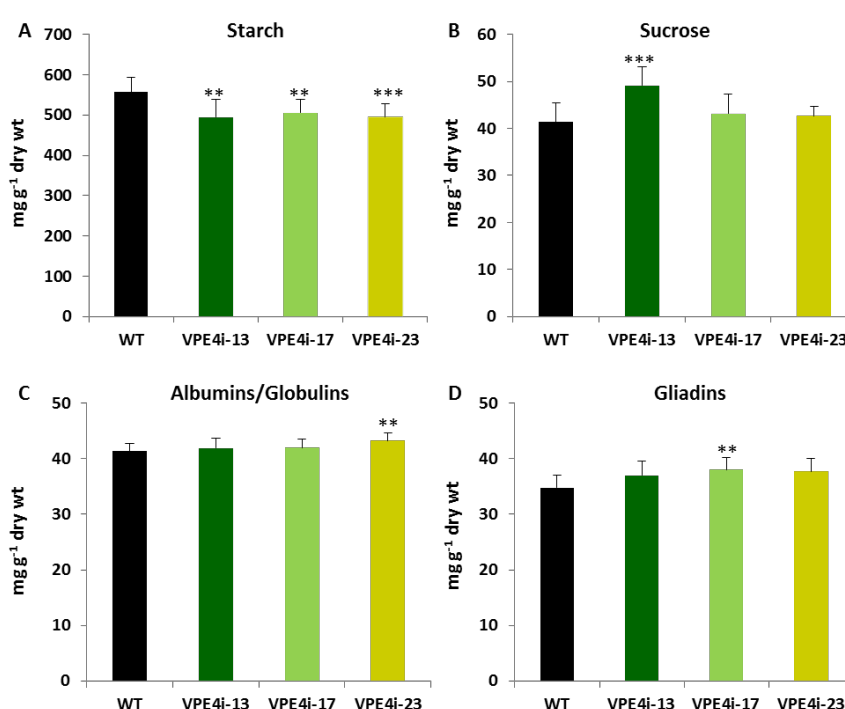


Figure 3.18 Content of starch (A), sucrose (B) and storage proteins (C, D) in mature grains of *VPE4* down-regulated transgenic grains in comparison to the wild type (GP). Data are means \pm SD, $n = 8$, * t significant at $P < 0.05$, ** t significant at $P < 0.01$ and *** t significant at $P < 0.001$.

3.2.7 Accumulation of metabolites in the *VPE4*-repressed pericarp during grain development

Levels of sucrose, hexoses and starch were measured in manually separated pericarp and endosperm fractions of transgenic and wild type caryopses at early development. There were not many differences in the sugar (sucrose and hexoses) contents between transgenic pericarps of lines *VPE4i-13* and *VPE4i-17* and wild type pericarp at 4 and 8 DAF (Fig. 3.19 A-

C). Sucrose was slightly increased in the VPE4i-13 transgenic pericarp while the levels of both fructose and glucose were slightly decreased at 4 DAF. The sucrose content in transgenic pericarps was similar to non-transgenic pericarp at 8 DAF (Fig. 3.19 A). Significantly higher glucose and fructose levels were detected only in the pericarp of line VPE4i-23 at 8 DAF (Fig. 3.19 B, C). While starch content tended to be higher at 4 DAF (significantly increased only in line VPE4i-17), it was decreased in the transgenic pericarp at 8 DAF albeit significantly only for lines VPE2i-13 and VPE2i-23 as compared to the wild type (Fig. 3.19 D).

In the transgenic endosperm fraction (Fig. 3.20 A), sucrose contents tended to be increased at 4 DAF (significantly only for the line VPE4i-23) and decreased at 8 DAF (two lines VPE4i-17 and VPE4i-23 showed significant decrease). There were no detectable trends in accumulation of hexoses in any of the lines or developing stages (Fig. 3.20 B, C). Starch levels were equal in the transgenic and wild type endosperms at 4 DAF (Fig. 3.20 D). At initiation of starch biosynthesis (8 DAF), endosperms of the transgenic seeds contain significantly more starch than the wild type (Fig. 3.20 D) albeit this is significantly different only for the lines VPE4i-17 and VPE4i-23.

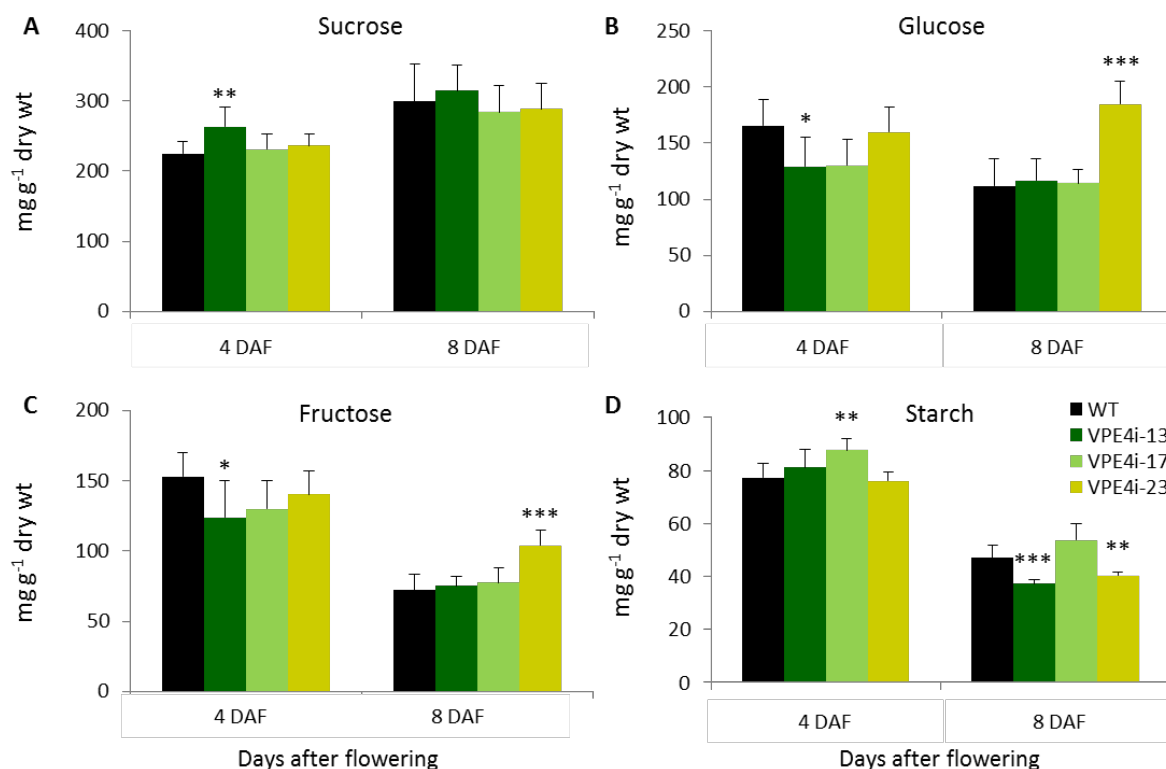


Figure 3.19 Accumulation of sucrose (A), glucose (B), fructose (C) and starch (D) in the developing pericarp of VPE4i transgenic grains compared to the wild type (WT). Data are means \pm SD, n = 6, *t significant at $P < 0.05$, **t significant at $P < 0.01$ and ***t significant at $P < 0.001$.

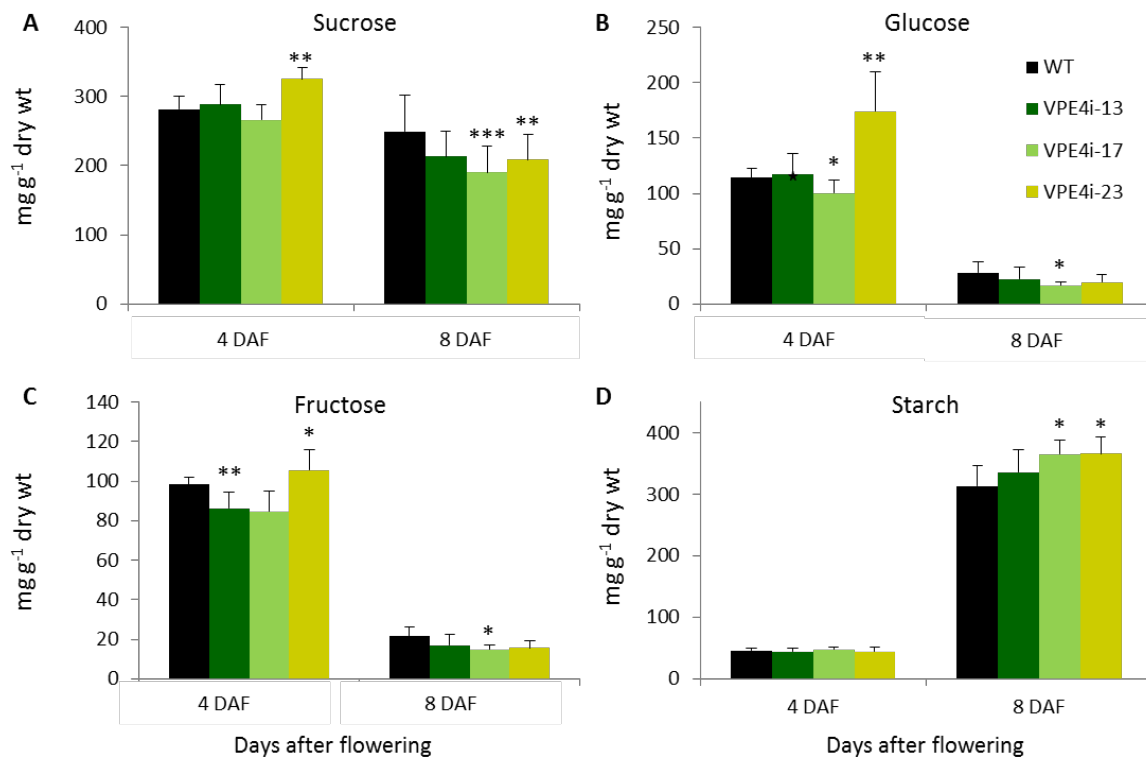


Figure 3.20 Accumulation of sucrose (A), glucose (B), fructose (C) and starch (D) in the endosperm fraction of developing barley grains of VPE4i transgenic plants compared to the wild type (WT). Data are means \pm SD, $n = 6$, * t significant at $P < 0.05$, ** t significant at $P < 0.01$ and *** t significant at $P < 0.001$.

To conclude, starch accumulation starts earlier in the transgenic endosperm (increased level 8 DAF when compared to WT). This correlates with the tendency to decreased sucrose levels (Fig. 3.20), which might be explained by a higher flux towards starch biosynthesis. Together with the decrease of caryopses fresh weight (Fig. 3.14) and increase in thickness of the pericarp (Figs. 3.15, 3.16) it is concluded that cell proliferation ceases earlier in the transgenic endosperm.

3.3 Analysis of the role of vacuolar processing enzymes on development of nucellar tissues

As presented in sub-chapter 3.1.3, the genes encoding vacuolar processing enzyme 2a (VPE2a), VPE2b and VPE2d are exclusively expressed in the nucellus and nucellar projection of developing barley grains (Fig. 3.5). However, only a partial cDNA sequence for VPE2a (called also *nucellain*; Linnestad *et al.*, 1998) gene was published (Linnestad *et al.*, 1998; Radchuk *et al.*, 2011). Hybridization *in situ* confirmed the presence of the VPE2a transcripts in nucellus and nucellar projection (Linnestad *et al.*, 1998). A physiological role of the VPEs in

PCD of the corresponding tissues was supposed (Linnestad *et al.*, 1998; Radchuk *et al.*, 2011) but not experimentally proved. Here, the impact of nucellar-specific VPE genes on grain development has been analyzed using an RNAi approach.

3.3.1 Cloning of the full-length VPE2a cDNA

Despite of several publications about *VPE2a* (Linnestad *et al.*; Radchuk *et al.*, 2011; Tran *et al.*, 2014), the full-length cDNA and the deduced protein sequence have never been reported. Therefore, full-length cDNA sequence for *VPE2a* was cloned at first. For this, the advantage of the full-length barley genome sequence (Barley Genomic Initiative, 2012) was used. Using *VPE2a* fragment as query, the HVVMRXALLhA0751I05_v23_c3 genomic region was found. As seen from the genomic fragment, the *VPE2a* gene consists of eight exons and seven introns (Fig. 3.21) and includes a promoter region of at least 1500 nt upstream of the putative ATG start codon.

Analyzing the very similar full-length cDNA sequences of *VPE2b-VPE2d* genes together with *VPE2a*, the putative ATG start codon for the *VPE2a* coding region was determined. Corresponding primers placed before the start and after the stop codon were designed. The full length *VPE2a* cDNA was amplified from reverse-transcribed mRNA derived from developing grains at 4 DAF, cloned into pGEM-T easy vector and sequenced. The longest cDNA sequence comprised a total of 1734 nucleotides. It encodes a protein of 484 amino acids in length with a calculated molecular mass of 53.74 kDa (Suppl. Fig. S1). The VPE2a protein contains a putative signal peptide of 26 amino acids and has been predicted to be localized to the vacuole (probability: 0.975) using the TargetP online software (<http://www.cbs.dtu.dk/services/TargetP/>). Full-length cDNA of *VPE2a* shares 94.7% and 92.4% identity to *VPE2b* and *VPE2d* cDNA, correspondingly. The deduced VPE2a protein shares the highest similarity to the barley VPE2b, VPE2d and VPE2c sequences being identical at 92.3% to VPE2b, 89.5% to VPE2d and 78.5% to VPE2c at amino acid level. All these proteins together with barley VPE1, rice OsVPE1 and OsVPE3 and Arabidopsis β VPE comprise the seed-specific sub-clade of VPEs (Fig. 3.22).

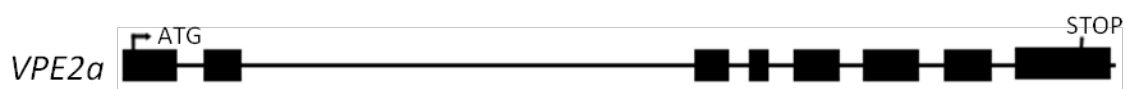


Figure 3.21 Exon-intron structure of the VPE2a gene. Exons are given by boxes, introns by lines.

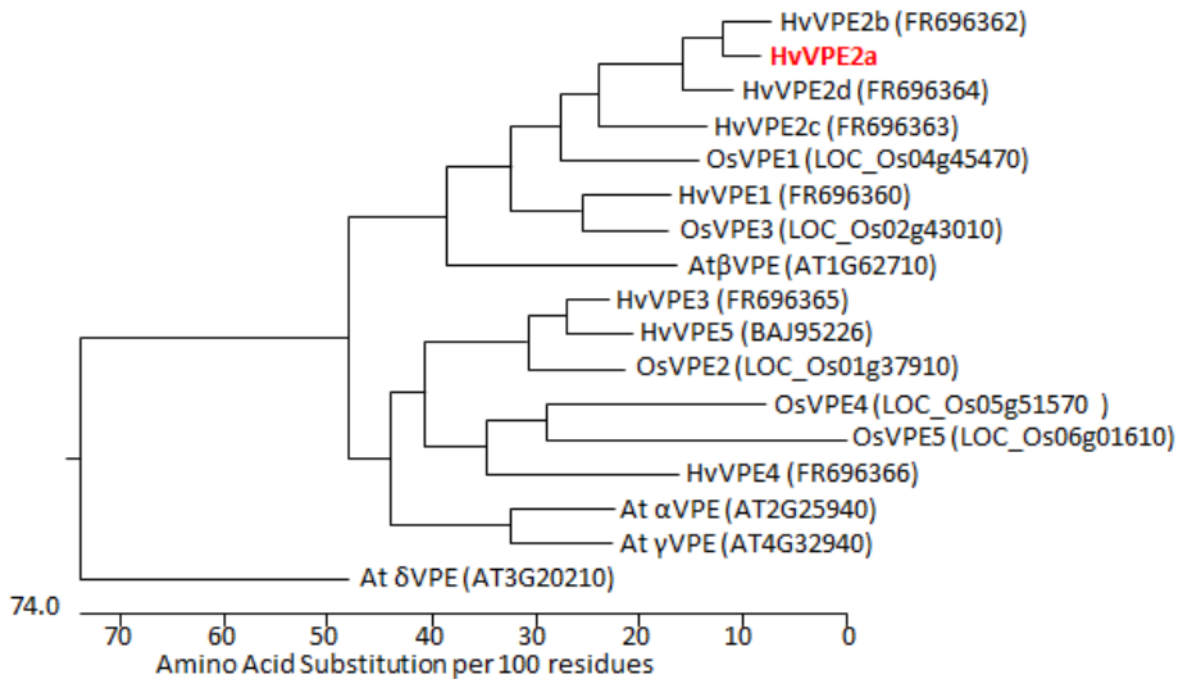


Figure 3.22 phylogenetic trees of barley, rice and Arabidopsis VPE2 proteins. The horizontal scale represents the evolutionary distance expressed as a number of substitutions per 100 amino acids. Barley VPE2a is shown in red color. GenBank accession numbers of the sequences are shown in brackets. Abbreviations: At, *Arabidopsis thaliana*; Hv, *Hordeum vulgare*; Os, *Oryza sativa*.

3.3.2 Repression of VPE activity in nucellar tissues

Because the deduced protein sequences of VPE2a, VPE2b and VPE2d are very similar (Fig. 3.22), and because expression of *VPE2a*, *VPE2b* and *VPE2d* genes is timely and spatially overlapping being predominantly detected in nucellus and nucellar projection of early developing barley grains (Fig. 3.5), functional redundancy among these proteins is highly expected. In this case, repression of only *VPE2a* transcripts may not result in phenotypic changes. Expression levels of the *VPE2b* gene are twice of those of *VPE2a* in the same tissue (Chapter 3.1). In order to repress the vacuolar processing enzyme activity in the nucellus and nucellar projection of the developing grains, a binary construct was produced capable to down-regulate the expression of *VPE2a-VPE2d* genes by RNAi (Fig. 2.2). For this, a fragment of *VPE2a* cDNA was selected which shares >96% identity to respective *HvVPE2b-HvVPE2d* regions and is expected to be sufficient for repression of the entire VPE activity in nucellus and nucellar projection.

3.3.3 Analysis of the VPE2i primary transformed plants and preparation of homozygous lines

In total, 22 putatively transgenic plants were recovered after transformation with the pVPE2i construct. The transgenic plants were characterized by Southern blot hybridization to identify the number of transgene copies integrated (Fig. 3.23). No *hpt* hybridization signal was detected for the non-transgenic control plant. Other lines showed integration of one (10 lines) and up to 4 copies (line 8).

Some of the selected lines were analysed for repression of *VPE2a-VPE2d* gene expression in developing grains by Northern blot analysis. Total RNA was extracted from four-day old caryopses and hybridized with a fragment of the *VPE2a* cDNA as a probe. Due to very high similarity of the *VPE2a* fragment to the *VPE2b* and *VPE2d* RNA, cross-hybridization of the probe with all transcripts of the subfamily is very likely. Analysis of gene-specific repression is therefore not possible by Northern blot analysis. The Northern blot data were however used to determine preliminary the levels of repression of *VPE2a-VPE2d* gene expression in caryopses of T₀ transgenic plants (Fig. 3.24).

Line 11 showed the strongest reduction of expression of *VPE2a-VPE2d* genes among all transgenic lines. The expression levels of lines 6 and 15 were similar to that of the wild type. The other lines showed different degrees of moderate reduction of the *VPE2a-VPE2d* transcript levels.

For further analyses the following lines were selected: VPE2i-11 with one transgene copy and strong reduction of the transcript level as a strong line; VPE2i-6 with one transgene copy and weak reduction of the transcript level as a weak line. Additionally, line VPE2i-5 was selected carrying two transgene copies. These transgenic copies co-segregated as registered in the following generations (Fig. 3.25).

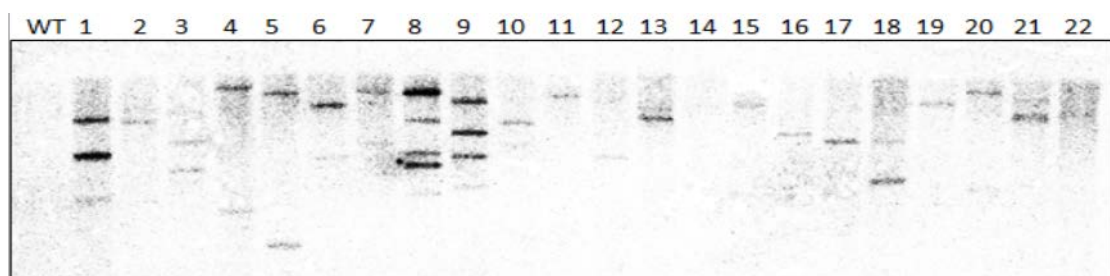


Figure 3.23 Southern blot hybridization of primary transgenic VPE2i plants using the *hpt* fragment as a probe. 1-22, number of regenerated plant lines; WT, untransformed control.

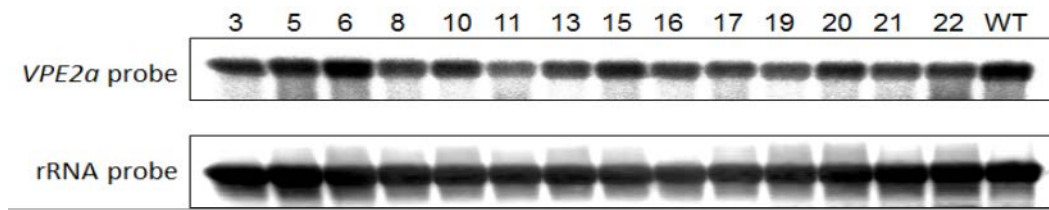


Figure 3.24 Expression of *VPE2a-VPE2d* genes in transgenic T_1 caryopses from plants transformed with pVPE2i construct. Because of high similarity between *VPE2a-VPE2d* nucleotide sequences, the data represent the transcript levels of all *VPE2a-VPE2d* genes after hybridization with the *VPE2a* probe (upper panel). 25S rRNA probe (below) was used as loading control. 3-22, independent transgenic lines; WT, wild type.

Stable integration of the transgene cassette was observed for the progenies of all selected lines as shown by PCR analysis of the T_2 generation. Segregation of transgenic *versus* non-transgenic plants was observed close to 3:1 as expected by Mendelian laws. Non-transgenic plants were discarded. One of these plants was selected for further propagation to the T_3 generation. Homozygous lines were selected from the self-pollinated progeny. Around 30 seeds from selected plants of the T_2 generation were sown and analyzed for the presence of the transgene in the T_3 generation by Southern blot hybridizations using the *hpt* gene fragment as a probe. VPE2i-6 and VPE2i-11 plants with a hybridization band in all progenies were considered as homozygous (Fig. 3.25). The homozygous line VPE2i-5 contained two transgene copies in its genome. These two copies were stably inherited to the following generations indicating that they were integrated in the same chromosome. The three homozygous lines shown in Fig. 3.25 were used for further characterization of the transgenic phenotype.

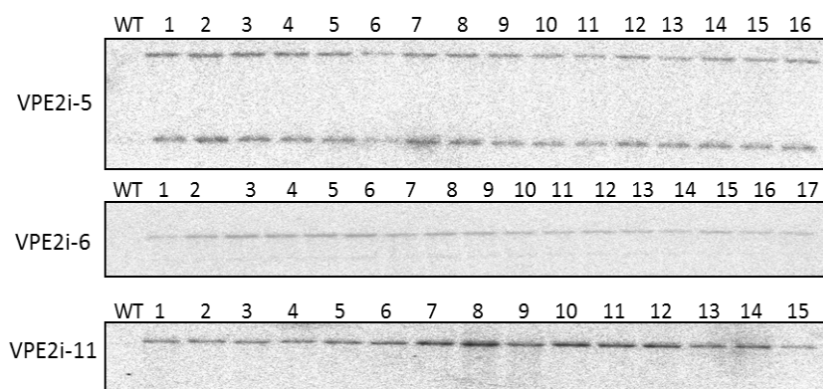


Figure 3.25 Representative Southern blots of the homozygote transgenic lines VPE2i-5 (above), VPE2i-6 (middle) and VPE2i-11 (below) after hybridization with the *hpt* gene fragment as a probe.

3.3.4 Analysis of expression of VPE2a to VPE2d genes in the homozygous VPE2i-transgenic plants

The expression of *VPE2a*, *VPE2b* and *VPE2d* genes was analyzed by qRT-PCR using gene-specific primers. The level of the *VPE2c* transcript was not analyzed because this gene is barely expressed in developing barley grains (Fig. 3.5; Tran *et al.*, 2014).

RNA was extracted from the manually dissected endosperm fraction of transgenic and control caryopses at 6 and 10 DAF, treated with DNase and used for reverse transcription and subsequent qRT-PCR. The *actin* gene was used as the reference gene to normalize all data. The primers for qRT-PCR were selected in gene-specific regions in order to distinguish

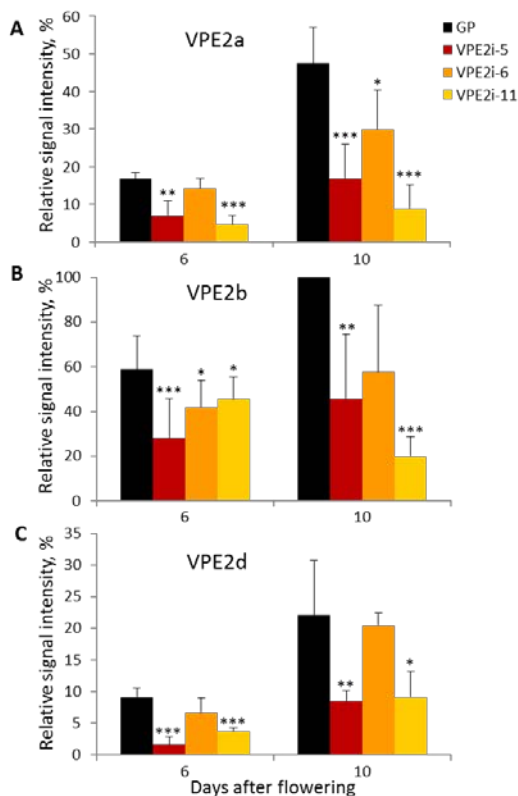


Figure 3.26 Analysis of *VPE2a* (A), *VPE2b* (B) and *VPE2d* (C) gene expression in the endosperm fraction of developing VPE2i-transgenic and untransformed control grains (GP) by qRT-PCR. Data are means \pm SD, n = 4, **t* significant at $P < 0.05$, ***t* significant at $P < 0.01$ and ****t* significant at $P < 0.001$.

between the gene family members (Radchuk *et al.*, 2011; Tran *et al.*, 2014). Significant repression of the *VPE2a* transcripts was detected for all transgenic lines at both developmental stages analyzed (Fig. 3.28 A). Strong *VPE2a* down-regulation was achieved in the lines VPE2i-5 and VPE2i-11, whereas line VPE2i-6 was characterized by weaker repression of *VPE2a* transcripts. Transcript levels of *VPE2b* and *VPE2d* genes were also down-regulated in all transgenic lines at both developmental stages (Fig. 3.26 B, C). However, the level of repression was reduced in comparison to the levels achieved for the *VPE2a* transcripts. As in the case of the *VPE2a* gene, the lines VPE2i-5 and VPE2i-11 showed stronger reduction of *VPE2b* and *VPE2d* transcripts, while line VPE2i-6 was characterized by weak down-regulation of *VPE2b* and no significant repression of *VPE2d* gene activity.

To conclude, selection of the conserved region for *VPE2a*, *VPE2b* and *VPE2d* genes for preparation of the RNAi construct resulted in successful transcriptional down-regulation of all these genes in the transgenic plants. Because the *VPE2b* gene is the most strongly expressed among all nucellar-specific VPEs, repression of its expression together with strong decrease of *VPE2a* transcript amount allow the speculation that enzyme activity of the nucellar specific VPE, as a protease with potentially caspase-1-like activity, might be decelerated.

3.3.5 Growth characteristics of VPE2i transgenic plants

Homozygous transgenic plants together with untransformed control plants were grown in the greenhouse and changes in the phenotypic characters were analyzed. No phenotypic differences between transgenic and wild type plants were observed until flowering. Phenotypic alterations were, however, visible during generative development, especially during late seed development.

Grain maturation and overall plant desiccation of the transgenic plants were delayed in comparison to non-transgenic control plants (Fig. 3.27 A). The transgenic plants required at least seven to 14 days longer to complete their life cycle. The plants of all three transgenic lines produced significantly lower numbers of seeds per spike compared with wild type plants (Fig. 3.27 C). Transgenic spikes of all analyzed lines frequently exhibited altered morphology compared to the wild type (Fig. 3.27 D). They were shorter than wild type spikes and often contained unfertilized or aborted seeds.

One or several small spikes were often formed at the basis of a main spike (Fig. 3.27 D). Formation of such additional spike is an indicator for internal or external stress factors (personal observation). Because secondary spikes were never or seldom built from wild type plants, it was concluded that such spike formation is due to VPE repression. In general, the extent of phenotypic alterations was dependent on the degree of down-regulation of *VPE2a-VPE2d* genes being strongly expressed in the VPE2i-11 line and to a lesser extent in VPE2i-5 and VPE2i-6 lines. Repression of the *VPE2a-VPE2d* expression resulted in phenotypic alterations of generative development in terms of spike morphology, grain number per spike and length of the growth period.

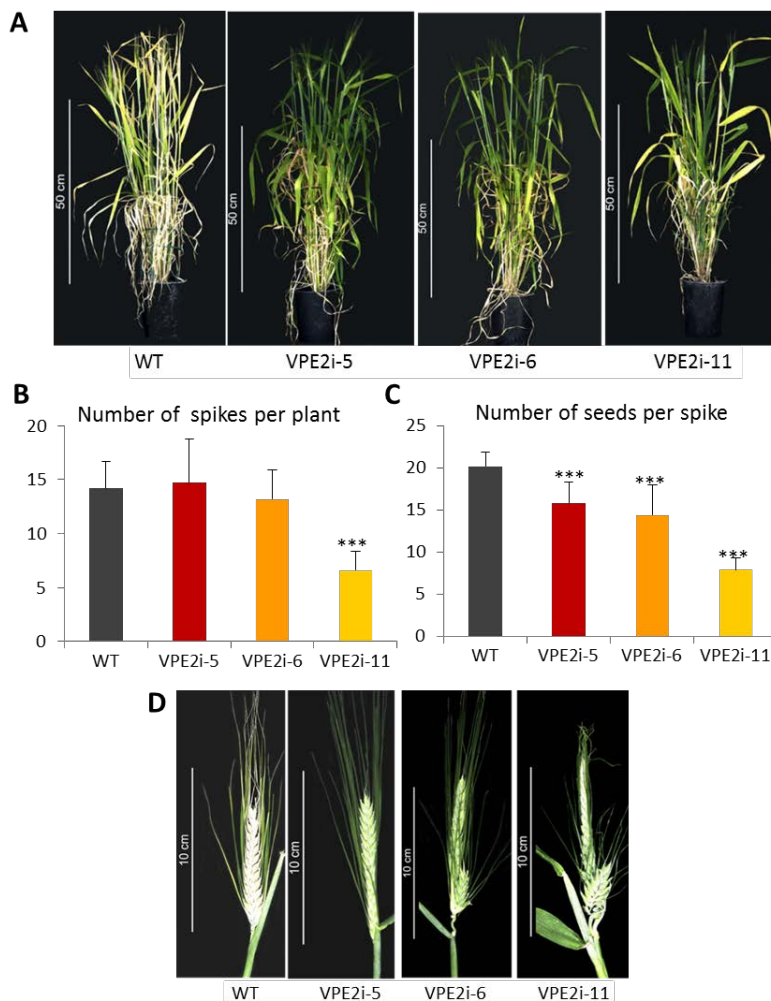


Figure 3.27. Phenotypic characters of the transgenic VPE2i-5, VPE2i-6 and VPE2i-11 plants compared to the untransformed control (WT). (A) General view on transgenic plants and untransformed control plant at seed storage phase. (B) Number of spikes per plant and (C) number of grains per spike in the VPE2i transgenic lines and WT. (D) General view on transgenic and untransformed spikes. Data are means \pm SD, $n = 10$ plants for (B) and $n = 30$ spikes from 10 plants for (B), *** t significant at $P < 0.001$.

3.3.6 Phenotype of mature seeds

Mature homozygous transgenic seeds are thinner than that of the wild type (Fig. 3.28 A). Significant reduction of transgenic grain weight was detected when compared to non-transgenic control seeds (Fig. 3.28 B). Seed width was not changed except in the VPE2i-6 lines where seed width was reduced (Fig. 3.28 C). All transgenic lines showed a tendency to longer seeds (Figure 3.30 D) with significant values for lines VPE2i-6 and VPE2i-11 (Fig. 3.28 D). However, despite increased seed length, seed weight was decreased for all transgenic lines (Fig. 3.10 B). This observation indicates that seed thickness has to be strongly reduced in all three transgenic lines pointing to disturbances in accumulation of storage compounds. Therefore, seed composition was analyzed in the mature grains. Proportion of total carbon was increased in grains of all transgenic lines compared to wild type grains (Fig. 3.29 A). Starch accumulation, however, was strongly decreased in mature seeds of all transgenic lines (Fig. 3.29 B).

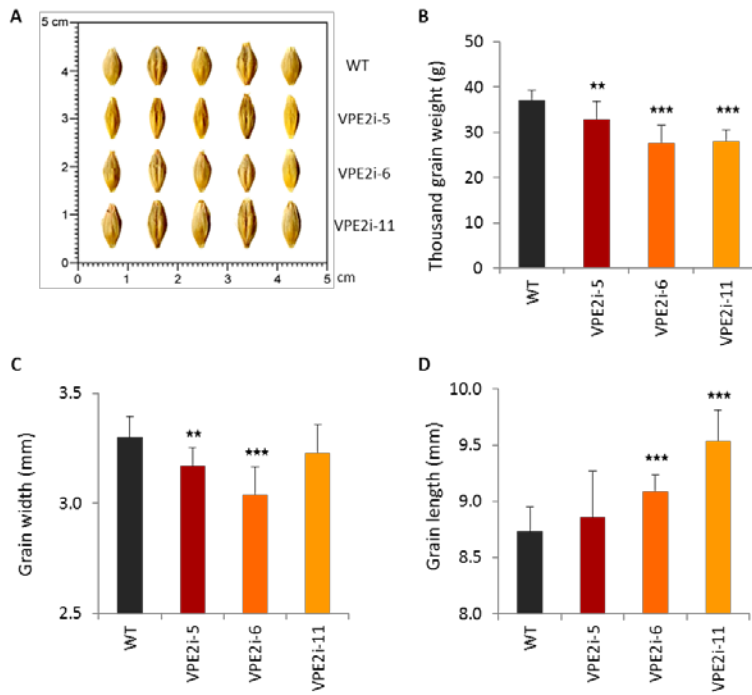


Figure 3.28. Phenotypic characters of mature VPE2i grains. (A) A general view on homozygous transgenic VPE2i grains compared to the wild type (WT). (B) Thousand grain weight, (C) grain width and (D) grain length of transgenic VPE2i-5, VPE2i-6 and VPE2i-11 grains and grains from non-transgenic control plants (GP). Data are means \pm SD, $n = 10$, * t significant at $P < 0.05$, ** t significant at $P < 0.01$ and *** t significant at $P < 0.001$.

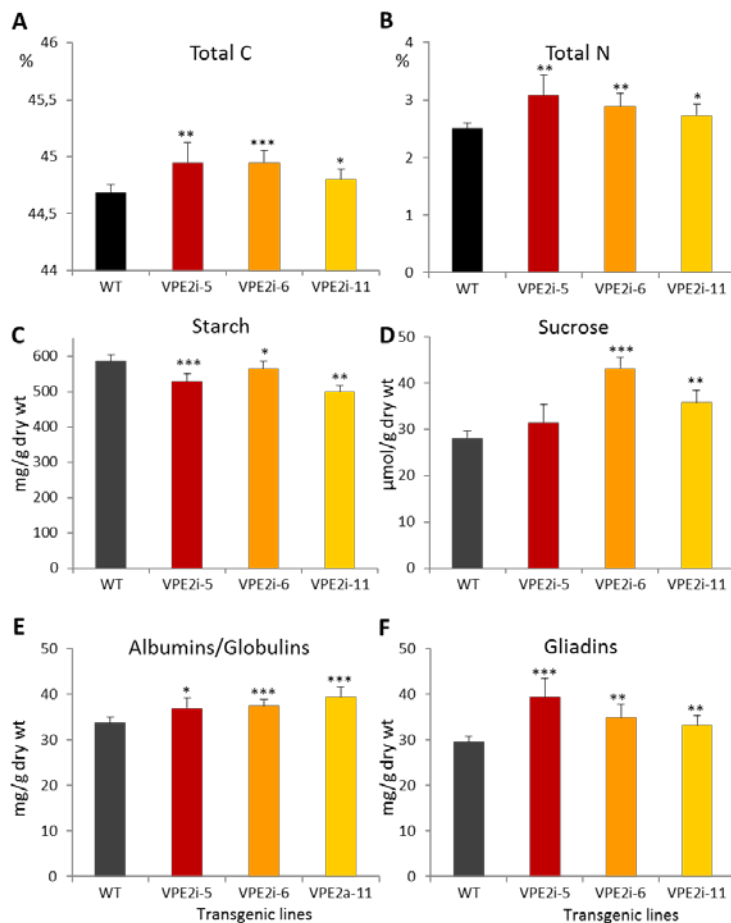


Figure 3.29. Composition of dry seeds. Total carbon (A), total nitrogen (B), starch (C), sucrose (D) and storage proteins (E, F) accumulation were detected in nature grains with repression of *VPE2a-VPE2d* genes and the wild type (WT) seeds. Data are means \pm SD, $n = 6$ for A and B, and $n = 10$ for C-D, * t significant at $P < 0.05$, ** t significant at $P < 0.01$ and *** t significant at $P < 0.001$.

The decrease in starch accumulation is well correlated with repression of *VPE2a-VPE2d* gene expression (Fig. 3.26). Because starch represents the bulk of storage compounds in dry barley seed, increase in total carbon was clearly not related to the starch fraction and must be due to accumulation of other storage compounds.

Levels of sucrose were increased in dry grains of all transgenic lines; however, this increase was significant only in lines VPE2i-6 and VPE2i-11 (Fig. 3.29 D). Total nitrogen content was also significantly increased in all transgenic seeds (Fig. 3.29 D) compared to wild type seeds. Total nitrogen content points to an increased protein level. To analyze the accumulation of different storage protein classes, total seed protein was extracted from mature grains and separated into the albumin/globulin and gliadin fractions. The amount of seed storage proteins of both fractions was increased in grains of all analyzed *VPE2*-repressed plants (Fig. 3.29 E, F). To conclude, repression of *VPE2a-VPE2d* expression resulted in lower amounts of accumulated starch, but increased sucrose and storage protein contents in mature grains.

3.3.7 Impact of down-regulation of nucellar-specific VPEs on seed germination

It has been reported that at least *VPE2b* is highly expressed in germinating seeds (Julian *et al.*, 2013). Reduced germination of VPE2i transgenic seeds was observed. This effect was analyzed in more details by germination tests in Petri dishes using seven biological repetitions with 25 seeds per repetition (Fig. 3.30). Wild type barley seeds germinated very prompt achieving nearly 100% of the germination rate already two days after imbibition. Transgenic seeds of all three lines showed reduced germination rate starting as early as one

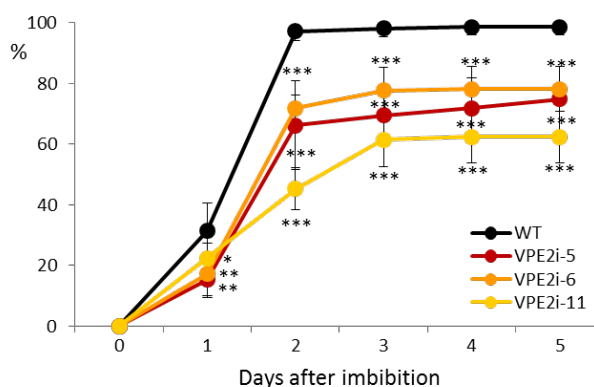


Figure 3.30 Germination rate of VPE2i-transgenic and non-transformed seeds. Data are means \pm SD, n = 7, *t significant at $P < 0.05$, **t significant at $P < 0.01$ and ***t significant at $P < 0.001$.

day after imbibition when compared to the wild type (Fig. 3.30). Maximum germination rate of line VPE2i-6 was around 80%, and only around 60% of the seeds of the VPE2i-11 line germinated. To conclude, the germination rate of the transgenic lines was significantly lower compared to the wild type indicating that down-regulation of the *VPE2a-d* gene subfamily interferes with seed germination.

3.3.8 Caspase-like activities in the endosperm fraction of VPE2i-repressed barley grains

Because VPE proteins are described to possess caspase-1-like activity, changes in this activity were measured in the endosperm fractions of developing transgenic grains with compromised expression of *VPE2a-VPE2d* genes (Fig. 3.31 A). Caspase-1-like activity was decreased in all transgenic grains especially at early development and this decrease correlated with combined repression of *VPE2a*, *VPE2b* and *VPE2d* genes at the corresponding stages of development (Fig. 3.26). Levels of caspase-4, caspase-6 and caspase-8-like activities decreased as well (Fig 3.33 B-D). To conclude, all analyzed caspase-like activities were strongly reduced in VPE2i transgenic grains.

The corresponding genes encoding proteins with caspase-4-like and caspase-8-like activities are still not described. However, it is known that caspase-6-like activity is performed by phytaspase in plants (Chichkova *et al.*, 2011). Of the three phytaspases found in barley, the *phytaspase 2* gene is predominantly active in nucellar tissues of developing barley grains (Tran *et al.*, 2014). Expression of this gene was analyzed by qRT-PCR.

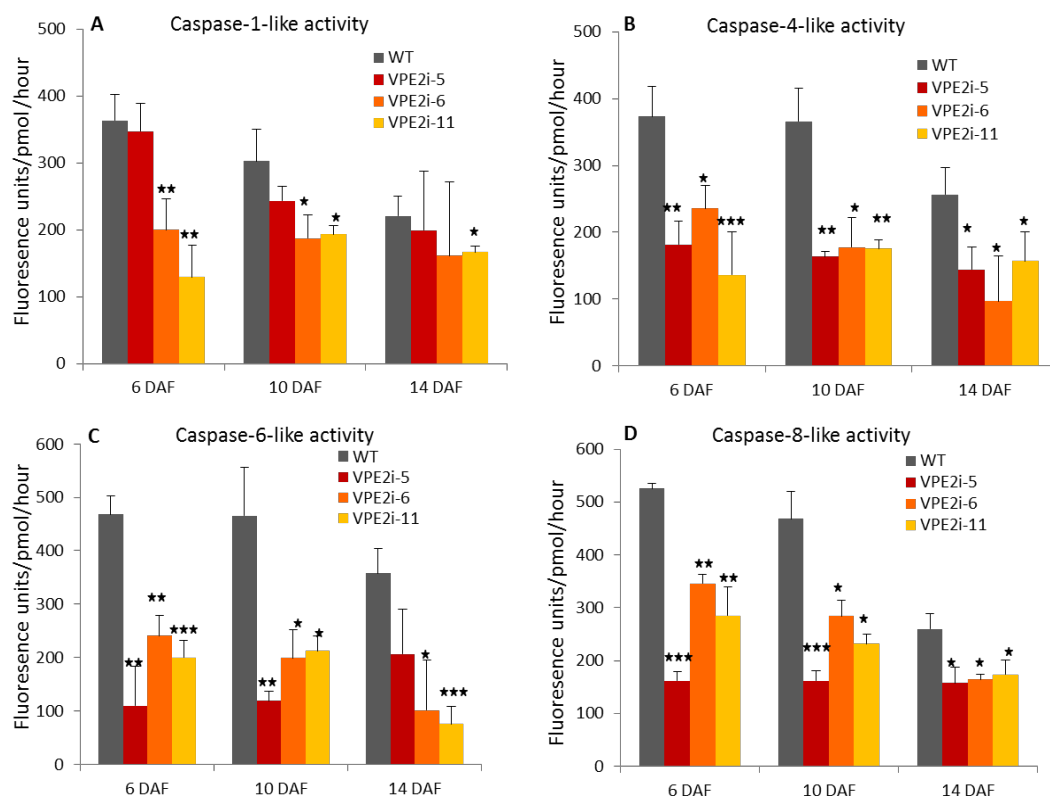


Figure 3.31 Caspase-1-like (A), caspase-4-like (B), caspase-6-like (C) and caspase-8-like (D) activities in developing grains of the three VPE2i-transgenic lines compared to the non-transformed control. Data are means \pm SD, n = 3, *t significant at $P < 0.05$, **t significant at $P < 0.01$ and ***t significant at $P < 0.001$.

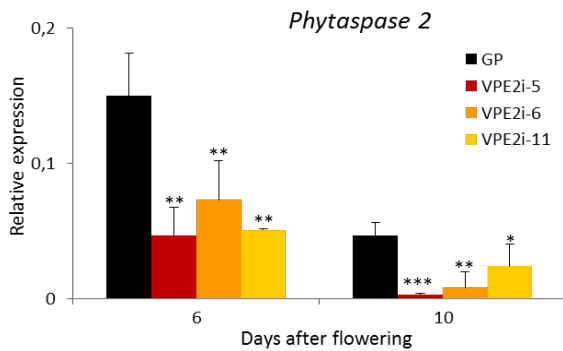


Figure 3.32 Analysis of *phytaspase 2* gene expression in the VPE2i-transgenic and untransformed control grains (GP) by qRT-PCR. Data are means \pm SD, n = 4, **t* significant at $P < 0.05$, ***t* significant at $P < 0.01$ and ****t* significant at $P < 0.001$.

Gene expression of *phytaspase 2* was strongly reduced in all three VPE2i transgenic lines compared to the wild type at both 6 and 10 DAF (Fig. 3.32).

Expression of the RNAi construct against *VPE2a* under control of *VPE2a* gene promoter resulted in transcriptional repression not only of *VPE2a* but also the very similar *VPE2b* and *VPE2d* genes. The results presented here have shown that down-regulation of the *VPE2a-VPE2d* genes reduced not only caspase-1-like activity but also caspase-4, caspase-6 and caspase-8-

like activities. Repression of *VPE2a-VPE2d* activity led to aberrant generative development of barley plants visible by changes in spike and grain morphology and extended plant life cycle. Knock-down of *VPE2a-VPE2d* genes in the developing grains resulted in decreased starch and increased seed storage protein accumulation. The dry weight of mature seeds was reduced in all transgenic lines reflecting negative influences on growth of the endosperm. The number of seeds reaching maturity was lower in all transgenic lines compared with the wild type, the number of spikes per plant and the numbers of seeds per spike were also reduced in VPE2-repressed transgenic plants.

3.4 Interaction of the MADS29 transcription factor with promoter sequences of *VPE2a* and *Jekyll* genes, both involved in PCD of nucellar tissues

3.4.1 Cloning and phylogenetic analysis of gene MADS29 from barley

A search in the barley full length cDNA database using the *MADS29* cDNA from rice sequence as query resulted in a hit, here denoted as barley *MADS29* (GenBank accession number AK375718). RT-PCR was applied to clone *HvMADS29* cDNA from total RNA isolated from early developing caryopses using gene-specific primers. The deduced *HvMADS29* peptide sequence shared 80.2% identity with *OsMADS29*, and belongs to the monocot sub-cluster of the B_{sister}-type of MADS box transcription factors (TF) (Fig. 3.33 A).

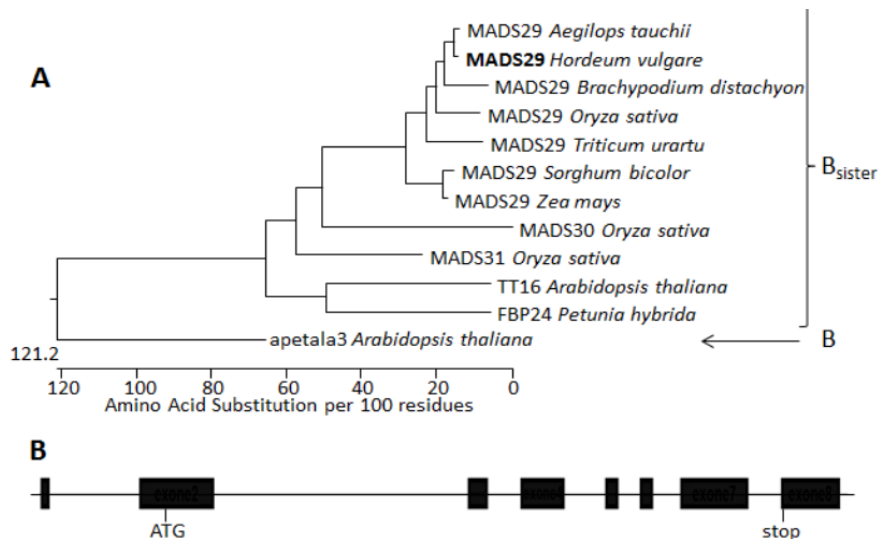


Figure 3.33 The phylogenetic tree of the B_{sister} clade of selected MADS box TFs (A) and the exon-intron structure of the barley MADS29 gene (B). The horizontal scale in (A) represents the evolutionary distance expressed as a number of substitutions per amino acid. The barley MADS29 is shown in bolt. Arabidopsis APETALA3 from the clade B is used for out-group. Exons in (B) are given by black boxes. GenBank accession numbers of the sequences are as follows: *Aegilops tauchii*, EMT28524; *Arabidopsis thaliana*, APETALA3, At3g54340, TT16, AT5G23260; *Brachypodium distachyon*, NP_001288325; *Hordeum vulgare*, BAK06913; *Oryza sativa*, MADS29, LOC_Os02g07430, MADS30, LOC_Os06g45650, MADS31, LOC_Os04g52420; *Petunia hybrida*, AAK21255; *Sorghum bicolor*, XP_002453370; *Triticum urartu*, EMS53774; *Zea mays*, CAC81053.

As deduced from the corresponding genomic fragment (Morex_contig50953) from full length barley genome sequence (International Barley Genome Sequencing Consortium, 2012), the genomic MADS29 sequence includes seven introns, the first of which is present in the 5' untranslated region (Fig. 3.33 B).

A search in the barley full length cDNA database using the MADS29 cDNA from rice sequence as query resulted in a hit, here denoted as barley MADS29 (GenBank accession number AK375718). RT-PCR was applied to clone HvMADS29 cDNA from total RNA isolated from early developing caryopses using gene-specific primers. The deduced HvMADS29 peptide sequence shared 80.2% identity with OsMADS29, and belongs to the monocot sub-cluster of the B_{sister} -type of MADS box transcription factors (TF) (Fig. 3.33 A). As deduced from the corresponding genomic fragment (Morex_contig50953) from full length barley genome sequence (International Barley Genome Sequencing Consortium, 2012), the genomic

MADS29 sequence includes seven introns, the first of which is present in the 5' untranslated region (Fig. 3.33 B).

3.4.2 MADS29 is expressed in the reproductive organs of barley

MADS29 expression was analyzed first by Northern blot in hand-separated pericarp, endosperm and embryo fractions. *HvMADS29* transcripts were detectable in the endosperm fraction between 2-14 days after flowering, but neither in the pericarp nor in the embryo fraction (Fig 3.36 A). The endosperm fraction represents a mixture of both filial (endosperm, endosperm transfer cells, aleurone layer and embryo-surrounding region) and maternal tissues (the nucellus, nucellar projection and chlorenchyma in some of the developmental stages) (Sreenivasulu *et al.*, 2006). To study the tissue-specific gene expression we used qRT-PCR of total RNA isolated from micro-dissected samples of these tissues from grains at different developmental stages. Expression of *HvMADS29* was restricted to the nucellus and nucellar projection, peaking at around two days after flowering (Fig. 3.34 B).

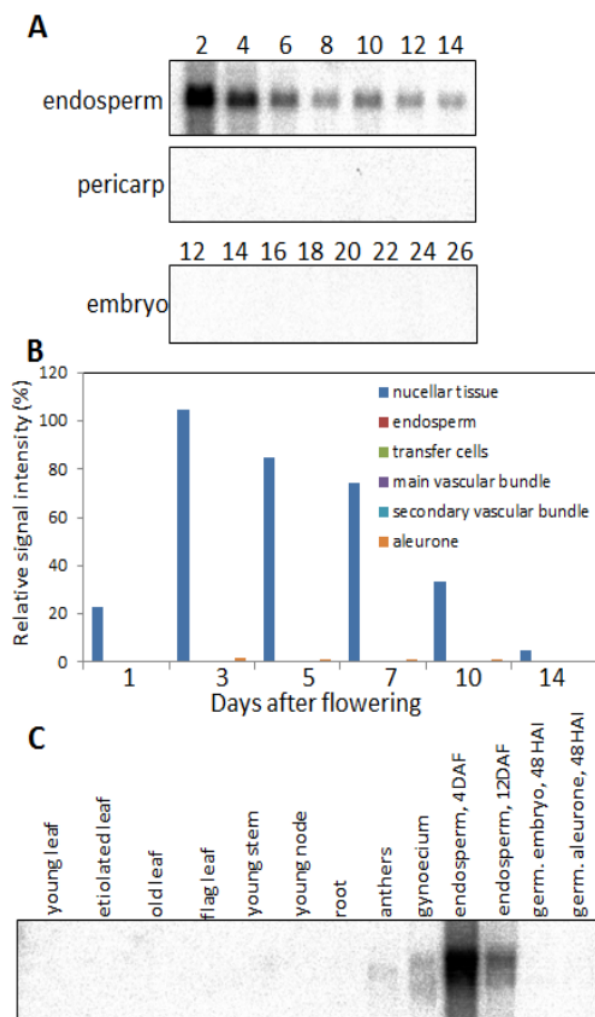


Figure 3.34. Expression of *MADS29* in barley. A) Northern blot analysis of *MADS29* expression in endosperm fraction, pericarp and embryo of developing barley grains. B) Expression profiles of *MADS29* in different tissues micro-dissected from developing barley grains as analysed by qRT-PCR. C) Presence of the *MADS29* transcripts in different barley tissues as detected by Northern blot analysis.

Transcripts were also detected at high level in the gynoecium of immature florets and at low level in the anthers, but neither in vegetative tissue nor in germinating grains (Fig. 3.34 C).

To conclude, *HvMADS29* is predominantly active in developing flowers and seeds. In developing seeds, *HvMADS29* is preferentially expressed in nucellus and nucellar projection, the nurse tissues that are devoted to PCD ensuring nutrient transfer to the filial organs and providing space for the expanding endosperm, respectively (Radchuk and Borisjuk, 2014).

3.4.3 *HvMADS29* binds to *Jekyll* and *VPE2a* gene promoter regions

Rice *MADS29* has been shown to regulate PCD in developing grains specifically recognizing *CARG cis*-motifs of target gene promoters (Yin and Xue, 2012). As shown in the subchapter 3.3, the *VPE2a* gene (together with *VPE2b* and *VPE2d*) is required for PCD in the nucellar tissues of developing barley grains. It was shown, that *Jekyll* is the regulator of PCD in nucellus and nucellar projection of developing barley grains (Radchuk *et al.*, 2006). The expression maximum of all three genes was detected in the endosperm fraction (which always contains nucellar tissues; Sreenivasulu *et al.*, 2006) during early grain development. No expression was detected in the pericarp fraction or in the developing embryo (Fig. 3.34). Expression profile of the *MADS29* gene largely coincides with those of *VPE2a* and *Jekyll* genes (Fig. 3.35) suggesting that *MADS29* may be a transcriptional regulator of *VPE2a* and *Jekyll* gene expression.

Promoter regions (1000 nt 5' upstream of the ATG start codon) of both *VPE2a* and *Jekyll* genes contain several *CARG*-like sequences (Fig. 3.36). There are four *CARG* motifs in the promoter of the *VPE2a* gene while the *Jekyll* promoter contains three *CARG*-like motifs. This finding further supports the hypothesis that *MADS29* can be a regulator of these genes.

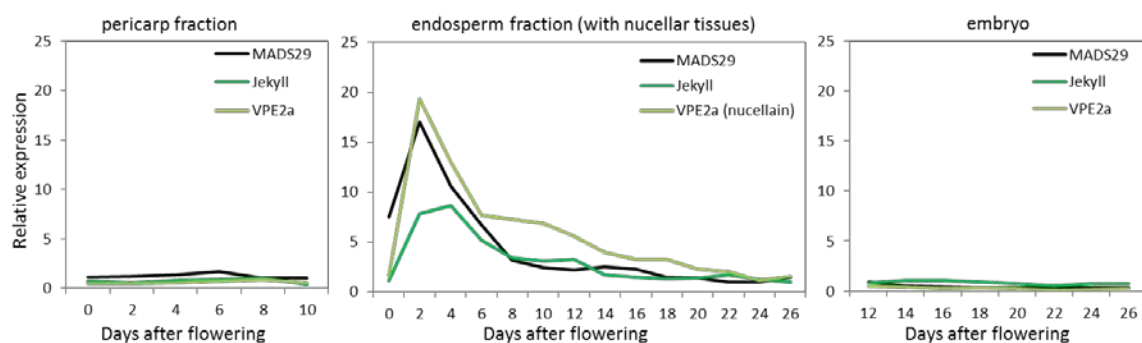


Figure 3.35 Co-expression of *MADS29* with *Jekyll* and *VPE2a* genes in developing barley grains (derived from the expression studies published by Sreenivasulu *et al.* 2006).

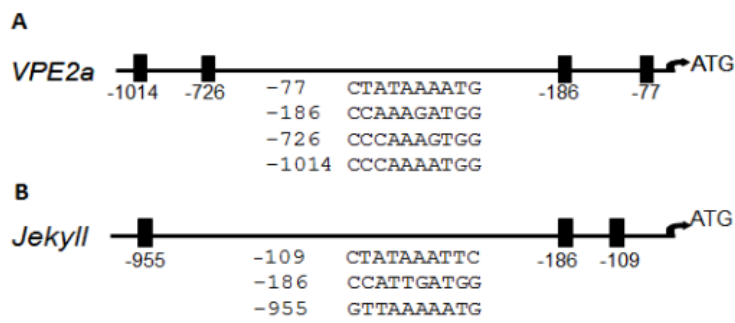


Figure 3.36 Positions (black boxes) and sequences of CAzG-like motifs in the 1000 nt promoter regions of *VPE2a* (A) and *Jekyll* (B) genes. Sequences of the corresponding CAzG motifs are shown below the scheme of the respective promoter.

In order to prove whether barley MADS29 may be a regulator of *VPE2a* and *Jekyll* gene expression, we analyzed the physical interaction of HvMADS29 with CAzG motifs of their promoter sequences.

3.4.4 Production of the recombinant MADS29 protein

Full-sized recombinant MADS29 protein was produced in *E. coli* cells. To express the recombinant MADS29 protein, the coding sequence of MADS29 was amplified by PCR introducing *Bam* HI and *Hind* III restriction sites, digested with the corresponding enzymes and cloned into pET32a in frame using the *Bam* HI/*Hind* III restriction sites (Fig. 3.37). The resulting recombinant protein consists of 429 amino acids with a calculated molecular mass of 47.5 kDa.

The MADS29 protein was produced in *E. coli* cells and purified using His-tag by Ni-NTA resin. Quality of the protein isolation was monitored by Coomassie Blue staining (Figure 3.39 B) and Western blot analysis using the monoclonal antibody against His-tag (Fig. 3.38 A). Produced and purified recombinant MADS29 protein was of the predicted weight (Fig. 3.38).

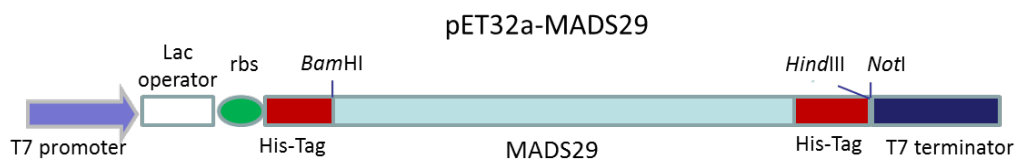


Figure 3.37 Schematic drawing of the construct pET32a-MADS29 for over-expression of the *MADS29* gene in *E. coli* cells.

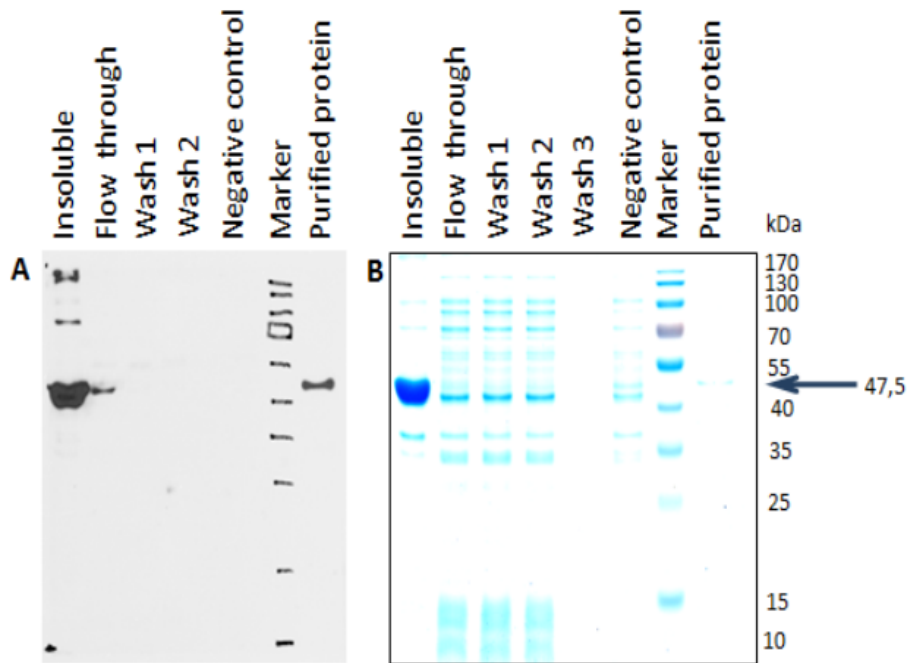


Figure 3.38 Purification of the barley MADS29 recombinant protein as confirmed by Western blot (A) and Coomassie Blue staining (B).

3.4.5 Binding of MADS29 protein to the CARG motifs of the VPE2a promoter

Binding of MADS29 to four CARG-like motifs of *VPE2a* was analyzed *in vitro* by an ELISA assay (Mönke *et al.*, 2004). The sequence from the *VPE2a* promoter without CARG motif was used as a control (Fig. 3.39 A). The MADS29 protein was able to bind to all CARG motifs albeit at different efficiency (Fig. 3.39 B). The strongest binding was observed to the CARG box located closest to the start codon. The farther the location of CARG motif was from the start codon, the weaker was the binding to MADS29 (Fig. 3.39 B). Artificial mutations introduced in every CARG *cis*-element resulted in either a strong decrease in binding or even to its abolition (Fig. 3.39 C). Addition of as little as 10 pmol of unlabeled DNA sequence with CARG box to the reaction almost completely competed binding of the MADS29 protein to labeled DNA (Fig. 3.39 D). To conclude, MADS29 protein recognizes and binds to CARG-like motifs of the sequences located 5'-upstream of the *VPE2a* coding region.

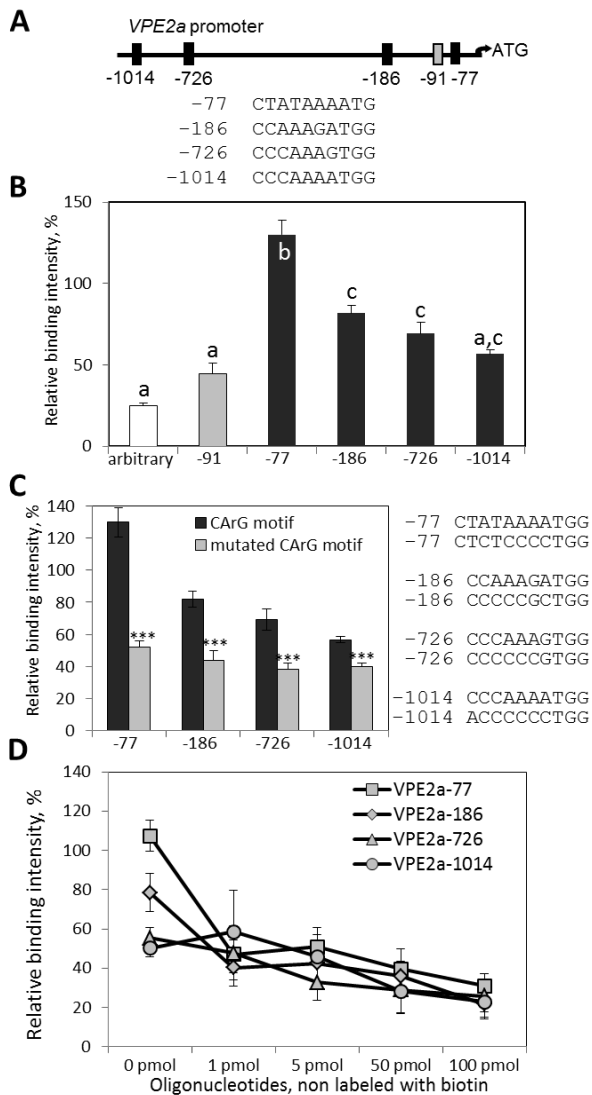


Figure 3.39 MADS29 protein binding to *HvVPE2a* promoter sequences. (A) The positions of the CARG-like motifs (black boxes) in the *HvVPE2a* promoter. Sequences of the corresponding motifs are shown below. Promoter fragment without CARG motif used for a control reaction is shown as a grey box. (B) Intensity of binding of MADS29 to CARG motifs of the *HvVPE2a* promoter (\pm SD, $n \geq 4$; different letters indicate significance between pairs according to *t* test at $P < 0.05$). Arbitrary sequence (white bar) and a sequence from the *VPE2a* promoter without CARG motif (grey bar) are used as negative controls. (C) Mutations of CARG-motifs (shown right) abolish binding of MADS29 to the corresponding CARG element (\pm SD, $n \geq 4$, ****t* significant at $P < 0.001$). (D) Unlabeled DNA fragments effectively compete the binding of MADS29 (average values \pm SD).

3.4.6 Binding of MADS29 protein to the CARG motifs of the *Jekyll* promoter

The ability of MADS29 to bind to the CARG-like motifs of the *Jekyll* gene promoter was also analyzed *in vitro* by ELISA (Mönke *et al.*, 2004). A promoter fragment without any CARG-like motif was selected as a negative control. MADS29 bound directly to all three CARG elements of the *Jekyll* promoter but not to arbitrary DNA or to the fragment of the *Jekyll* promoter without CARG motif (Fig. 3.40 B). Artificial mutations in every CARG *cis*-element by changing adenine by cytosine residues strongly decreased the MADS29-CARG motif interaction (Fig. 3.40 C) indicating that MADS29 specifically bind to the CARG elements of the promoter. Adding of unlabeled DNA fragments with the corresponding CARG motif to the reaction effectively competes out the MADS29 interaction with biotin-labeled DNA confirming the specificity of the reaction (Fig. 3.40 D).

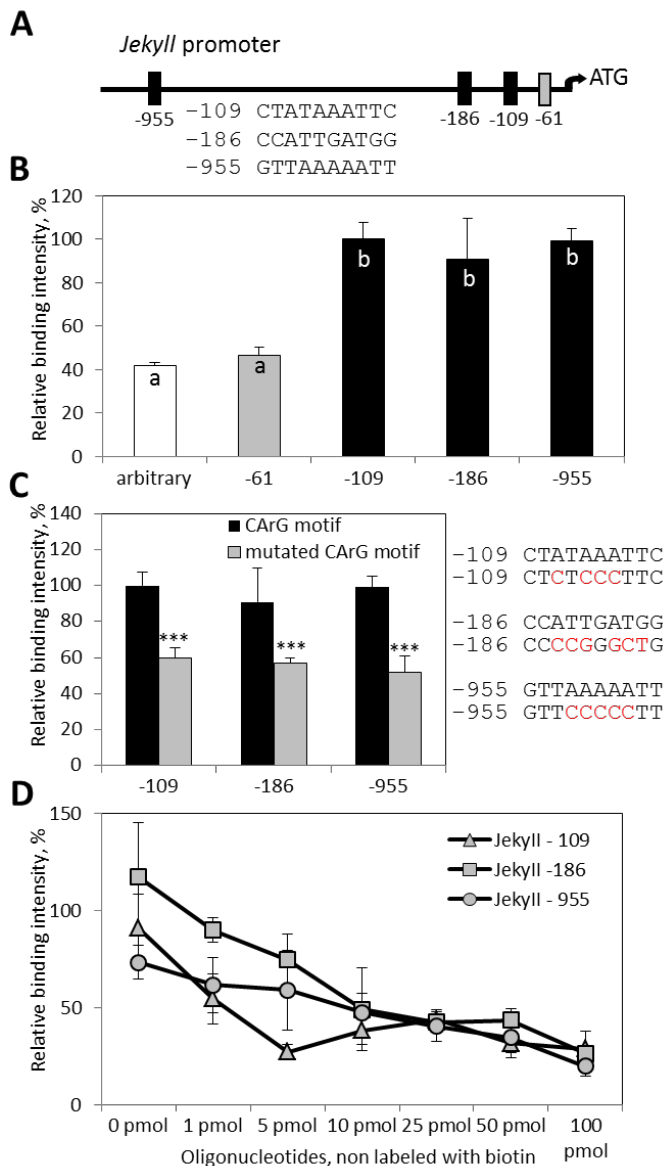


Figure 3.40 MADS29 protein binding to *Jekyll* promoter sequences. (A) The positions of the CARG-like motifs (black boxes) in the *Jekyll* promoter. Sequences of the corresponding motives are shown below. The promoter fragment without CARG motif used for a control reaction is shown as a grey box (-61). (B) Intensity of binding of MADS29 to CARG elements of the *Jekyll* promoter (\pm SD, $n \geq 4$; different letters indicate significance between pairs according to *t* test at $P < 0.001$). Arbitrary sequence (white bar) and a sequence from the *Jekyll* promoter without CARG motif (grey bar) are used for negative controls. (C) Mutations of CARG-boxes abolish binding of MADS29 to the corresponding CARG element (\pm SD, $n \geq 4$, ****t* significant at $P < 0.001$). CARG motif nucleotides changed by mutations are showed at right. (D) Unlabeled DNA fragments effectively compete out the binding of MADS29 (average value \pm SD).

3.4.7 Multiple copies of CARG cis-elements are present in the promoter sequences of genes transcriptionally active in the nucellar tissues

The presence of CARG-like motives in the promoters of genes which are both active in the nucellar tissues and potentially involved in PCD was taken as *prima facie* evidence of their likely transcriptional regulation by HvMADS29. *MADS29*, *Jekyll* and *VPE2a* genes are co-expressed with 37 other genes from sub-cluster 3_1 described in Sreenivasulu *et al.* (2006), (Table S1). We assumed that the majority of these genes might be expressed in the nucellar tissues. Potentially PCD-related *VPE2b*, *VPE2d* and *phytopase2* genes are predominantly active in the nucellar tissues (Tran *et al.* 2014). Promoter regions (1,000 nt 5' upstream of

the ATG start codon) of 20 genes with proven or tentative nucellar-specific expression were depicted from the whole barley genome sequence (International Barley Genome Sequencing Consortium, 2012) and analyzed for the presence of CARG-like motifs. The majority of the promoter sequences harbored multiple *cis* CARG elements (Fig. 3.41, Table 3.1 and 3.2). For example, the *VPE2b* and *VPE2d* promoters each harbor four CARG *cis*-elements. It was shown in chapter 3 that *VPE2b* and *VPE2d* participate in PCD of nucellar tissues. The promoter region of *phytaspase 2* harbored five *cis* CARG elements. *Phytaspase 2* is predominantly expressed in the nucellar tissues of early developing barley grains (Tran *et al.*, 2014) and potentially possesses caspase-6-like activity thereby being involved in PCD. In most of the cases, the *cis* CARG elements are duplicated or even triplicated at short segments of the promoter (Fig. 3.41).

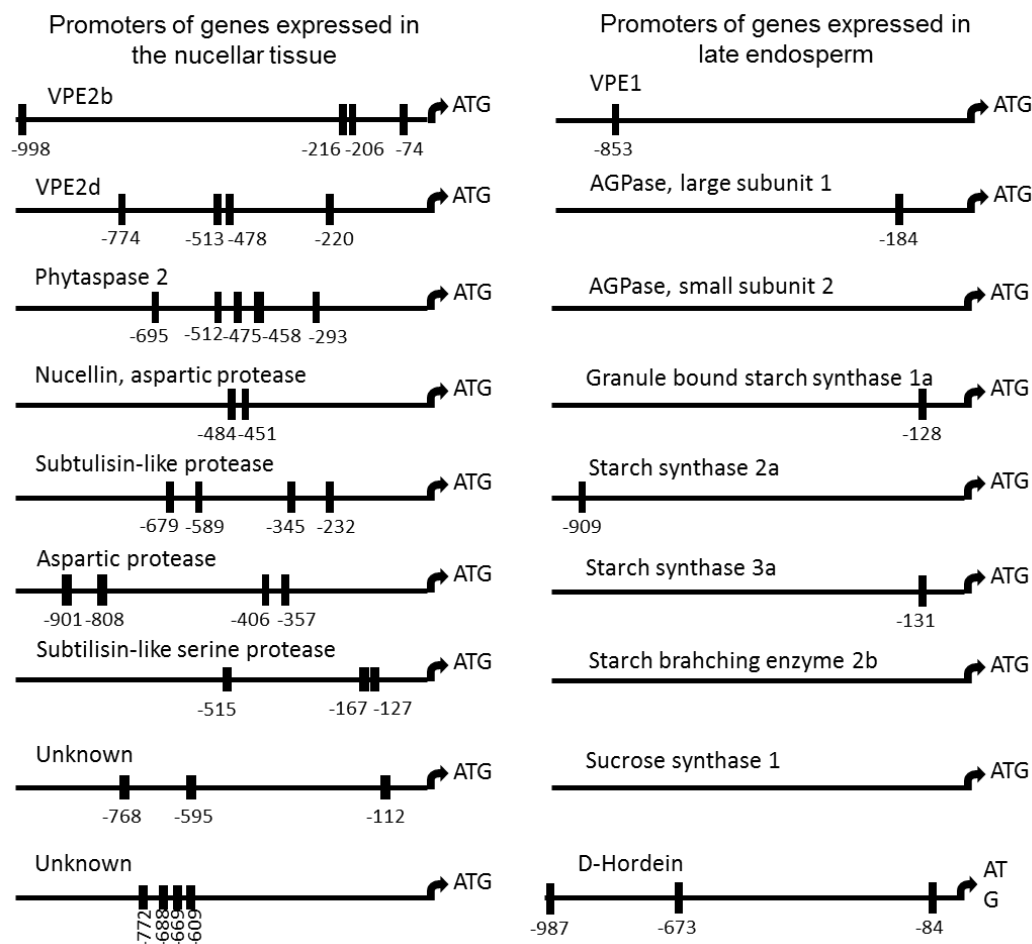


Figure 3.41 Presence of CARG-like motifs in promoters of genes expressed in nucellar tissues and late endosperm. The presence and positions of CARG-like motifs (black boxes) in selected promoters of genes predominantly expressed in the nucellar tissues (left) and in late endosperm (right).

Table 3.1 CARG-like cis-elements in selected promoter sequences of genes predominantly expressed in the endosperm.

Genbank acc. (EST)	Gene annotation	Genbank acc. (full length cDNA)	Genbank acc. (genomic region with corresponding gene promoter)	Positions and sequences of the detected CARG-like motifs				
BQ472756	ADP-glucose transporter	AY560327	CAJW011568487	-106	CATTTT TAGG	-327	CTATATT TAG	
AL507015	AGPase large subunit 1	X67151	CAJW010135957	-184	CCCATGAAAG			
BU983885	AGPase small subunit 2	AF537363	CAJW010041650		no			
BU982243	Granule bound starch synthase 1a	AF486518	CAJW010049158	-128	CTTATGTTTG			
BU966952	Starch synthase 2a	AY133250	CAJW010161604	-909	CTTATATTAG			
BU970315	Starch synthase 3a	JN256950	CAJW010041334	-131	CCAATTTTAG			
BU967173	Starch branching enzyme 2b	AF064561	CAJW010063263		no			
BU973936	pullanase	AF122050	CAJW010121135	-535	CACATGAAAG			
BU985795	Vacuolar processing enzyme 1 (VPE1)	FR696360	CAJW010274612	-853	CAATTAAAGG			
AL506916	alpha-amylase inhibitor,	U47641	CAJW010049644	-777	CTCATATTAG			
CA020993	Sucrose synthase 1	AK248622.1	CAJW011561797		no			
BU972873	vacuolar targeting receptor	AK374393	CAJW010049686	-180	CCATATTTGG			
AL511111	aminocyclopropane-1-carboxylate synthase (EC 4.4.1.14) 2 - wheat	AK364695	CAJW010136941	-214	CTATAAATAG			
AL509489	alpha-hordothionin precursor	AK366145	CAJW010135103	-400	CATTATATG	-728	CAAAATAAAG	-858 CTTATGTAGG
BQ459861	beta-hordothionin	AK374439	CAJW010275278		no			
BU968623	Cysteine proteinase 1	AK361896	CAJW010085326	-580	CTCTATTTTG	-665	CTTATAATAG	-898 CACTATATTG
BU971796	D-Hordein	AK373042	CAJW010273630	-84	CCTATAAAAG	-673	CAATTAGTTG	-987 CAATTATAAG
AL512203	Gamma-Hordein 3	AK251750.1	CAJW010052005	-96	CTATAAATAG	-208	CACTTGTAAG	
BU988592	endopeptidase	AK375678	CAJW010244144	-673	CCTAAATTAG			
BU967017	aspartic proteinase	AK252296.1	CAJW010048756	-191	CTAATTAAGG	-241	CCTAATTTTG	
BQ472349	DegP2 protease	AK376618	CAJW010042584	-538	CATAATGTGG	-549	CAAAAAGATG	-591 CCTAAAGATG

Table 3.2 CARG-like cis-elements in selected promoter sequences of genes predominantly expressed in nucellar tissues.

	Genbank acc. (EST)	Gene annotation	Genbank acc. (full length cDNA)	Genbank acc. (genomic region with corresponding gene promoter)	Positions and sequences of the detected CARG-like motifs
Genes with known localization of expression predominantly in the nucellar tissues	AL510768	VPE2a	FR696361	CAJW010245248	-77 CTATAAAATG -186 CCAAAGATGG -196 CATTTTGAAG -726 CCCAAAGTGG -747 CAATTTTTGG -1014 CCCAAAATGG
	AL507464	VPE2b	FR696362	CAJW012552891	-74 CTATAAAATG -206 CAAAAAATGG -216 CATTTTGAAG -998 CCATAGGATG
	N/A	VPE2d	FR696364	CAJW010136091	-220 CATTTTGAAG -478 CTATTTTTTG -513 CCCAAAGAAG -774 CCCTTTTTTG
	N/A	Phytaspase 2	AK356015	CAJW010049548	-293 CACTTGTAAG -458 CAATTATATG -475 CCCAATGATG -512 CTAAAATAG -695 CTTTTTTTTG
	N/A	Phytaspase 3	AK358242	CAJW010138503	-802 CAATAAATGG
	BU980232	nucellin	U87149	CAJW010038970	-451 CATTAAATTTG -489 CAAAAATATG
	BU976203	Jekyll2	AK375232	CAJW010045863	-953 CTCTAAGTTG -999 CTATAAAATG
Genes with predicted localization of expression in the nucellar tissues	FD527996	subt. protease	AK356656	CAJW011645383	-232 CCTTAGGATG -245 CAAATTTTTG -589 CACATATATG -679 CATTTTTTATG
	BU983421	nucellin-like aspartic protease	AK368577	CAJW011566115	-357 CTCTAGAAAG -406 CATTTTAAAG -888 CTCTAAAAAG -901 CCTTTATTGG
	AL511831	subtilisin-like serine protease	AK372403	CAJW010136296	-127 CACATAATTG -167 CATAAGATAG -515 CAAATTAAGG
	BQ460303	endo-beta-1,4-glucanase	AK375111	CAJW010046932	-606 CTTTAAAATG -975 CCATTGAATG
	CB883749	unknown	AK372388	CAJW010135588	-591 CACATTTTGG -942 CAAAAGATAG
	BU982383	Lipid transfer protein 3	AK376365	CAJW010136343	-919 CCATTTATTG -1050 CACAAAATGG
	BQ460163	unknown	AK375143	CAJW011586546	-112 CCCATATAAG -595 CAATATATAG -768 CATTTTGAGG
	HA31N07	unknown (nucellus specific)	AK377005	CAJW010159836	-609 CAATAATTTG -669 CTAAAATGG -722 CATTATTTTG -788 CTTTAGATTG
	BU981685	putative cell wall protein	AK376582	CAJW010101421	-560 CTAATGAAAG -892 CCATTAATGG
	BU980354	nodulin MtN21/EamA-like transporter family protein	AK373532	CAJW010051049	-789 CACTTGAAG -814 CCAATGATAG
	BQ469810	Proline-rich protein	AK252852.1	CAJW010245610	-105 CTCATGGTTG -650 CTAATGGTTG -902 CATATAATTG
	BU978933	calcium-binding EF-hand family protein	AK376205	CAJW010134001	-144 CTATTGTTGG -388 CCATTTGTTG -601 CTATTTTATG
	BU973392	unknown	AK373045	CAJW010056123	no
	BU981494	unknown	AK377005	CAJW010159836	-609 CAATAATTTG -669 CTAAAATGG -722 CATTATTTTG -788 CTTTAGATTG

Promoters of genes specifically expressed in the late developing endosperm, such as VPE1 (Radchuk *et al.* 2011) and genes encoding enzymes of starch biosynthesis (Radchuk *et al.* 2009), were used for control. These genes together with more than 800 other genes belong to the sub-cluster 5_3 of genes active during late grain development (Sreenivasulu *et al.* 2006). Promoters from 20 randomly selected genes of sub-cluster 5_3 were analyzed. CArG elements were infrequent in the promoters of this control set of genes. For example, the promoters of the genes encoding sucrose synthase 1, small subunit 2 of AGPase and β -hordothionin all lack a CArG-like sequence (Figure 3.42; Table 3.1 and 3.2). In those cases when more than two CArG elements were present, they were not duplicated (e.g., the *hordein D* promoter). The promoters of the genes encoding cysteine proteinase 1, aspartic proteinase and DegP2 protease harbored either two or three CArG motifs.

Taken together, the promoters of genes active in the nucellus harbor 2.95 ± 1.19 CArG-like motives, while those associated with endosperm-specific transcription harbor just 1.33 ± 1.02 motives; the difference is statistically significant ($P < 0.001$).

The results presented in the subchapter 3.4 have shown that the *MADS29* TF is exclusively expressed in the nucellus and nucellar projection of developing barley grains. ELISA assay revealed the interaction *in vitro* between the *MADS29* protein and CArG-like boxes of the promoter regions of *Jekyll* and *HvVPE2a* genes, both required for PCD of nucellar tissues.

4. Discussion

Programmed cell death (PCD) is an essential part in the life of any multicellular organism. Whole development of the barley grain and other cereal seeds is accompanied by regular cellular disintegration. In this dissertation, PCD events in maternal tissues of the developing barley caryopsis have been visualized by TUNEL assay and correlated with known processes of cellular disintegration. Several caspase-like activities have been determined in both pericarp and endosperm fraction with coinciding patterns to PCD events in the respective tissue. Further, the role of vacuolar processing enzymes (VPE4) and VPE2a-VPE2d in PCD execution has been studied. Finally, a potential transcriptional regulator HvMADS29 of *VPE2a* and *Jekyll* genes, both involved in PCD of nucellar tissues, was cloned and its abilities to bind to specific promoter elements has been analyzed.

4.1 Caspase-like activities is associated with PCD events in developing barley grains

When a barley seed starts to develop after double fertilization, maternal tissues compose a bulk of caryopsis and consist of pericarp, integuments and nucellus. As indicated by TUNEL staining, nucellus is the first tissue undergoing PCD after beginning of caryopsis development (Fig.3.1 B), besides the antipodals and synergid cells, which however belong to the gametophyte. The first TUNEL-labeled nuclei were detectable at the margins of the nucellus facing the developing endosperm very soon after fertilization in barley (Fig. 3.1 B), similarly to the nucellus degeneration in the developing wheat grain (Domingues *et al.*, 2001). With endosperm growth, PCD in nucellus expands to outward cell layers finally resulting in complete disappearing of the tissue at 4–5 DAF (Fig. 3.1 C) except the cells adjacent to the main vascular bundle, which develop to the nucellar projection (Radchuk *et al.*, 2011; Thiel *et al.*, 2008). The nucellar projection together with the opposite endosperm transfer cells operate as a main conduit for nutrient supply from the main vascular bundle to the endosperm (Hands *et al.*, 2012; Radchuk *et al.*, 2006). The first TUNEL-positive nuclei appear at margins of the nucellar projection facing the endosperm transfer cells around 6 DAF (Fig. 3.1 E). Thereafter, the degenerating nuclei at margins of the nucellar projection are detectable till late grain maturation (Fig. 3.1 K, M). Permanent cell turnover seems to occur in the nucellar projection. New cells are produced in the mitotic region, then cells elongate, produce thick cell walls (Weschke *et al.*, 2000) and become functionally active before they

degenerate thereby directing cell content and cell remnants into the apoplastic space. This mechanism of nutrient delivery is not fully understood, despite its importance for endosperm filling and grain yield (Offler *et al.*, 2003). There are no symplastic connections between nucellar projection and endosperm transfer cells, and nutrient transport across maternal/filial border occurs apoplastically (Radchuk and Borisjuk, 2014). As deduced from thick cell walls of elongating cells (Weschke *et al.*, 2000) and expression of many transporters (Thiel *et al.*, 2008), the nutrient transfer through nucellar projection involves both symplastic and apoplastic pathways and evidently requires PCD at the site of the nucellar projection (Radchuk *et al.*, 2006). Impaired PCD in nucellar tissues affects endosperm development and grain weight in barley (Radchuk *et al.*, 2006) and rice (Yin *et al.*, 2012).

Activation of caspases is a hallmark of apoptosis and inflammatory response in animals (Degterev *et al.*, 2003; Jin and El-Deiry, 2005). Caspase-like activities become also markedly enhanced upon induction of PCD in plants (Bonneau *et al.*, 2008; Woltering *et al.*, 2002). The caspase-1-like, caspase-3-like, caspase-4-like, caspase-6-like, caspase-8-like and caspase-9-like activities were measured in separated pericarp and endosperm fractions of the developing grain (Figs. 3.3, 3.4). Because the manually separated endosperm fraction always includes nucellus and nucellar projection (Radchuk *et al.*, 2011; Radchuk *et al.*, 2009), the first increase in almost all caspase-like activities, except of caspase-9-like, in the endosperm fraction (Fig. 3.4) may be related to PCD of nucellus and nucellar projection. The increase in caspase-1-like activity may be acquired by VPE2a, VPE2b and VPE2d proteases, which potentially exhibit this activity in plants. The respective genes are exclusively expressed in nucellus and nucellar projection during grain development (Fig. 3.5). The caspase-1-like activity of VPE2b (HvLeg2) has been already proven (Julian *et al.*, 2013). Expression of phytaspase 2 and phytaspase 3, encoding an enzyme with caspase-6-like activity (Vartapetian *et al.*, 2011), is higher during early grain development (Tran *et al.*, 2014) coinciding with caspase-6-like activity (Fig. 3.4) and indicating that these genes may be responsible for the corresponding activity. PCD processes in the distinct grain tissues and possibly involved proteases are summarized in Fig. 4.1.

After nucellus degeneration, the endosperm enlarges on costs of pericarp cells which undergo PCD starting from the innermost cell layer of mesocarp between 4 and 5 DAF, as seen from distribution of TUNEL-positive nuclei (Fig. 3.1 D).

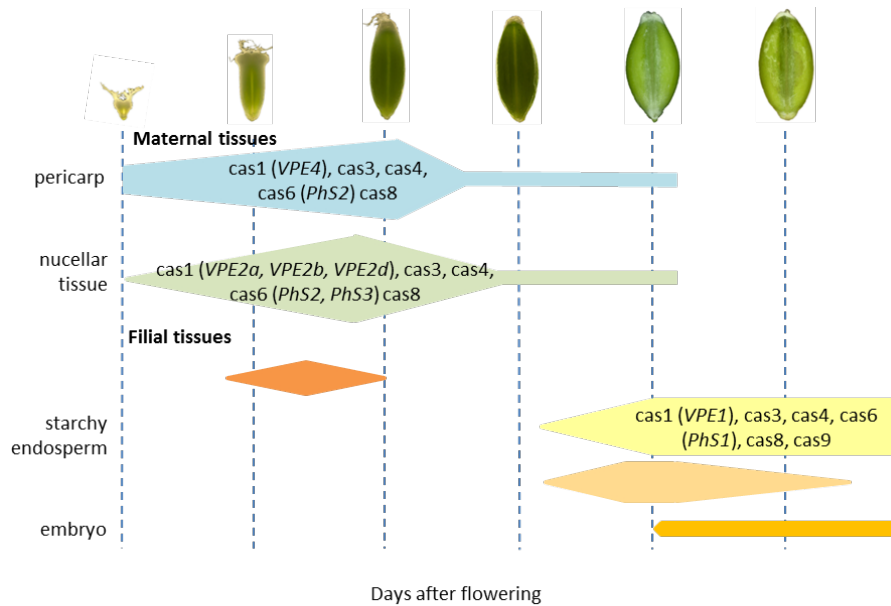


Figure 4.1 Scheme illustrating programmed cell death processes together with potentially involved activities and genes (in brackets) in distinct tissues of developing barley grains (scheme is taken from: Tran *et al.*, 2014). Activities: cas1, caspase-1-like; cas3, caspase-3-like; cas4, caspase-4-like; cas6, caspase-6-like; cas8, caspase-8-like; cas9, caspase-9-like. Genes: VPE, vacuolar processing enzyme; PhS, phytaspase.

The lateral and dorsal parts of the pericarp disintegrate till 8–10 DAF (Fig. 3.1 H) whereas the ventral region around the main vascular bundle persists undergoes later a gradual degeneration until grain maturation (Fig. 3.1 I, J). The green and photosynthetically active chlorenchyma layer (Rolletschek *et al.*, 2004) however does not show any TUNEL-positive signals during the developmental phases that have been investigated (Fig. 3.1). Probably this layer disintegrates during desiccation when the color of the maturing grain turns from green to yellow. Obviously, the chlorenchyma plays an important role for caryopsis development. Perception of light by this photosynthetically active seed layer is thought to represent a strategy to sense environment and provide a means of tuning grain metabolism according to the changing conditions (Radchuk and Borisjuk, 2014).

Coinciding with PCD progression in the pericarp and the abundance of TUNEL positive nuclei, the increase of the caspase-1-like, caspase-3-like, caspase-4-like, caspase-6-like and caspase-8-like but not caspase-9-like activities were detected towards 10 DAF and their decline thereafter (Fig. 3.3). The transcript profile of the earlier described pericarp-expressed *VPE4* gene (Radchuk *et al.*, 2011) coincides with the pattern of caspase-1-like activity (Fig. 3.3)

further supporting that VPE4 may be responsible for the activity. Additionally, expression of *phytaspase 2* (Tran *et al.*, 2014) coincides with increase of caspase-6-like activity in the pericarp (Fig. 3.3) and with accumulation of TUNEL-positive nuclei (Fig. 3.1 B-L) further supporting that phytaspase 2 might be responsible for the caspase-6-like activity required for PCD in pericarp.

In both pericarp and endosperm fractions of developing grains, distinct caspase-like activities showed similar profiles albeit their relative activity levels were different. Coordinated increase of diverse caspase-like activities coincides with cell disintegration processes in the corresponding tissues.

Based on these observations, I tempt to conclude that co-action of caspase-like protease activities may execute and regulate PCD processes in plant tissues similar to that occurring in animal cells (Degterev *et al.*, 2003; Slee *et al.*, 1999).

In animals, the caspases are classified into inflammatory, apoptotic initiator and apoptotic effector groups (Jin and El-Deiry, 2005). The latter group is processed and activated by upstream caspases and performs downstream steps cleaving multiple cellular substrates. The effector caspases are usually more abundant and active than initiator caspases (Jin and El-Deiry, 2005). In the barley grains, caspase-6-like activity is highest in both pericarp and early endosperm fractions followed by the caspase-3-like activity (both effector activities in animals) while caspase-8-like and especially caspase-9-like activities were substantially lower (Figs. 3.3 and 3.4). Referring to the animal model, I speculate that proteases with caspase-6-like and caspase-3-like activities may fulfill an effector role in plant PCD while proteases with caspase-8-like and caspase-9-like activities are PCD initiators. Caspase-like proteases executing PCD may differ among distinct plant tissues. For instance, the caspase cascade in the pericarp and early endosperm fractions may not include caspase-9-like activity, because the latter has been barely measurable in these tissues. In contrast, the potential caspase coaction in the maturing endosperm includes caspase-9-like activity but caspase-6-like activity may play minor role (Fig. 3.4). The possible co-action of proteases with caspase-like activities in acquisition and execution of plant PCD needs further experimental confirmation. The caspase-4-like activity was detected in plants for the first time. Its patterns of activity in both pericarp and endosperm (Figs. 3.3 and 3.4) coincide with the degeneration processes in the respective tissue (Fig. 3.1). The specific protease inhibitor could strongly inhibit the

caspase-4-like activity. The specific protease responsible for the newly detected caspase-4-like activity remains to be detected.

The presented data imply that pericarp-specific VPE4 and nucellus-specific VPE2a, VPE2b and VPE2d are involved in execution of PCD in the corresponding tissues. Therefore, the further investigations were concentrated on the study of their role during grain development.

4.2 VPE4 is required for cell death of the pericarp in developing barley grains

In angiosperms, endosperm and embryo develop after fertilization being covered by maternal tissues (Radchuk and Borisjuk, 2014) those not only defend the new establishing organism from detrimental environment but also supply it with nutrients. Besides, the expansion of endosperm and embryo is only possible on costs of maternal tissues that must undergo progressive and highly coordinated cell death (Radchuk *et al.*, 2011). In barley grains, the expression of *VPE4* is restricted to the pericarp (Radchuk *et al.*, 2011), the main maternal tissue at early development. Transgenic barley plants were generated in which *VPE4* gene expression was down-regulated by an RNAi construct driven by the gene's own promoter (Fig. 2.1). The VPE4i transgenic plants showed stable integration of the transgene cassette over generations (Figs. 3.8 and 3.10) and displayed normal phenotype until flowering. The beginning of flowering and following grain development of VPE4i lines were also not phenotypically different from those in wild type but required 7-10 days longer for seed maturation (Fig. 3.12). The accumulation of fresh weight in transgenic caryopses was delayed at early stages (Fig. 3.14) indicating slower development. The extent of phenotypic alteration was largely depended on the repression level of *VPE4* expression in the transgenic pericarp (Fig. 3.11).

Number of cell rows and cell width is progressively diminish in lateral and, especially, dorsal regions of the pericarp at ongoing seed development (Radchuk *et al.*, 2011) leading to pericarp thinning. However, the pericarp remains thick in the *VPE4*-repressed line VPE4i-23 until middle development (Figs. 3.15 and 3.16). The effect is caused not only by a higher number of cell rows but also by thicker (more roundish) cells (Fig. 3.15). The delayed degradation of pericarp cells explains the levelling up of fresh weight accumulation in transgenic and wild type caryopses between 10 and 16 DAF (Fig. 3.14): while fresh weight accumulation in wild type seeds coincide with pericarp disintegration, expanding VPE4i

transgenic caryopses still preserve a number of vital pericarp cells. DNA fragmentation, a typical feature of PCD, was detected in the pericarp starting at an early stage of seed development by gel electrophoresis (Radchuk *et al.*, 2011) and TUNEL assay (Fig. 3.1). These results show that death for the pericarp cells starting from inner cell rows is programmed by ongoing seed development. *VPE4* transcripts spatially and temporally expressed in pericarp cells (Radchuk *et al.*, 2011) and *VPE4* suppression delays the targeted cell death (Fig. 3.15). The *VPE3* gene of barley, which is also weakly expressed in the pericarp (Radchuk *et al.*, 2011), is not able to compensate the effect of *VPE4* down-regulation. Therefore, *VPE4* is a key player in the developmental cell death of the barley pericarp, which occurs during seed coat formation. Similarly, the seed specific δVPE of Arabidopsis is responsible for PCD of two inner cell layers of the early seed coat (Nakaune *et al.*, 2005). In δVPE -deficient mutants, PCD is delayed and the seed coat remains thick throughout early development (Nakaune *et al.*, 2005). The later stages of development of *VPE4*-repressed barley seeds were not studied. However, compression of the pericarp at the final stage is possible based on necrosis as a result of mechanical pressure by the growing endosperm. In Arabidopsis δVPE mutant, the inner integuments were finally diminished by necrotic cell death at the full-sized-embryo stage, resulting in formation of thin seed coats in the dry seeds (Nakaune *et al.*, 2005).

VPE has been shown to exhibit enzymatic properties similar to that of caspase-1, which is a cysteine protease that mediates the PCD pathway in animals (Hatsugai *et al.* 2015). *VPEs* probably represent the most important example of a caspase-like protease in plants (Hatsugai *et al.*, 2015). Despite many caspase-like activities being detected, no true caspase homologues exist in plant genomes (Vercammen *et al.*, 2008). The caspase-1-like activity was decreased in the pericarp of the transgenic developing grains (Fig.3.17 A) correlating with down-regulation of *VPE4* expression (Fig. 3.11). While the ability of the *VPE4* protein to cleave caspase-1 substrate has not been analyzed so far, the results presented here demonstrate that *VPE4* may be responsible for caspase-1-like activity in the pericarp. The results are consistent with other published observations. Tobacco *VPEs* exhibiting caspase-1-like activity are involved in *Tobacco mosaic virus*-induced hypersensitive cell death (Hatsugai *et al.*, 2004). Arabidopsis δVPE protease is able to cleave caspase-1 substrate and this activity is inhibited by a caspase-1 inhibitor (Nakaune *et al.*, 2005). The Arabidopsis *vpe*-null mutant, which lacks all *VPE* genes in the genome, shows neither *VPE* activity nor caspase-1-like activity (Kuroyanagi *et al.*, 2005).

The developing barley pericarp exhibits different caspase-like activities (Fig. 3.3); the level of most of them increases with aging of pericarp. The *VPE4*-repressed barley pericarp displays not only decreased caspase-1-like activity but also decreased caspase-3, caspase-4, caspase-6 and caspase-8-like activities (Fig. 3.17). It is possible that *VPE4*, besides of caspase-1-like activity, possesses also some other caspase-like activities. So, poppy VPE displays besides caspase-1-like also weak caspase-3-like (20% of caspase-1-like activity) and caspase-8-like (40%) activities (Bosch *et al.*, 2010). Barley *VPE2b* (*HvLeg-2*) and *VPE3* (*HvLeg-4*) possess both strong caspase-1-like activity and weak caspase-6-like activity which reaches only 20% of caspase-1-like activity (Julian *et al.*, 2013). However, these weak activities cannot explain strong increase of diverse caspase-like activities in the aging pericarp (Fig. 3.3) and other proteins as VPE must display corresponding activities, e.g. phytaspase (Chichkova *et al.*, 2010). Besides, it was not shown so far that decrease in VPE and in corresponding caspase-1-like activity is reflected also in the decrease of other caspase-like activities. Therefore, the results rather support the above mentioned speculation (chapter 4.1) that co-action of caspase-like protease activities may execute and regulate PCD processes in plant tissues similar to that occurring in animal cells (Degterev *et al.*, 2003).

VPE4-repressed caryopses accumulate less fresh weight compared to the wild type ones (Fig. 3.14) despite of longer development of the transgenic seeds indicating for decreased ability of the endosperm in transgenic grains to accumulate storage products. Indeed, mature transgenic seeds are smaller (Fig. 3.12 B) which is reflected in lower thousand grain weight (Fig. 3.13 A) due to lower seed width and possibly thickness (Fig. 3.13 B). At maturity, transgenic seeds accumulate significantly less starch but the level of storage proteins is not changed or slightly increased (Fig. 3.18). Based on these observations, it can be concluded that PCD in pericarp during early seed development affects later grain filling. Several mechanisms can be supposed to explain how PCD in pericarp can control endosperm filling. First, due to delayed PCD in *VPE4*-repressed pericarp, endosperm does not have enough space for cell proliferation and expansion at early development leading to less or smaller cells in the endosperm. The total number of cells in endosperm is believed to influence final grain size and starch accumulation (Trafford *et al.*, 2013). Second, because early pericarp functions as transient storage tissue (Radchuk *et al.*, 2009), starch and storage protein remobilization is hampered by delayed PCD in the transgenic pericarp resulting in shortage of nutrient delivery to the endosperm. A combination of both assumptions is also possible.

While a direct evidence for any assumption is missing I tend to favour the predominant role of space limitation because of following reasons. Despite of retarded PCD and alleged holdup of storage product remobilization, sucrose as well as hexose levels are not significantly increased in the *VPE4*-repressed pericarp in two of three lines studied (Fig. 3.19 A-C). The increase in glucose and fructose but not sucrose level was observed only for the lines *VPE4i-23* with the strongest *VPE4* down-regulation. The levels of starch have even decreased with aging of the transgenic pericarp compared to the wild type (Fig. 3.19 D) indicating that starch remobilization is not directly connected with PCD in pericarp. In the transgenic endosperm, no trends in sucrose, hexose or starch accumulation are visible at 4 DAF (Fig. 3.20). At 8 DAF, however, transgenic endosperms accumulate less sucrose and more starch compared to the wild type (Fig. 3.20). Starch biosynthesis in cereal endosperm starts following endosperm cellularization (Olsen, 2004). Assuming that starch accumulation rate is similar in wild type and transgenic endosperm, higher starch levels in the transgenic endosperms at 8 DAF indicate earlier start of starch synthesis in the this tissue possibly due to an earlier beginning or shortage of the cell division period and accelerated differentiation of the endosperm cells. However, earlier start of starch accumulation does not result in higher starch accumulation at maturity. Transgenic grains accumulated significantly less starch than wild type (Fig. 3.18). The transition from the syncytial to the cellularized state is critical for endosperm development and likely determines seed size (Hehenberger *et al.*, 2012). In Arabidopsis, early cellularization leads to reduced nuclear proliferation and reduced seed size. Delayed cellularization correlates with increased nuclear proliferation and increased seed size (Liu *et al.*, 2014). In maize, rice and wheat, increased nuclear proliferation increases the grain sink strength and grain weight (Liang *et al.*, 2001; Jones *et al.*, 1996; Chojecki *et al.*, 1986; Singh and Jenner, 1982; Radley, 1978; Brocklehurst, 1977). In maternally-effected barley mutant *seg8*, abnormal cellularization/differentiation of the shrunken endosperm leads to reduced starch accumulation and smaller seeds (Sreenivasulu *et al.*, 2010). The reduction of both thousand grain weights and thickness of *seg8* grains is caused by a lower number and reduced ploidy level of endosperm cells.

To conclude, the delayed removal of cell rows in *VPE4*-repressed pericarp relieves a physical restraint for the growing endosperm prompting the latter for early cellularization. Thus, endosperm cell division and/or cell expansion and finally grain filling and seed size are determined by growth characteristics of the early pericarp.

4.3 Nucellar PCD, mediated by VPE activity, is required for proper assimilate transfer to the endosperm

As seen from the expression profiles, VPE activity in the nucellar tissues is mediated by three very similar genes: *VPE2a*, *VPE2b* and *VPE2d* (Fig. 3.5). The expression patterns of these genes are largely overlapping indicating functional redundancy. Therefore, to repress the whole VPE activity, a nucleotide region of *VPE2a*, highly conserved in the *VPE2b* and *VPE2d* cDNA, was used for an RNAi construct and the construct was ectopically expressed in barley driven by the *VPE2a* promoter (Fig. 2.2). The VPE2i transgenic plants showed stable integration of the transgene cassette over generations (Fig. 3.25). Using the RNAi approach, transcriptional repression not only of the *VPE2a* gene (which cDNA fragment was used for the RNAi construct) but also of *VPE2b* and *VPE2d* expression were achieved (Fig. 3.26). Distinct transgenic lines show similar levels of down-regulation of the expression of *VPE2a*, *VPE2b* and *VPE2d* transcripts being weak in the line VPE2i-6 and strong in the lines VPE2i-5 and VPE2i-11. These results indicate that levels of knock-down for all these genes depend on the expression of the RNAi transgenic construct in individual transgenic lines. To conclude, the RNAi technique is a reliable approach to transcriptionally repress not only a single gene but also a family of very similar genes in order to overcome functional redundancy.

Transgenic plants displayed a normal phenotype during vegetative growth. However, phenotypic changes occurred already at the tillering stage: VPE2i transgenic plants produced less tillers and, as a consequence, less spikes per plant (Fig.3.29 A, B), although this change was significant only for the line VPE2i-11 with the strongest down-regulation of *VPE2a-VPE2d* genes. The overall reproductive development of the transgenic grains took at least seven days longer compared to the wild type. The number of seeds per spike was also drastically reduced in all transgenic lines (Fig. 3.27 C). The value of phenotypic changes correlates well with level of the *VPE2a-VPE2d* down-regulation. These observations suggest that some or all genes of the *VPE2* subfamily are expressed in vegetative and generative meristems playing a pivotal role for their development and differentiation besides being important for seed development. Repression of the *VPE2* gene subfamily resulted not only in delayed germination but also in strongly reduced germination rate (Fig. 3.30). It is known that at least *VPE2a* (*HvLeg-2*) is highly expressed in the germinating aleurone and its expression is further induced by gibberellin treatment (Julian *et al.*, 2013). Therefore,

reduced germination rate of the transgenic lines might be a result of reduced expression of *VPE2b* during germination while the impact of the *VPE2a*, *VPE2c* and *VPE2d* genes cannot be excluded. Which genes from the VPE2 subfamily are active in which tissue and how they influence meristem development and seed germination remain to investigate.

High levels of all caspase-like activities, with exclusion of the caspase-9-like activity, were detected during early endosperm development (Fig. 3.4). The endosperm fraction is always co-isolated with the nucellus and nucellar projection by manual dissection (Radchuk *et al.*, 2009; Sreenivasulu *et al.*, 2006). It was concluded above that these caspase-like activities are attributed to the disintegrative cellular processes occurring in the nucellar tissues. *VPE2a*, *VPE2b* and *VPE2d* altogether are major candidates for caspase-1-like activity in these tissues. Ability of barley *VPE2b* to cleave the caspase-1 substrate has been already proved (Julian *et al.*, 2013). Transgenic grains with down-regulated expression of the genes of the VPE2 subfamily are characterized by reduced caspase-1-like activity (Fig. 3.31 A) and the level of reduction coincides with the transcript level (Fig. 3.26). Besides reduced caspase-1-like activity, caspase-4, caspase-6 and caspase-8-like activities were also decreased in the transgenic grains (Fig. 3.31). The cascade of caspase-like activities is required for PCD execution also in nucellar tissues. It has been shown that phytaspase 2 and 3, both proteases with potential caspase-6-like activity, are up-regulated in the nucellar tissues of the developing barley grains (Tran *et al.*, 2014). Indeed, expression of phytaspase 2 was down-regulated in the transgenic grains (Fig. 3.32) and the level of repression correlated with the decrease of caspase-6-like activity (Fig. 3.31 C). These data further support the suggestion that diverse caspase-like activities are performed by different proteases. As seen from coordinated changes in the expression of *VPE2a*, *VPE2b*, *VPE2d* and *phytaspase 2* genes, the PCD in plants may be regulated at transcriptional level. This is different from apoptosis in animals where apoptotic regulation occurs post-translationally (Degterev, 2003).

Expression of the *VPE2a*, *VPE2b* and *VPE2d* genes was found predominantly in the nucellar tissues of developing barley grains (Fig. 3.5; Linnestad *et al.*, 1998). Nucellus undergoes PCD during early development providing nutrients and space for the expanding endosperm (Fig. 3.1 B-D). After nucellus degeneration and differentiation of the nucellar projection, the latter together with the endosperm transfer cells are established as a main route for assimilate transfer (Hands *et al.*, 2012). PCD in the nucellar projection is an integral part of the assimilate transfer (Radchuk and Borisjuk, 2014; Melkus *et al.*, 2011; Radchuk *et al.*, 2006).

The VPE2i transgenic plants were not analyzed at the cytological level. However, the delayed or diminished PCD process in nucellus and nucellar projection is probable. In such case, endosperm of the transgenic grains would be deprived in development due to nutrient starvation. Further development of the endosperm would be affected due to decrease or interruption of nutrient transfer from the maternal seed part leading to less filled seeds. Indeed, all transgenic lines with repressed *VPE2a-VPE2d* expression were characterized by smaller seeds resulting in lower seed weight due to decreased seed width and thickness (Fig. 3.28). The seed length, however, was increased (Fig. 3.28 D). The final size of the barley caryopsis is determined predominantly by cell expansion of the early pericarp (Pielot *et al.*, 2015). Impaired nutrient transfer *via* the nucellar projection may lead to abnormal accumulation of assimilates (sucrose) in pericarp that in turn activate elongation processes in the tissue. The transgenic grains with decreased final seed weight accumulated less starch further supporting the idea that PCD in the nucellar projection is involved in assimilate transfer. Mature grains of three transgenic lines show increased percentages of total nitrogen (Fig. 3.29), which reflects higher grain protein content. The increased content of storage proteins of both albumin/globulin and gliadin fractions in the transgenic grains can be explained by well-known negative correlation between starch accumulation and grain protein content (Sinclair, 1998; Simmonds, 1995). However, it was shown that VPE2b (HvLeg-2) protein is able to degrade globulins *in vitro* (Julian *et al.*, 2013). Higher globulin content in the mature VPE2i-repressed grains is correlated with lower amounts of VPE transcript, and probably VPE protease. The amounts not only of globulins but also of gliadins were increased. The latter, however, is not target of VPE2b proteolytic activity (Julian *et al.*, 2013). Furthermore, *VPE2a*, *VPE2b* and *VPE2d* transcripts were not detected in the endosperm (Fig. 3.5) where preliminary globulins accumulate (Weber *et al.*, 2010). Thus, VPE activity and globulin accumulation are topographically separated. In fact, there is a weak expression of *VPE2c* in endosperm (Fig. 3.5). However, because the RNAi construct is driven by *VPE2a* gene promoter and is active only in tissues where *VPE2a* gene is expressed, it is unlikely that *VPE2c* in endosperm could be also down-regulated by the same RNAi construct. Besides, as concluded from the pattern of *VPE2c* gene expression (less than 1% of *VPE2b* transcript abundance; Fig. 3.5), even decreased VPE2c activity is probably too low to cause strong changes of such abundant product as storage globulins. Based on all those considerations, it can be excluded that the increase in storage protein content is a direct result of reduced VPE

activity. Secondary effect changing the starch-protein balance might be suggested resulting from disturbances of nutrient transfer towards the developing endosperm.

4.4 The barley MADS29 transcription factor regulates expression of genes involved in PCD in nucellar tissue of the developing barley grain

Contrary to ubiquitously-expressed caspases in animals, genes encoding plant proteases with caspase-like activities show tissue- and time-specific profiles of expression (Radchuk *et al.*, 2011; Julian *et al.*, 2013; Nakaune *et al.*, 2005). Therefore, the expression of these genes must be regulated at transcriptional level. It was shown that the MADS29 transcription factor (TF) of rice regulates PCD in nucellar tissues of the developing grains (Yin and Xue, 2012). I have cloned the corresponding *MADS29* gene from barley and analyzed its possibility to interact with specific promoter fragments of *Jekyll* and *VPE2a* genes, both required for PCD in the nucellar tissues.

Barley MADS29 belongs to the B_{sister} clade of the class B floral identity genes, as concluded from phylogenetic analysis (Fig. 3.33, Becker *et al.*, 2002). The presence of close homologs of *HvMADS29* in the genomes of monocotyledonous species indicates that their products probably have a common function, a conclusion supported by the conservation of *MADS29* transcription profiles. The wheat gene *WBSis* is active exclusively in the nucellus (Yamada *et al.*, 2009), while the rice gene *OsMADS29*, although transcribed in the florets, exhibits its peak level of both transcript and protein in the nucellus and nucellar projection of the developing grain (Yang *et al.*, 2012; Yin and Xue, 2012; Nayar *et al.*, 2013). Two hypotheses have been recently published regarding the function of rice MADS29. One group showed the role of *OsMADS29* in the transcriptional regulation of PCD in seed nucellar tissues (Yin and Xue, 2012). Another group, based on immunochemical localization of *OsMADS29*, supposed that the protein is involved in the regulation of embryo development and endosperm filling (Nayar *et al.*, 2013). Contrary to rice *MADS29*, barley *MADS29* transcripts were exclusively detected in the nucellus and nucellar projection of the young immature grain (Fig. 3.34 A, B). No MADS29 expression was found either in embryo or developing endosperm including aleurone layer (Fig. 3.34 A, B). Because no protein transport is known from maternal tissues into endosperm and embryo, the results support the first hypothesis and imply the role of *HvMADS29* in the nucellar tissues of the developing barley grains. The strong tissue



Figure 4.1 The sequence logo of the CARg motif derived from a comparison of all detected CARg sequences in the promoters of nucellar-specific genes.

and nucellar projection contribute to feed the endosperm (Hands *et al.*, 2012; Krishnan and Dayanandan, 2003).

The rice MADS29 was functionally characterized as a key transcriptional regulator of PCD in maternal tissues of the developing grains (Yin and Xue, 2012). The OsMADS29 protein binds directly to the putative promoter regions of genes that encode a Cys protease and nucleotide binding site-Leu-rich repeat proteins (Yin and Xue, 2012). However, no one of analyzed proteins was shown to be directly involved in PCD. The HvMADS29 protein interacts with CarG-like *cis*-elements present in the promoters of certain genes required for PCD in the barley nucellar tissues. The product of the *Jekyll* gene is a pivotal regulator of terminal differentiation of nucellar cells switching their fate to cell death (Radchuk *et al.*, 2006). The *VPE2a* gene is exclusively expressed in the deteriorating nucellus and nucellar projection and supposed to be an executor of PCD in these tissues (Fig. 3.5). Similarly to the expression of *MADS29* (Fig. 3.34 C), both *Jekyll* and *VPE2a* genes are active in anthers and gynoecia of developing flowers (Radchuk *et al.*, 2012). In developing grains, expression of *Jekyll* and *VPE2a* coincides with that of *MADS29* (Fig. 3.35) indicating that MADS29 may regulate expression of *Jekyll* and *VPE2a* genes. Promoter regions of both genes contain several CARg-like motifs partially grouped nearby to each other (Figs. 3.40 A and 3.41 A). MADS29 binds physically to each of these CARg motifs of both *Jekyll* and *VPE2a* gene promoters (Figs. 3.40 B and 3.41 B) albeit at different efficiency. The specificity of this binding was shown by control experiments demonstrating that MADS29 fails to bind to destroyed CARg motifs or to motifs without CARg-like sequence (Figs. 3.40 C and 3.41 C).

The canonic sequence for CARg box is C(C/t/a)(T/A)₆(G/t/a)G (De Folter and Angenet, 2006). However, barley MADS29 is also able to recognize CARg-like sequences in which one A/T is replaced by G (CCATTGATGG sequences at -186 position of *Jekyll* promoter and the

specificity shown for *HvMADS29* may reflect differences between barley and rice in the importance of the nucellus for endosperm development. In the barley grain, the nucellar projection provides the major conduit for assimilate delivery to the endosperm (Melkus *et al.*, 2011), whereas in the rice grain, both the nucellar epidermis

sequences CCAAAGATGG and CCCAAAGTGG at -186 and -726 positions of *VPE2a* promoter, correspondingly). However, MADS29 binding to these CArG motifs is weaker as its binding to the canonical C(A/T)8G sequence (Figs. 3.39 B and 3.41. B). It is also unknown whether and how MADS29 binds to the promoter regions of the analyzed genes *in vivo*. The results described here show that the minimal consensus CArG sequence (Fig. 4.2) is sufficient for the HvMADS29 binding to DNA.

MADS29 may also regulate other genes involved in PCD of the nucellar tissues since their promoters harbor multiple CArG-like *cis*-elements, frequently in duplicate (Table 3.1 and 3.2; Fig. 3.41). In order to be translocated into the nucleus, OsMADS29 generates either homo- or heterodimers (for example with OsMADS8, Nayar *et al.* 2013). In addition to HvMADS29, at least three other MADS box TF genes (*HvMADS8*, *HvMADS9* and *HvMADS58*) are expressed in the barley nucellar projection (Thiel *et al.*, 2008). Their transcription profiles resemble that of *HvMADS29* (Sreenivasulu *et al.*, 2006). Thus it is possible that HvMADS29 interacts with one or more of these factors to enable its translocation to the nucleus. Because CArG-like elements are very common in plant genomes, it is also possible that interaction of MADS29 with other factors is necessary for proper regulation of target genes. The accepted ABC model for determining floral organ identity proposes that a combination of two dimers generates a tetrameric complex (de Folter and Angenent, 2006; Theissen and Saedler, 2001). Experimentally, it has been demonstrated that the binding of the tetrameric complex of SEEDSTICK and SEPALLATA3 to two adjacent CArG *cis*-elements is essential for the formation of the DNA loop required to activate the relevant promoter (Mendes *et al.*, 2013). Duplication of the CArG motif may therefore be important for the ability of HvMADS29 complex to activate its target genes in the nucellus. The promoter of the nucellus-specific *NUC1* gene encoding a still unknown protein (Doan *et al.*, 1996) contains four *cis* CArG elements, organized as two duplicated sequences (Fig. 3.41). Because the *NUC1* transcription profile is similar to that of *Jekyll* and *VPE2a*, it may also be involved in the PCD of the nucellus. The *HvMADS29* promoter itself harbors no *cis* CArG elements, so it is unlikely that its activity is maintained by an auto-regulatory loop, as is the case for many other B-type MADS box proteins (de Folter and Angenent, 2006). Given that the promoter sequences of genes encoding starch synthesis enzymes contain at most one *cis* CArG element (Fig. 3.41), their transcription is most likely not regulated by MADS box proteins. However, several genes transcribed in the late endosperm and potentially involved in PCD

(Sreenivasulu *et al.* 2006) do contain duplicated CArG elements in their promoter sequences (Table 3.1 and 3.2). However, since *HvMADS29* is not transcribed in the late endosperm, these genes are probably regulated by some other MADS box TFs. Despite this, no MADS box factor could be identified in a search of over 800 genes active in the late endosperm (Sreenivasulu *et al.*, 2006).

The data presented here imply that *HvMADS29* binds to the specific fragments of genes related to PCD in the nucellus and nucellar projection of the developing barley grain being a potential transcriptional regulator of these genes. Duplication of CArG-like *cis*-elements appears to be important for binding of the MADS-box factor to its target gene. It remains still unclear whether *HvMADS29* regulates transcription of *Jekyll*, *VPE2a* and other genes *in planta* and whether other TFs may be required to trigger the expression of the genes responsible for PCD in the nucellar tissues.

4.5 Concluding remarks

A short comparison of the PCD in pericarp and nucellar tissues of developing barley grains

Different tissues of maternal origin in developing barley grains undergo the developmental type of PCD by their own way. The pericarp disintegrates progressively during early grain development providing space and, possibly, nutrients to the expanding endosperm. At grain maturity, pericarp remnants together with other maternal seed parts form a protective hull. Nucellus also disappears completely within several days after flowering providing space and nutrients for growing endosperm and embryo. However, nucellar cells opposite of the main vascular bundle differentiate into the nucellar projection. Nucellar projection together with endosperm transfer cells becomes a main route for assimilate transfer to the endosperm (Melkus *et al.*, 2011). Because there are no symplastic connections between maternal seed parts and endosperm, assimilate transfer must occur apoplastically and evidently requires PCD (Radchuk *et al.*, 2006). There is a continuous cell turnover as a part of nutrient transfer process at margins of the nucellar projection (Thiel *et al.*, 2008).

PCD in both pericarp and nucellus/nucellar projection is accompanied by an increase of diverse caspase-like activities. Among them, the caspase-1-like activity is observed in pericarp and early developing endosperm fraction harboring nucellar tissues. Vacuolar processing enzymes (VPEs) are known to possess caspase-1-like activity in plants (Hatsugai *et*

al., 2015). Disintegration processes in pericarp and nucellar tissues coincide with transcriptional activation of specific VPE genes: *VPE4* is up-regulated in the pericarp whereas *VPE2a*, *VPE2b* and *VPE2d* are strongly and specifically activated in nucellar tissues. RNAi-mediated down-regulation of *VPE4* expression results in decrease of caspase-1-like activity in the transgenic pericarp. Similarly, simultaneous repression of *VPE2a*, *VPE2b* and *VPE2d* transcription in the nucellus and nucellar projection leads to lower caspase-1-like activity. These results suggest that *VPE4* and all or some of *VPE2a*, *VPE2b* and *VPE2d* proteases are responsible for specific caspase-1-like activity in barley grains. However, other caspase-like activities were also decreased in *VPE4*-repressed pericarp as well as in *VPE2*-subfamily repressed nucellus and nucellar projection. It is concluded that a cascade of caspase-like activities are required to execute PCD in plants similarly to the function of caspases in animal apoptosis (Degterev *et al.*, 2003; Slee *et al.*, 1999). Because transcriptional repression of VPE resulted in the decrease of not only caspase-1-like activity but in a number of other activities, it can be supposed that VPEs act upstream of other caspase-like activities.

Further, it was found that *VPE4* knock-down and repression of caspase-like activities impairs PCD in pericarp confirming that *VPE4* is required for PCD in pericarp. While cytological studies have not been finished with *VPE2*-repressed caryopses yet, it can be assumed that transcriptional repression of *VPE2a*, *VPE2b* and *VPE2d* genes resulted in delayed or aborted PCD in the nucellar tissues confirming the importance of *VPE* genes for PCD in the nucellus and nucellar projection.

Knock-down of tissue-specific *VPE* genes in both pericarp and nucellus/nucellar projection resulted in smaller and less filled seeds at maturity mainly due to lower starch accumulation indicating that PCD events in maternal seed tissues are coordinated with endosperm development. Caryopses with defective *VPE4* or *VPE2a* function developed a reduced sink and storage capacity during the major storage period. Despite a similar phenotypic effect, the nature of these changes might be different. Because endosperm develops being fully covered by pericarp, delayed PCD in the pericarp may hamper endosperm expansion leading to alterations in the coenocyte cellularization. That in turn may reduce the potential for starch storage. As concluded from the data, potentially decelerated nutrient remobilization from pericarp might have remarkable influence on endosperm development. Thus, growth and development of the early pericarp are important yield-related parameters controlling final grain size and shape.

As seen from impaired storage product accumulation in transgenic grains with repressed expression of *VPE2* gene subfamily, PCD in the nucellus and nucellar projection have also an impact on endosperm development. The lower starch accumulation in the *VPE2*-affected grains is probably due to disrupted assimilate transfer route from the nucellar projection to endosperm. Sucrose, amino acid and hormone transport commonly occurs *via* the same transport route (Kamboj *et al.*, 1998; Yang *et al.*, 2002). In this context, an operational nucellar projection is required for endosperm development. Therefore, it is proposed that *VPE2a-VPE2d* represents a further mechanism for maternal control during seed development.

The experiments have shown that expression of *VPE2a* and *Jekyll* genes, both important for PCD in the nucellar tissues, may be regulated by the MADS29 TF which temporal and spatial expression coincides with the two genes. Barley MADS29 can specifically bind to the CArG-like motifs in the *VPE2a* and *Jekyll* promoters. MADS29 might be a potential regulator also of *VPE2b* and *VPE2d* genes as well as a number of other PCD-related genes in the nucellar projection because the promoter regions of these genes contain several CArG-like motives often organized in duplicate. The promoter of the pericarp-specific *VPE4* gene does not have any CArG-like element and therefore must be regulated on a different way.

5. Summary

Barley grain development depends on both, growth and cellular disintegration. One of the major players in cellular disintegration is programmed cell death (PCD). Cysteine proteases called caspases were found to be main executors of PCD in animals. In plants, PCD is known to play a role in cellular degeneration of the starchy endosperm and in germination but the molecular events driving PCD in maternal grain tissues are barely understood. Caspase-like activities accompany PCD also in plants but performed by specific proteases those are different from animal caspases. Caspase-1-like activity is executed by vacuolar processing enzymes (VPEs). The general aim of this study is a detailed analysis of seed-specific barley VPEs to elucidate its role in PCD in maternal tissues (pericarp and nucellar tissues) of the developing barley grain. In developing grains, *VPE4* gene is pericarp-specific while small VPE subfamily consisting of *VPE2a*, *VPE2b* and *VPE2d* genes is expressed in nucellar tissues.

Degradation of DNA and disintegration of nuclei are common features of PCD that can be detected by the terminal deoxynucleotidyl transferase-mediated dUTP nick end labeling (TUNEL) of the 3'-OH groups. Distribution of TUNEL-positive nuclei in the barley pericarp reveals that degradation of pericarp tissues starts around 4 DAF from inner mesocarp cells spreading to the outer pericarp layers during further grain development. The nucellus disintegrates soon after fertilization between 0 and 2 days after flowering (DAF) besides the region in close proximity to main vascular bundle which differentiates to the nucellar projection, one of the major players in assimilate transfer to the endosperm. Caspase-like activities were detected in pericarp and nucellar tissues coinciding with the abundance of TUNEL positive nuclei.

The possible involvement of barley *VPE4* and *VPE2a-VPE2d* in PCD of maternal tissues of the developing barley grain was studied by RNAi suppression under control of the respective gene-specific promoter. Homozygous transgenic barley plants with suppressed VPE expression were selected, and grain development was analysed compared to that of the non-transgenic control. *VPE4*-reduced grains showed reduction in thousand grain weight coinciding with delayed pericarp degradation and reduced caspase-1-like activity which is related to decreased amounts of starch detected in mature transgenic grains. However, also caspase-4-like, caspase-6-like and caspase-8-like activities were reduced in developing grains. *VPE2*-RNAi plants showed a pleiotropic phenotype with reduced number of tillers and

grains per spike as well as impaired grain development. The transgenic grains were significantly thinner than that of the wildtype indicating disturbances in storage product accumulation during grain filling. Related to that, starch accumulation was reduced but proteins were increased in mature grains when compared to the control. The phenotype of VPE2i grains correlates with reduced caspase-1-like, caspase-4-like, caspase-6-like and caspase-8-like activities in developing grains. The germination rate also was reduced in VPE2i lines. The barley MADS29 transcription factor regulates expression of genes involved in PCD of nucellar tissues of developing barley grains. This was suggested first from co-expression studies. The MADS29 mRNA profile clusters together with that of Jekyll and VPE2a genes in developing grains. Jekyll regulates PCD in nucellar tissues (Radchuk *et al.*, 2006), VPE2a is responsible for PCD in the same tissue as show in this study. Furthermore, MADS29 binds specifically to CArG motives in the Jekyll and VPE2a promoter investigated by *in vitro* studies. A consensus sequence of the CArG motif in the promoters of nucellus-specific genes was derived.

It can be concluded that PCD in pericarp and nucellar tissues of developing barley grains is related to an increase of diverse caspase-like activities encoded by VPE genes. Suppression of VPE gene expression results in impaired grain development, either resulting in delayed degradation of the pericarp (VPE4) or diminished transfer of assimilates to the developing endosperm (VPE2). Expression of the nucellus-specific VPE genes might be controlled by the transcription factor MADS29 as concluded from protein interaction with promoter *cis* elements.

6. Zusammenfassung

Die Entwicklung von Gerstenkörnern wird sowohl durch das Wachstum als auch durch den zellulären Abbau bestimmt. Cysteinproteasen, genannt Caspasen, sind die Hauptkomponenten des programmierten Zelltods (PCD) in Tieren. In Pflanzen spielt der PCD eine Rolle beim Zelltod des Endosperms und bei der Keimung. Jedoch sind die molekularen Mechanismen des PCD in den maternalen Geweben der sich entwickelnden Getreidekörner wenig verstanden. Zellulärer Abbau und PCD in Pflanzen sind verbunden mit der Aktivität von vakuolären Prozessingenzymen (VPEs). In dieser Promotionsarbeit sollen die kornspezifischen VPEs in Gerste detailliert analysiert werden. Das Ziel der Arbeit besteht darin, die Rolle der VPEs im PCD der maternalen Gewebe von Gerstenkörnern aufzuklären.

Übliche Merkmale des PCD sind DNA-Abbau und Desintegration der Zellkerne. Diese Prozesse können sichtbar gemacht werden mittels TUNEL (*terminal deoxynucleotidyl transferase-mediated dUTP nick end labelling*) der 3'-OH-Gruppen. Die Analyse der Verteilung der TUNEL-positiven Zellkerne im Gerstenpericarp zeigte, dass die Degradation etwa am 4. Tag nach der Bestäubung (DAF) im inneren Mesocarp beginnt und sich während der weiteren Entwicklung in den äußeren Zellschichten des Perikarps fortsetzt. Der Abbau des Nucellus beginnt unmittelbar nach der Blüte (Anthese bis 2 DAF). Nicht betroffen davon ist die Region gegenüber dem Hauptleitbündel. Dieser Bereich des Nucellus differenziert zur nuzellaren Projektion. Dieses Gewebe vermittelt den Assimilattransfer von den maternalen Kornteilen zum sich entwickelnden Endosperm. Sowohl im Perikarp als auch in den nuzellaren Geweben wurden Caspase-ähnliche Aktivitäten nachgewiesen, die mit der Häufigkeit von TUNEL-positiven Zellkernen in Verbindung stehen.

Die Gene *VPE2a-VPE2d* und das Perikarp-spezifische Gen *VPE4* codieren für Enzyme mit Caspase-1-ähnlicher Aktivität. In sich entwickelnden Körnern ist die Expression der *VPE2*-Gene spezifisch für die nuzellaren Gewebe.

Die postulierte Rolle der Gerste-spezifischen Enzyme *VPE4* und *VPE2a* im PCD der maternalen Gewebe des sich entwickelnden Gerstenkorns wurde analysiert mittels RNAi-Suppression unter Kontrolle des entsprechenden genspezifischen Promotors. Homozygote transgene Gerstenpflanzen mit supprimierter *VPE*-Expression wurden selektiert, die Kornentwicklung wurde analysiert und mit der nicht-transgenen Kontrolle verglichen. *VPE4i*-transgene Körner zeigten eine Reduktion im Tausendkorngewicht, die einherging mit

einem verspäteten Abbau des Perikarps und reduzierter Caspase-1-ähnlicher Aktivität während der Kornentwicklung. Damit korreliert die Verminderung der Stärkemenge in den reifen transgenen Körnern. Ebenso waren die Caspase-4-, die Caspase-6- und die Caspase-8-ähnliche Aktivität vermindert. VPE2-RNAi-Pflanzen zeigten einen pleiotropen Phänotyp mit einer reduzierten Zahl an Bestockungstrieben und einer verminderten Kornzahl pro Ähre, aber auch Einflüsse auf die Kornentwicklung. Die transgenen Körner waren signifikant dünner als die der Kontrolle, was auf eine Störung der Kornfüllung hinweist. Damit korreliert die Reduktion der Stärkemenge in den reifen transgenen Körnern; jedoch war die Proteinmenge erhöht. Der Phänotyp der reifen VPE2i-Körner korreliert mit reduzierter Caspase-1-, Caspase-4-, Caspase-6- und Caspase-8-ähnlicher Aktivität in den sich entwickelnden Körnern. Die Keimungsrate der VPE2i-Linien war auch reduziert.

Der Gersten-spezifische Transkriptionsfaktor MADS29 reguliert möglicherweise die Expression von PCD-assoziierten Genen in den nuzellaren Geweben. Das wurde zunächst abgeleitet aus Koexpressionsstudien. Das Expressionsprofil des MADS29-Gens korreliert mit dem des Jekyll- und des VPE2a-Gens in sich entwickelnden Körnern. Jekyll reguliert den PCD in nuzellaren Geweben (Radchuk *et al.*, 2006), VPE2 ist eine Komponente des Zelltods in demselben Gewebe, wie in dieser Arbeit gezeigt wurde. Weiterhin wurde die spezifische Bindung von MADS29 an CArG-Motive im Jekyll- und VPE2a-Promotor *in vitro* nachgewiesen. Eine Konsensus-Sequenz für das CArG-Motiv in den Promotoren Nuzellus-spezifischer Gene wurde abgeleitet.

Zusammenfassend kann geschlussfolgert werden, dass der PCD im Perikarp und in den nuzellaren Geweben des sich entwickelnden Gerstenkorns verbunden ist mit einem Anstieg definierter Caspase-ähnlicher Aktivitäten, die durch VPE-Gene kodiert werden. Die Suppression der VPE-Genexpression hat negativen Einfluss auf die Kornentwicklung und führt entweder zu einem verzögerten Perikarp-Abbau (VPE4) oder zu einer Behinderung des Assimilattransfers in Richtung des sich entwickelnden Endosperms (VPE2). Die Expression der Nuzellus-spezifischen VPE-Gene wird möglicherweise durch den Transkriptionsfaktor MADS29 kontrolliert, worauf Interaktionen des Proteins mit Promotor-*cis*-Elementen hinweisen.

7. References

- Arnaud, C., Bonnot, C., Desnos, T., Nussaume, L.** (2010). The root cap at the forefront. *C. R. Biol.* **333**: 335–343.
- Arora, R., Agarwal, P., Ray S., Singh A., Singh V., Tyagi A.K., Kapoor S.** (2007). MADS-box gene family in rice: Genome-wide identification, organization and expression profiling during reproductive development and stress. *BMC Genomics* **8**: 242–263
- Bar-Dror, T., Dermastia, M., Kladnik, A., Znidaric, M.T., Novak, M.P., Meir, S., Burd, S., Philosoph-Hadas, S., Ori, N., Sonogo, L., Dickman, M.B., Lers, A.** (2011). Programmed cell death occurs asymmetrically during abscission in tomato. *Plant Cell* **23**: 4146–4163.
- Baskin, T.I., Busby, C.H, Larry C. Fowke, L.C., Saturant M., Gubler, F.** (1992). Improvements in immunostaining samples embedded in methacrylate: localization of microtubules and other antigens throughout developing organs in plants of diverse taxa. *Planta* **187**(3): 405-13.
- Becker, A., Kaufmann, K., Freialdenhoven, A., Vincent, C., Li M.A., Saedler, H., Theissen, G.** (2002). A novel MADS-box gene subfamily with a sister-group relationship to class B floral homeotic genes. *Mol. Genet. Genomics* **266**: 942–950.
- Becraft, P.W., Gutierrez-Marcos, J.** (2012). Endosperm development: dynamic processes and cellular innovations underlying sibling altruism. *Wiley Interdiscip. Rev. Dev. Biol.* **1**: 579-593.
- Beers, E.P.** (1997). Programmed cell death during plant growth and development. *Cell Death Differ.* **4**: 649–661.
- Boatright, KM., Salvesen G.S.** (2003). Mechanisms of caspase activation. *Current Opinion in Cell Biology.* **15**: 725–731
- Bonneau, L., Ge, Y., Drury, G.E., Gallois P.** (2008). What happened to plant caspases? *J. Exp. Bot.* **59**: 491–499.
- Bosch M, Franklin-Tong V.E.,** (2008) Self-incompatibility in Papaver: signalling to trigger PCD in incompatible pollen. *J. Exp. Bot.* **59**: 481-490.
- Borén, M., Höglund, A.S., Bozhkov, P., Jansson, C.** (2006). Developmental regulation of a VEIDase caspase-like proteolytic activity in barley caryopsis. *J. Exp. Bot.* **57**: 3747-3753.
- Bozhkov, P.V., Filonova, L.H., Suarez, M.F.** (2005). Programmed cell death in plant embryogenesis. *Curr. Top. Dev. Biol.* **67**: 135-179.
- Bozhkov, P.V., Suarez, M.F., Filonova, L.H., Daniel, G., Zamyatnin, A.A. Jr, Rodriguez-Nieto, S., Zhivotovsky, B., Smertenko, A.** (2005). Cysteine protease mclI-Pa executes programmed cell death during plant embryogenesis. *Proc. Natl. Acad. Sci. USA* **102**: 14463-14468.
- Breeze, E., Harrison, H., McHattie, S.** (2011). High-resolution temporal profiling of transcripts during Arabidopsis leaf senescence reveals a distinct chronology of processes and regulation. *Plant Cell* **23**: 873-894.
- Brocklehurst, P.** (1977). Factors controlling grain weight in wheat. *Nature* **266**: 348–349.

- Cai, Y.M., Yu, J., Gallois, P.** (2014). Endoplasmic reticulum stress-induced PCD and caspase-like activities involved. *Front. Plant Sci.* **5**: 41.
- Chen, F., Foolad, M.R.** (1997). Molecular organization of a gene in barley which encodes a protein similar to aspartic protease and its specific expression in nucellar cells during degeneration. *Plant Mol. Biol.* **35**: 821–831.
- Church, G.M., Gilbert, W.** (1984). Genomic sequencing. *Proc Natl Acad Sci USA.* **81**: 1991-5.
- Chichkova, N.V., Shaw, J., Galiullina, R.A., Drury, G.E., Tuzhikov, A. I., Kim, S.H., Kalkum, M., Hong, T.B., Gorshkova, E.N., Torrance, L., Vartapetian, A.B., Taliansky, M.** (2010). Phytaspase, a relocalisable cell death promoting plant protease with caspase specificity. *EMBO J.* **29**: 1149–1161.
- Chojecki, A., Bayliss, M., Gale, M.** (1986). Cell production and DNA accumulation in the wheat endosperm, and their association with grain weight. *Ann. Bot.* **58**: 809–817.
- Christiansen, M.W., Gregersen, P.L.** (2014). Members of the barley NAC transcription factor gene family show differential co-regulation with senescence associated genes during senescence of flag leaves. *J. Exp. Bot.* **65**: 4009-4022.
- Christoff, A.P., Turchetto-Zolet, A.C., Margis, R.** (2014). Uncovering legumain genes in rice. *Plant Sci.* **215-216**: 100-109.
- Cochrane, MP, Duffus, C.M.** (1980). The nucellar projection and modified aleurone in the crease region of developing caryopses of barley (*Hordeum vulgare* L. var. *distichum*). *Protoplasma* **103**: 361-375.
- Coffeen, W.C., Wolpert, T.J.** (2004). Purification and characterization of serine proteases that exhibit caspase-like activity and are associated with programmed cell death in *Avena sativa*. *Plant Cell* **16**: 857–873.
- Cohen, S.N., Chang, A.C., Hsu, L.** (1972). Nonchromosomal antibiotic resistance in bacteria: genetic transformation of *Escherichia coli* by R-factor DNA. *Proc. Natl. Acad. Sci. USA*, **69**: 2110-2114.
- Courtois-Moreau, C.L., Pesquet, E., Sjödin, A., Muñiz, L., Bollhöner, B., Kaneda, M., Samuels, L., Jansson, S., Tuominen, H.** (2009) A unique program for cell death in xylem fibers of *Populus* stem. *Plant J.* **58**: 260–274.
- Dangl, J.L., Jones, J.D.** (2001). Plant pathogens and integrated defense responses to infection. *Nature* **411**: 826–833.
- Degtarev, A., Boyce, M., Yuan, J.** (2003). A decade of caspases. *Oncogene.* **22**: 8543–8567.
- Delaney TP, Uknes S, Vernooij B, Friedrich L, Weymann K, Negrotto D, Gaffney T, Gut-Rella M, Kessmann H, Ward, E.** (1994). A central role of salicylic acid in plant disease resistance. *Science*: **266**:1247–1250.
- de Folter, S., Angenent, G.C.** (2006). trans meets cis in MADS science. *Trends Plant Sci.* **118(1)**:224–231.
- Della Mea, A., Serafini-Fracassini, D., Del Duca, S.** (2007). Programmed cell death: similarity and differences in animals and plants. A flower paradigm. *Amino Acids* **33**: 395–404.
- del Pozo, O., Lam, E.** (1998). Caspases and programmed cell death in the hypersensitive response of plants to pathogens. *Curr. Biol.* **8**: 1129–1132.

- Doan, D., Linnestad, C., and Olsen, O.A.** (1996). Isolation of molecular markers from the barley endosperm coenocyte and the surrounding nucellus cell layers. *Plant Mol. Biol.* **31**, 877–886.
- Domínguez, F., Moreno, J., Cejudo, F.J.** (2001). The nucellus degenerates by a process of programmed cell death during the early stages of wheat grain development. *Planta* **213**: 352–360.
- Domínguez F., Cejudo F.J.** (1998). Germination-related genes encoding proteolytic enzymes are expressed in the nucellus of developing wheat grains. *Plant J.* **15**: 569–574.
- Drew, M.C., He, C.J., Morgan, P.W.** (2000). Programmed cell death and aerenchyma formation in roots. *Trends Plant Sci.* **5**: 123–127.
- Ekert, P.G., Silke, J., Vaux, D.L.** (1999) Inhibition of apoptosis and clonogenic survival of cells expressing crmA variants: optimal caspase substrates are not necessarily optimal inhibitors. *EMBO J.*, **18**, 330–338
- Escamez, S., André, D., Zhang, B., Bollhöner, B., Pesquet, E., Tuominen, H.** (2016) METACASPASE9 modulates autophagy to confine cell death to the target cells during Arabidopsis vascular xylem differentiation. *Biol. Open* **5**: 122-129.
- Escamez, S., Tuominen, H.** (2014). Programmes of cell death and autolysis in tracheary elements: when a suicidal cell arranges its own corpse removal. *J. Exp. Bot.* **65**: 1313–1321.
- Fagundes, D., Bohn, B., Cabreira, C., Leipelt, F., Dias, N., Bodanese-Zanettini, M.H., Cagliari, A.** (2015). Caspases in plants: metacaspase gene family in plant stress responses. *Funct. Integr. Genomics* **15**: 639-649.
- Farage-Barhom, S., Burd, S., Sonogo, L., Perl-Treves, R., Lers, A.** (2008). Expression analysis of the BFN1 nuclease gene promoter during senescence, abscission, and programmed cell death-related processes. *J. Exp. Bot.* **59**: 3247–3258.
- Fendrych, M., Van Hautegeem, T., Van Durme, M., Olvera-Carrillo, Y., Huysmans, M., Karimi, M., Lippens, S., Guérin, C.J., Krebs, M., Schumacher, K., Nowack, M.K.** (2014). Programmed cell death controlled by ANAC033/SOMBRERO determines root cap organ size in Arabidopsis. *Curr. Biol.* **24**: 931–940.
- Fernández, M.B., Daleo, G.R., Guevara, M.G.** (2015). Isolation and characterization of a *Solanum tuberosum* subtilisin-like protein with caspase-3 activity (StSBTc-3). *Plant Physiol. Biochem.* **86**: 137-46.
- Filonova, L.H., Bozhkov, P.V., Brukhin, V.B., Daniel, G., Zhivotovsky, B., von Arnold, S.** (2000). Two waves of programmed cell death occur during formation of development of somatic embryos in the gymnosperm, Norway spruce. *J. Cell Sci.* **113**: 4399–4411.
- Friedman, W.E., Ryerson, K.C.** (2009). Reconstructing the ancestral female gametophyte of angiosperms: insights from Amborella and other ancient lineages of flowering plants. *Am. J. Bot.* **96**: 129–143.
- Fukuda, H.** (1996). Xylogenesis: initiation, progression, and cell death. *Annu. Rev. Plant Physiol. Plant Mol. Biol.* **47**: 299–345.

- Gavireli, Y., Sherman, Y., Ben-Sasson, S.A.** (1992). Identification of programmed cell death in situ via specific labelling of nuclear DNA fragmentation. *Journal of Cell Biology* **119**, 493–501.
- Gechev, T.S., Van Breusegem, F., Stone, J.M., Denev, I., Laloi, C.** (2006). Reactive oxygen species as signals that modulate plant stress responses and programmed cell death. *BioEssays* **28**: 1091–1101.
- Gepstein, S., Glick, B.R.** (2013). Strategies to ameliorate abiotic stress-induced plant senescence. *Plant Mol. Biol.* **82**: 623–633.
- Greenberg J.T.** (1997). Programmed cell death in plant-pathogen interactions. *Annu. Rev. Plant Physiol. Plant Mol. Biol.* **48**: 525–545.
- Greenberg, J.T.** (1996). Programmed cell death: a way of life for plants. *Proc. Natl. Acad. Sci. USA* **93**: 12094–12097.
- Greenberg, J.T., Guo, A., Klessig, D.F., Ausubel, F.M.** (1994). Programmed cell death in plants: a pathogen-triggered response activated coordinately with multiple defense functions. *Cell* **77**: 565–577.
- Gregersen, P.L., Holm, P.B., Krupinska, K.** (2008), Leaf senescence and nutrient remobilisation in barley and wheat. *Plant Biol.* **10**: 37–49.
- Gubatz, S., Weschke, W.** (2014). Barley grain: development and structure. In: Shewry, P.R., Ullrich, S. (Eds.): *Barley: chemistry and technology*, 2nd ed. St. Paul, Minnesota: AACC International Inc. pp. 11–54. ISBN 978-1-891127-79-3
- Gunawardena, A.H.L.A.N., Greenwood, J.S., Dengler, N.G.** (2004). Programmed cell death remodels leaf shape during development. *Plant Cell* **16**: 60–73.
- Gunawardena A.H.L.A.N.** (2008) Programmed cell death and tissue remodelling in plants. *J. Exp. Bot.* **59**: 445–451.
- Han, J.J., Lin, W., Oda, Y., Cui, K.M., Fukuda, H., He, X.Q.** (2012). The proteasome is responsible for caspase-3-like activity during xylem development. *Plant J.* **72**: 129–141.
- Hanamata, S., Kurusu, T., Kuchitsu, K.** (2014). Roles of autophagy in male reproductive development in plants. *Front. Plant Sci.* **5**: 457.
- Hands, P., Kourmpetli, S., Sharples, D., Harris, R.G., Drea, S.** (2012). Analysis of grain characters in temperate grasses reveals distinctive patterns of endosperm organization associated with grain shape. *J. Exp. Bot.* **63**: 6253–6266.
- Hara-Nishimura, I., Hatsugai, N., Nakaune, S., Kuroyanagi, M., Nishimura, M.** (2005). Vacuolar processing enzyme: an executor of plant cell death. *Current Opinion in Plant Biology.* **8**: 404–408.
- Hara-Nishimura, I., Maeshima, M.** (2000). Vacuolar processing enzymes and aquaporins. In *Vacuolar Compartments in Plants*, A.D.G. Robinson and J.C. Rogers, eds (London: Sheffield Academic Press), pp. 20–42.
- Hara-Nishimura, I., Nishimura, M.** (1987). Proglobulin processing enzyme in vacuoles isolated from developing pumpkin cotyledons. *Plant Physiol.* **85**: 440–445.
- Hatsugai, N., Yamada, K., Goto-Yamada, S., Hara-Nishimura, I.** (2015). Vacuolar processing enzyme in plant programmed cell death. *Frontiers in Plant Science.* **6**: 234.

- Hatsugai, N., Kuroyanagi, M., Nishimura, M., Hara-Nishimura, I.** (2006). A cellular suicide strategy of plants: vacuole-mediated cell death. *Apoptosis* **11**: 905-911.
- Hatsugai, N., Kuroyanagi, M., Yamada, K., Meshi, T., Tsuda, S., Kondo, M., Nishimura, M., Hara-Nishimura, I.** (2004). A plant vacuolar protease, VPE, mediates virus-induced hypersensitive cell death. *Science* **305**: 855-858.
- Hatsugai, N., Iwasaki, S., Tamura, K., Kondo, M., Fuji, K., Ogasawara, K., Nishimura, M., Hara-Nishimura, I.** (2009). A novel membrane fusion-mediated plant immunity against bacterial pathogens. *Genes Dev.* **23**: 2496-2506.
- He, R., Drury, G. E., Rotari, V. I., Gordon, A., Willer M., Farzaneh, T.** (2008). Metacaspase-8 modulates programmed cell death induced by ultraviolet light and H₂ O₂ in Arabidopsis. *J. Biol. Chem.* 283 774–783.
- Heath, M.C.** (2000). Hypersensitive response-related death. *Plant Mol. Biol.* **44**: 321–334.
- Hehenberger, E., Kradolfer, D., Kohler, C.** (2012). Endosperm cellularization defines an important developmental transition for embryo development. *Development* **139**: 2031–2039.
- Heydlauff, J., Gross-Hardt, R.** (2014). Love is a battlefield: programmed cell death during fertilization. *J. Exp. Bot.* **65**: 1323–1330.
- Hengartner, M.O.** (2000). The biochemistry of apoptosis. *Nature* **407**: 770–776.
- Hensel, G., Kastner, C., Oleszczuk, S., Riechen, J., Kumlehn, J.** (2009). Agrobacterium-mediated gene transfer to cereal crop plants: current protocols for barley, wheat, triticale, and maize. *Int. J. Plant Genomics* 2009: 835608.
- Hiraiwa, N., Nishimura, M., and Hara-Nishimura, I.** (1999). Vacuolar processing enzyme is self-catalytically activated by sequential removal of the C-terminal and N-terminal propeptides. *FEBS Lett.* **447**, 213–216
- Hofius, D., Tsitsigiannis, D.I., Jones, J.D.G., Mundy, J.** (2007). Inducible cell death in plant immunity. *Sem. Cancer Biol.* **17**: 166-187.
- Huang, S., Mira, M.M., Stasolla, C.** (2016). Dying with style: death decision in plant embryogenesis. *Methods Mol. Biol.* **1359**: 101-115.
- Jibrán, R., Hunter, D., Dijkwel, P.** (2013). Hormonal regulation of leaf senescence through integration of developmental and stress signals. *Plant Mol. Biol.* **82**: 547-561.
- Jin, Z., El-Deiry, W.S.** (2005). Overview of cell death signaling pathways. *Cancer Biol. Therapy* **4**: 139-163.
- Jones, A.M.** (2000). Does the plant mitochondrion integrate cellular stress and regulate programmed cell death? *Trends Plant Sci.* **5**: 225–230.
- Jones, J.D., Dangl, J.L.** (2006). The plant immune system. *Nature* **444**: 323–329.
- Julian, I., Gandullo, J., Santos-Silva, L.K., Diaz, I., Martinez, M.** (2013). Phylogenetically distant barley legumains have a role in both seed and vegetative tissues. *J. Exp. Bot.* **64**: 2929–2941.
- Kamboj, J.S., Blake, P.S., and Baker, D.A.** (1998). Cytokinins in the vascular saps of *Ricinus communis*. *Plant Growth Regul.* **25** 123–126.

- Kater, M.M., Dreni, L., Colombo, L.** (2006). Functional conservation of MADS-box factors controlling floral organ identity in rice and *Arabidopsis*. *J. Exp. Bot.* **57**: 3433–3444.
- Kim, S., Kim, S., Wang, Y., Yu, S., Choi, I.** (2011) The RNase activity of rice probenazole-induced protein1 (PBZ1) plays a key role in cell death in plants. *Mol Cells* 31: 25–31
- Kinoshita, T., Yamada, K., Hiraiwa, N., Kondo, M., Nishimura, M., Hara-Nishimura, I.** (1999). Vacuolar processing enzyme is up-regulated in the lytic vacuoles of vegetative tissues during senescence and under various stressed conditions. *Plant J.* **19**: 43–53.
- Kladnik, A., Chamusco, K., Dermastia, M., Chourey P.** (2004). Evidence of programmed cell death in post-phloem transport cells of the maternal pedicel tissue in developing caryopsis of maize. *Plant Physiology.* **136**: 3572-3581.
- Kohl, S., Hollmann, J., Erban, A., Kopka, J., Riewe, D., Weschke, W., Weber, H.** (2015). Metabolic and transcriptional transition in barley glumes reveal a role as transitory resource buffers during endosperm filling. *J. Exp. Bot.* **66**: 1397-1411.
- Kozloski, G.V., Rocha, J.B.T., Ribeiro Filho, H. and Perottoni, J.** (1999). Comparison of acid and amyloglucosidase hydrolysis for estimation of non-structural polysaccharides in feed samples. *Journal of the Science of Food and Agriculture*, 79, 1112-1116.
- Korthout, H.A., Berecki, G., Bruin, W., van Duijn, B., Wang, M.** (2000). The presence and subcellular localization of caspase 3-like proteinases in plant cells. *FEBS Lett.* **475**: 139–144.
- Koukalova, B., Kovarik, A., Fajkus, J., Siroky, J.** (1997). Chromatin fragmentation associated with apoptotic changes in tobacco cells exposed to cold stress. *FEBS Lett.* **414**: 289–292.
- Kraus, D.** (2014). Daniel's XL Toolbox addin for Excel, version 6.10.
<http://xltoolbox.sourceforge.net>.
- Krishnan S., Dayanandan, P.** (2003). Structural and histochemical studies on grain-filling in the caryopsis of rice (*Oryza sativa L.*). *J. Biosci.* 28 455–469
- Kroemer, G., Galluzzi, L., Vandenabeele, P., Abrams, J., Alnemri, E., et al.** (2009). Classification of cell death: recommendations of the Nomenclature Committee on Cell Death. *Cell Death Differ.* **16**: 3–11.
- Kubo, M., Udagawa, M., Nishikubo, N., Horiguchi, G., Yamaguchi, M., Ito, J., Mimura, T., Fukuda, H., Demura, T.** (2005). Transcription switches for protoxylem and metaxylem vessel formation. *Genes Dev.* **19**: 1855–1860.
- Kuroyanagi, M., Yamada, K., Hatsugai, N., Kondo, M., Nishimura, M., Hara-Nishimura, I.** (2005). Vacuolar processing enzyme is essential for mycotoxin-induced cell death in *Arabidopsis thaliana*. *J. Biol. Chem.* **280**: 32914–32920.
- Kuroyanagi, M., Nishimura, M., and Hara-Nishimura, I.** (2002). Activation of Arabidopsis vacuolar processing enzyme by self-catalytic removal of an auto-inhibitory domain of the C-terminal propeptide. *Plant Cell Physiol.* 43: 143–151
- Lam, E.** (2004). Controlled cell death, plant survival and development. *Nat. Rev. Mol. Cell Biol.* 5, 305–315.
- Liang, J., Zhang, J., Cao, X.** (2001). Grain sink strength may be related to the poor grain filling of indica-japonica rice (*Oryza sativa*) hybrids. *Plant Physiol.* **112**: 470–477.

- Linnestad, C., Doan, D.N., Brown, R.C., Lemmon, B.E., Meyer, D.J., Jung, R., Olsen, O.A.** (1998). Nucellain, a barley homolog of the dicot vacuolar-processing protease, is localized in nucellar cell walls. *Plant Physiol.* **118**: 1169–1180.
- Liu, P., Qi, M., Wang, Y., Chang, M., Liu, C., Sun, M., Yang, W., Ren, H.** (2014). Arabidopsis RAN1 mediates seed development through its parental ratio by affecting the onset of endosperm cellularization. *Mol. Plant* **7**: 1316–1328.
- Lohmann, J.U., Weigel, D.** (2002). Building beauty: The genetic control of floral patterning. *Dev. Cell* **2**: 135–142.
- Lombardi, L., Ceccarelli, N., Picciarelli, P., Lorenzi, R.** (2007). DNA degradation during programmed cell death in *Phaseolus coccineus* suspensor. *Plant Physiol. Biochem.* **45**: 221–227.
- Lopez-Fernandez, M.P., Maldonado, S.** (2015) Programmed cell death in seeds of angiosperms. *J Integr Plant Biol* **57**: 996–1002
- Lord, C.E.N., Gunawardena, A.H.L.A.N.** (2011). Environmentally induced programmed cell death in leaf protoplasts of *Aponogeton madagascariensis*. *Planta* **233**: 407–421.
- Love A.J., Milner J.J. & Sadanandom A.** (2008) Timing is everything: regulatory overlap in plant cell death. *Trends in Plant Science* **13**, 589–595.
- Masclaux-Daubresse, C., Reisdorf-Cren, M., Orsel, M.** (2008). Leaf nitrogen remobilisation for plant development and grain filling. *Plant Biol.* **10**: 23–36.
- Matsumoto, T., Tanaka, T., Sakai, H., Amano, N., Kanamori, H., Kurita, K., Sato, K.** (2011). Comprehensive Sequence Analysis of 24,783 Barley Full-Length cDNAs Derived from 12 Clone Libraries. *Plant Physiology.* **156**(1), 20–28.
- Melkus G., Rolletschek H., Fuchs J., Radchuk V., Grafahrend-Belau E., Sreenivasulu N.** (2011). Dynamic ¹³C/¹H NMR imaging uncovers sugar allocation in the living seed. *Plant Biotechnol. J.* **9** 1022–1037
- Milhinhos, A., Miguel, C.M.** (2013). Hormone interactions in xylem development: a matter of signals. *Plant Cell Rep.* **32**: 867–883.
- Mino M., Murata N., Date S., Inoue M.** (2007). Cell death in seedlings of the interspecific hybrid of *Nicotiana gossei* and *N. tabacum*; possible role of knob-like bodies formed on tonoplast in vacuolar-collapse-mediated cell death. *Plant Cell Rep.* **26**: 407–419.
- Mittler R, Simon L, Lam E.** (1997) Pathogen-induced programmed cell death in tobacco. *J Cell Sci* **110**:1333–1344.
- Mönke, G., Altschmied, L., Tewes, A., Reidt, W., Mock, H.P., Bäumlein, H., Conrad, U.** (2004). Seed-specific transcription factors ABI3 and FUS3: molecular interaction with DNA. *Planta* **219**: 158–166.
- Müntz, K.** (2007). Protein dynamics and proteolysis in plant vacuoles. *J. Exp. Bot.* **58**: 2391–2407.
- Müntz, K., and Shutov, A.** (2002). Legumains and their functions in plants. *Trends Plant Sci.* **7**: 340–344
- Nakaune, S., Yamada, K., Kondo, M., Kato, T., Tabata, S., Nishimura, M., Hara-Nishimura, I.** (2005). A vacuolar processing enzyme, δ VPE, is involved in seed coat formation at the early stage of seed development. *Plant Cell* **17**: 876–887.

- Navarre, D.A., Wolpert, T.J.** (1999). Victorin induction of an apoptotic/senescence-like response in oats. *Plant Cell* **11**: 237–249.
- Nayar, S., Kapoor, M., Kapoor, S.** (2014). Post-translational regulation of rice MADS29 function: homodimerization or binary interactions with other seed-expressed MADS proteins modulate its translocation into the nucleus. *J. Exp. Bot.* **65**: 5339-5350.
- Nayar, S., Sharma, R., Tyagi, A.K., Kapoor, S.** (2013). Functional delineation of rice MADS29 reveals its role in embryo and endosperm development by affecting hormone homeostasis. *J. Exp. Bot.* **64**: 4239-4253.
- Nawkar, G.M., Maibam, P., Park, J.H., Sahi, V.P., Lee, S.Y., Kang, C.H.** (2013). UV-induced cell death in plants. *Int. J. Mol. Sci.* **14**: 1608-1628.
- Nesi, N., Debeaujon, I., Jond, C., Stewart, A.J., Jenkins, G.I., Caboche, M., Lepiniec, L.** (2002). The *TRANSPARENT TESTA16* locus encodes the ARABIDOPSIS BSISTER MADS domain protein and is required for proper development and pigmentation of the seed coat. *Plant Cell* **14**: 2463–2479.
- Oflfer, C.E., McCurdy, D.W., Patrick J.W., Talbot, M.J.** (2003) Transfer cells: cells specialized for a special purpose. *Annu Rev Plant Biol* 54 431–454
- Olsen, O.A.** (2004). Nuclear endosperm development in cereals and *Arabidopsis thaliana*. *Plant Cell* **16**: S214–S227.
- Orman-Ligeza, B., Parizot, B., Gantet, P.P., Beeckman, T., Bennett, M.J., Draye, X.** (2013). Post-embryonic root organogenesis in cereals: branching out from model plants. *Trends Plant Sci.* **18**: 459–467.
- Overmyer, K., Tuominen, H., Kettunen, R., Betz, C., Langebartels, C., Sandermann, H., Kangasjarvi, J.** (2000). Ozone-sensitive Arabidopsis *rcd1* mutant reveals opposite roles for ethylene and jasmonate signaling pathways in regulating superoxide-dependent cell death. *Plant Cell* **12**: 1849–1862.
- Olvera-Carrillo, Y., Van Bel, M., Van Hautegeem, T., Fendrych, M., Huysmans, M., Simaskova, M., van Durme, M., Buscaill, P., Rivas, S, Coll, N.S., Coppens, F., Maere, S., Nowack, M.K.** (2015). A conserved core of programmed cell death indicator genes discriminates developmentally and environmentally induced programmed cell death in plants. *Plant Physiol.* **169**: 2684-2699.
- Palotta M., Graham R., Langridge P., Sparrow D., Barker S.** (2000). RFLP mapping of manganese efficiency in barley. *Theor. Appl. Genet.* **101**: 1100–1108.
- Parish, R.W., Li, S.F.** (2010). Death of a tapetum: a program of developmental altruism. *Plant Sci.* **178**: 73–89.
- Pennel, R.I., Lamb, C.** (1997). Programmed cell death in plants. *Plant Cell* **9**: 1157–1168.
- Pielot, R., Kohl, S., Manz, B., Rutten, T., Weier, D., Tarkowská, D., Rolčík, J., Strnad, M., Volke, F., Weber, H., Weschke, W.** (2015). Hormone-mediated growth dynamics of the barley pericarp as revealed by magnetic resonance imaging and transcript profiling. *J. Exp. Bot.* **66**: 6927-6943.
- Plackett, A.R., Thomas, S.G., Wilson, Z.A., Hedden, P.** (2011). Gibberellin control of stamen development: a fertile field. *Trends Plant Sci.* **16**: 568–578.

- Prasad, K., Zhang, X., Tobon, E., Ambrose, B.A.** (2010). The *Arabidopsis* B-sister MADS-box protein, GORDITA, represses fruit growth and contributes to integument development. *Plant J.* **62**: 203–214.
- Radchuk, V., Borisjuk, L.** (2014). Physical, metabolic and developmental functions of the seed coat. *Front. Plant Sci.* **5**: 510.
- Radchuk V., Kumlehn J., Rutten T., Sreenivasulu N., Radchuk R., Rolletschek H.** (2012). Fertility in barley flowers depends on Jekyll functions in male and female sporophytes. *New Phytol.* **194** 142–157
- Radchuk, V., Weier, D., Radchuk, R., Weschke, W., Weber, H.** (2011). Development of maternal seed tissue in barley is mediated by regulated cell expansion and cell disintegration and co1, ordinated with endosperm growth. *J. Exp. Bot.* **62**: 1217–1227.
- Radchuk, V.V., Borisjuk, L., Sreenivasulu, N., Merx, K., Mock, H.P., Rolletschek, H., Wobus, U., Weschke, W.** (2009). Spatio-temporal profiling of starch biosynthesis and degradation in the developing barley grain. *Plant Physiol.* **150**: 190–204.
- Radchuk, V., Borisjuk, L., Radchuk, R., Steinbiss, H.H., Rolletschek, H., Broeders, S., Wobus, U.** (2006). Jekyll encodes a novel protein involved in the sexual reproduction of barley. *Plant Cell* **18**: 1652–1666.
- Radley M.** (1978). Factors affecting grain enlargement in wheat. *J. Exp. Bot.* **29**: 919–934.
- Rantong, G., Evans, R., Gunawardena, A.H.L.A.N.** (2015). Lace plant ethylene receptors, AmERS1a and AmERS1c, regulate ethylene-induced programmed cell death during leaf morphogenesis. *Plant Mol. Biol.* **89**: 215-227.
- Rantong, G., Gunawardena A.H.L.A.N.** (2014). Programmed cell death: genes involved in signaling, regulation, and execution in plants and animals. *NRC Res. Press Botany* **93**: 193-210.
- Reape, T. J., and McCabe, P. F.** (2010) Apoptotic-like regulation of programmed cell death in plants. *Apoptosis* **15**: 249–256.
- Reape, T. J., and McCabe, P. F.** (2008) Apoptotic-like programmed cell death in plants. *New Phytologist* **180**: 13–26.
- Rolletschek, H., Weschke, W., Weber, H., Wobus, U., and Borisjuk, L.** (2004). Energy state and its control on seed development: starch accumulation is associated with high ATP and steep oxygen gradients within barley grains. *J. Exp. Bot.* **55**: 1351-1359.
- Rojo, E., Martin, R., Carter, C., Zouhar, J., Pan, S., Plotnikova, J., Jin, H., Paneque, M., Sánchez-Serrano, J.J., Baker, B., Ausubel, F.M., Raikhel, N.V.** (2004). VPEy exhibits a caspase-like activity that contributes to defense against pathogens. *Curr. Biol.* **14**: 1897–1906.
- Rubinstein, B.** (2000). Regulation of cell death in flower petals. *Plant Mol. Biol.* **44**: 303–318.
- Sambrook, J., Russell, D. W.** (2001). Molecular cloning. *Cold Spring Harbor Laboratory manual* 2001.
- Scott, I., Logan, D.C.** (2008). Mitochondrial morphology transition is an early indicator of subsequent cell death in *Arabidopsis*. *New Phytol.* **177**: 90–101.

- Senatore, A., Trobacher, C.P., Greenwood, J.S.** (2009). Ricinosomes predict programmed cell death leading to anther dehiscence in tomato. *Plant Physiol.* **149**: 775-790.
- Shimada, T., Yamada, K., Kataoka, M., Nakaune, S., Koumoto, Y., Kuroyanagi, M., Tabata, S., Kato, T., Shinozaki, K., Seki, M., Kobayashi, M., Kondo, M., Nishimura, M., Hara-Nishimura, I.** (2003). Vacuolar processing enzymes are essential for proper processing of seed storage proteins in *Arabidopsis thaliana*. *J. Biol. Chem.* **278**: 32292-32299.
- Simmonds, N.W.** (1995). The relation between yield and protein in cereal grain. *J. Food Agric.* **67**: 309-315.
- Sinclair, T.R.** (1998). Historical changes in harvest index and crop nitrogen accumulation. *Crop Sci.* **38**: 638-643.
- Singh, B., Jenner, C.** (1982). Association between concentration of organic nutrients in the grain, endosperm cell number and grain dry weight within the ear of wheat. *Funct. Plant Biol.* **9**: 83-95.
- Slee, E.A., Harte, M.T., Kluck, R.M., Wolf, B.B., Casiano, C.A.** (1999) Ordering the cytochrome c-initiated caspase cascade: hierarchical activation of caspases-2, -3, -6, -7, -8, and -10 in a caspase-9-dependent manner. *J Cell Biol* **144**: 281-292.
- Smertenko, A.P., Bozhkov, P.V., Filonova, L.H., von Arnold, S., Hussey, P.J.** (2003). Re-organisation of the cytoskeleton during developmental programmed cell death in *Picea abies* embryos. *The Plant Journal* **33**: 813-824.
- Solis, M.T., Chakrabarti, N., Corredor, E., Cortes-Eslava, J., Rodriguez-Serrano, M., Biggiogera, M., Risueno, M.C., Testillano P.S.** (2014) Epigenetic changes accompany developmental programmed cell death in tapetum cells. *Plant Cell Physiol.* **55**: 16-29
- Sreenivasulu, N., Radchuk, V., Alawady, A., Borisjuk, L., Weier, D., Staroske, N., Fuchs, J., Miersch, O., Strickert, M., Usadel, B., Wobus, U., Grimm, B., Weber, H., Weschke, W.** (2010). De-regulation of abscisic acid contents causes abnormal endosperm development in the barley mutant *seg8*. *Plant J.* **64**: 589-603.
- Sreenivasulu, N., Graner, A., Wobus, U.** (2008). Barley genomics: an overview. *Int. J. Plant Genomics* ID486258, 13 pp.
- Sreenivasulu, N., Radchuk, V., Strickert, M., Miersch, O., Weschke, W., Wobus, U** (2006). Gene expression patterns reveal tissue-specific signaling networks controlling programmed cell death and ABA-regulated maturation in developing barley seeds. *Plant J.* **47**: 310-327.
- Steffens, B., Kovalev, A., Gorb, S.N., Sauter, M.** (2012). Emerging roots alter epidermal cell fate through mechanical and reactive oxygen species signaling. *Plant Cell* **24**: 3296-3306.
- Suarez, M.F., Filonova, L.H., Smertenko, A., Savenkov, E.I., Clapham, D.H., von Arnold, S., Zhivotovsky, B., Bozhkov, P.V.** (2004). Metacaspase-dependent programmed cell death is essential for plant embryogenesis. *Curr. Biol.* **14**: R339-340.
- Swidzinski, J.A., Sweetlove, L.J., Leaver, C.J.** (2002). A custom microarray analysis of gene expression during programmed cell death in *Arabidopsis thaliana*. *Plant J.* **30**: 431-446.
- Theissen, G., Saedler, H.** (2001). Plant biology. Floral quartets. *Nature.* **409**(1):469-471

- Thiel, J., Müller, M., Weschke, W., Weber, H.** (2009). Amino acid metabolism at the maternal-filial boundary of young barley seeds: a microdissection-based study. *Planta* **230**: 205-213.
- Thiel, J., Weier, D., Sreenivasulu, N., Strickert, M., Weichert, N., Melzer, M., Czauderna, T., Wobus, U., Weber, H., Weschke, W.** (2008). Different hormonal regulation of cellular differentiation and function in nucellar projection and endosperm transfer cells: a microdissection-based transcriptome study of young barley grains. *Plant Physiol.* **148**: 1436–1452.
- Thomas, H.** (2013). Senescence, ageing and death of the whole plant. *New Phytol.* **197**: 696–711.
- Thomas, S.G., Franklin-Tong, V.E.** (2004). Self-incompatibility triggers programmed cell death in *Papaver* pollen. *Nature* **429**: 305-309.
- Trafford, K., Haleux, P., Henderson, M., Parker, M., Shirley, N.J., Tucker, M.R., Fincher, G.B., Burton, R.A.** (2013). Grain development in *Brachypodium* and other grasses: possible interactions between cell expansion, starch deposition, and cell-wall synthesis. *J. Exp. Bot.* **64**: 5033-5047.
- Tran, V., Weier, D., Radchuk, R., Thiel, J., Radchuk, V.** (2014). Caspase-like activities accompany programmed cell death events in developing barley grains. *PLoS One* **9**: e109426.
- van Doorn, W.G., Beers, E.P., Dangl, J.L.** (2011). Morphological classification of plant cell deaths. *Cell Death Differ.* **18**: 1241–1246.
- van Doorn, W.G.,** (2011). Classes of programmed cell death in plants, compared to those in animals. *J. Exp. Bot.* **62** (14): 4749-4761.
- van Doorn, W.G., Woltering, E.J.** (2005). Many ways to exit? Cell death categories in plants. *Trends Plant Sci.* **10**: 117–122.
- van Doorn W.G.** (2004). Is petal senescence due to sugar starvation? *Plant Physiology.* **134**:35-42
- Van Hautegeem, T., Waters, A.J., Goodrich, J., Nowack, M.K.** (2015). Only in dying, life: programmed cell death during plant development. *Trends Plant Sci.* **20**: 102-113.
- Varda, S.B., Nurit, K., Hilal, Z.** (2008) Uncovering the role of VDAC in the regulation of cell life and death. *J Bioenerg Biomembr* **40**: 183–191.
- Vartapetian, A.B., Tuzhikov, A.I., Chichkova, N.V., Taliansky M., Wolpert T.J.** (2011). A plant alternative to animal caspases: Subtilisin-like proteases. *Cell Death and Differ.* **18**, 1289–1297.
- Vercammen, D., Declercq, W., Vandenabeele, P., Van Breusegem, F.** (2007). Are metacaspases caspases? *J. Cell Biol.* **179**: 375–380.
- Vercammen, D., van de Cotte, B., De Jaeger, G., Eeckhout, D., Casteels, P., Vandepoele, K., Vanderberghe, I., Beeumen, J., Inze, D., van Breusegem, F.** (2004). Type II metacaspases Atmc4 and Atmc9 of *Arabidopsis thaliana* cleave substrates after arginine and lysine. *J. Biol. Chem.* **279**: 54329-45336.

- Wang, H., Li, J., Bostock, R.M., Gilchrist, D.G.** (1996). Apoptosis: a functional paradigm for programmed plant cell death induced by a host-selective phytotoxin and invoked during development. *Plant Cell* **8**: 375–391.
- Weber, H., Sreenivasulu, N., Weschke, W.** (2010). The molecular physiology of seed maturation and seed storage protein biosynthesis. In: Pua, E.C., Davey, M. (Eds.), *Plant Developmental Biology — Biotechnological Perspectives*, Vol. 2. Springer, Heidelberg.
- Weschke, W., Panitz, R., Sauer, N., Wang, Q., Neubohn, B., Weber, H.** (2000). Sucrose transport into barley seeds: molecular characterization and implications for seed development and starch accumulation. *Plant J.* **21**: 455–467.
- Wilkins, K.A., Poulter, N.S., Franklin-Tong, V.E.** (2014). Taking one for the team: self-recognition and cell suicide in pollen. *J. Exp. Bot.* **65**: 1331–1342.
- Williams B. & Dickman M.** (2008) Plant programmed cell death: can't live with it; can't live without it. *Molecular Plant Pathology* **9**, 531–544.
- Wobus, U., Sreenivasulu, N., Borisjuk, L., Rolletschek, H., Panitz, R., Gubatz, S., Weschke, W.** (2004). Molecular physiology and genomics of developing barley grains. *Recent Res. Dev. Plant Mol. Biol.* 21–29.
- Woltering, E.J., van der Bent, A., Hoeberichts, F.A.** (2002) Do plant caspases exist? *Plant Physiol* **130**: 1764–1769
- Wu, H.M. and Cheung, A.Y.** (2000). Programmed cell death in plant reproduction. *Plant Molecular Biology* **44**, 267–281.
- Xu, Q., Zhang, L.** (2009). Plant caspase-like proteases in plant programmed cell death. *Plant Signal. Behav.* **4**: 902–904.
- Yamada, K., Saraike, T., Shitsukawa, N., Hirabayashi, C., Takumi, S., Murai, K.** (2009). Class D and Bsister MADS-box genes are associated with ectopic ovule formation in the pistil-like stamens of alloplasmic wheat (*Triticum aestivum* L). *Plant Mol Biol.* **71**: 1–14
- Yamada, T., Ichimura, K., van Doorn W.G.,** (2006b). DNA degradation and nuclear degeneration during programmed cell death in petals of *Antirrhinum*, *Argyranthemum*, and *Petunia*. *Journal of Experimental Botany*; **57**:3543-3552
- Yamada, T., Takatsu, Y., Ichimura, K., van Doorn W.G.,** (2006a). Nuclear fragmentation and DNA degradation during programmed cell death in petals of morning glory (*Ipomoea nil*). *Planta.* **224**:1279-1290.
- Yamada, T., Takatsu, Y., Manabe, T., Kasumi, M., Marubashi, W.,** (2003). Suppressive effect of trehalose on apoptotic cell death leading to petal senescence in ethylene-insensitive flowers of *Gladiolus*. *Plant Science.* **164**:213-221
- Yamaguchi, T., Hirano, H.Y.** (2006). Function and diversification of MADS-box genes in rice. *Sci. World J.* **6**: 1923–1932.
- Yang, J., Zhang, J., Huang, Z., Wang, Z., Zhu, Q., and Liu, L.** (2002). Correlation of cytokinin levels in the endosperms and roots with cell number and cell division activity during endosperm development in rice. *Ann. Bot.* **90**: 369–377

- Yang, X., Wu, F., Lin, X., Du, X., Chong, K., Gramzow, L., Schilling, S., Becker, A., Theissen, G., Meng, Z.** (2012). Live and let die - the B_{sister} MADS-box gene *OsMADS29* controls the degeneration of cells in maternal tissues during seed development of rice (*Oryza sativa*). PLoS One **7**: e51435.
- Yin, L.L., Xue, H.W.** (2012). The *MADS29* transcription factor regulates the degradation of the nucellus and the nucellar projection during rice seed development. Plant Cell **24**: 1049-1065.
- Young TE, Gallie D.R.,** (2000). Programmed cell death during endosperm development. Plant Molecular Biology. 44: 283-301
- Young, T.E., Gallie, D.R., DeMason, D.A.** (1997). Ethylene mediated programmed cell death during maize endosperm development of wild type and *shrunk2* genotypes. Plant Physiol. **115**: 737–751.
- Zhu, J., Lou, Y., Xu, X., Yang, Z.N.** (2011). A genetic pathway for tapetum development and function in Arabidopsis. J. Integr. Plant Biol. **53**: 892–900.
- Zentgraf U, Laun T, Miao Y.** (2010). The complex regulation of WRKY53 during leaf senescence of *Arabidopsis thaliana* . European Journal of Cell Biology **89**, 133–137.

8. Publications and Presentations (during PhD study)

8.1 Publications

Van Tran, Diana Weier, Ruslana Radchuk, Johannes Thiel, Volodymyr Radchuk (2014), "Caspase-like activities accompany programmed cell death events in developing barley grain.", PLOS One, 9: e109426. [Dx.doi.org/10.1371/journal.pone.0109426](https://doi.org/10.1371/journal.pone.0109426).

8.2 Presentations at meetings and conferences

Van Tran, Radchuk R., Weier D., Hensel G., Fuchs J., Weschke W., Borisjuk L., Radchuk V. (2016), "Programmed cell death of maternal tissues in the developing barley grain is required for endosperm growth and grain filling.", Abstracts of Plant Proteases 2016 Conference, April 10-12, 2016, Oxford, UK

Van Tran, Conrad U., Weschke W., Radchuk V. (2015), "MADS29 transcription factor regulates programmed cell death in the nucellar projection of barley grains by direct interaction with Jekyll and VPE2a gene promoters.", Abstracts of 28th Conference of Molecular Biology of Plants, February 24-27, 2015; Dabringhausen, Germany

Van Tran, Radchuk R., Hensel G., Kumlehn J., Conrad U., Weber H., Weschke W., Radchuk V. (2014), "Down-regulation of the vacuolar processing enzymes in maternal seed tissues affects grain development of barley.", Abstracts of International Conference "Translational Cereal Genomics"; February 09 - 12, 2014; Vienna, Austria; p. 37.

Van Tran, Radchuk V., Radchuk R., Hensel G., Kumlehn J., Conrad U., Weber H., Weschke W. (2013), "Vacuolar processing enzymes and programmed cell death in developing barley grains.", IPK Evaluation Meeting; 25-26 September, 2013.

9. Acknowledgements

I would like to express special thanks to Dr. Volodymyr Radchuk, for supervision and providing me the opportunity to pursue this work. I am most thankful for his teachings, his dedication, the fruitful discussions concerning the scientific interpretation of the results deriving from this work and especially the honesty that has been a hallmark of the past five years.

I would like to express my gratitude to Dr. Weschke Winfriede for giving me the opportunity to work on this project, providing the prerequisites for a successful scientific work within the Seed Development Group as well as special thanks to Dr. Weschke Winfriede, Prof. Dr. Udo Conrad and Dr. Volodymyr Radchuk for their critical revisions of the thesis and the suggestions to improve content.

I would like to express my appreciation to Prof. Dr. Thomas Altmann to all the wonderful kindness and support, and also the helpful suggestions.

It is big pleasure to thank to all member of the Seed development group, I am most grateful to all my lab colleagues, Dr. Ruslana Radchuk, Dr. Hans Weber, Dr. Stefan Kohl and my friends, Dr. Cao Xuan Hieu, Dr. Vu Thi Ha Giang, Thirulogachandar Venkatasubbuchan who have been an integral part of this adventure and. I thank them all for the help given during the prosecution of this work and supported me in any respect throughout the years during good and hard time. I am particularly thankful our technicians at the IPK, Angela Stegmann, Elsa Fessel, Uta Siebert, Heiko Weichert, Kathrin Blaschek, and Angela Schwarz, for their excellent assistance in harvesting, preparing and analysing the plant material.

My great thank go to all the staff for making scientific life easier at IPK, especially Dr. Britt Leps for great help and assisting with all administrative issues.

For the financial supports, I am grateful to the Vietnamese government, the Ministry of Education and Training of Vietnam (MOET), the Ministry of Agricultural and Rural Development of Vietnam and the Leibniz-Institute of Plant Genetics and Crop Plant Research (IPK), Gatersleben, Germany.

Finally, I want to express my heartfelt thanks to my husband Nguyen Trong Tuat, my lovely son Nguyen Quoc Khanh and Nguyen Trong Khoi for their love, tender care, patience and sympathy. I would like to thank whole family for their ongoing care, support and encouragement throughout my work.

Thank you for everything!

10. Curriculum Vitae

Full name: Tran Thi Thuy Van
Date of birth: 15.02.1975
Nationality: Vietnam
Marital Status: Married, 2 children
Contacts detail: Leibniz Institute of Plant Genetics and Crop Plant Research (IPK)
Molecular Genetic Department, Seed Development Group
Corrensstrass.3, 06466 Seeland, OT Gatersleben, Germany
Telephone: 0394825352
Email: tran@ipk-gatersleben.de or thuyvank38@gmail.com
Current address: IPK Guest-house 1, Room No.17, Selkeweg 4a,
06466 Gatersleben (Germany).

Education and employment

08/2011 – present: PhD student at Seed development group, Molecular Genetics Department, Leibniz Institute of Plant Genetics and Crop Plant Research (IPK)
08/2008 – 07/2011: Researcher as Agricultural Science Institute of Northern Central Vietnam
07/2006 to 08/2008: Master student in Centre for Plant Breeding and Genetics, Tamil Nadu Agricultural University – Coimbatore 003 – Tamil Nadu State – India.
Title of thesis: "Genetic studies on two-line and three- line hybrid rice involving cytoplasmic male sterile lines."
01/1998 to 06/2006: Researcher as Center for Agricultural and Rural Development – Northern Central Region, Vietnam
09/1993 to 01/1998: Bachelor student in Agronomy, Hanoi Agricultural University No1 – Vietnam.

11. Declarations

“I, Tran Thi Thuy Van, declare that all the work presented in this dissertation was my own, carried out solely at the Seed Development Group of the Leibniz Institute of Plant Genetics and Crop Plant Research (IPK) Gatersleben. I have not used any other than the permitted reference sources or materials. All references and sources used in the presented work have been appropriately acknowledged. The content of this work has not been previously submitted for a degree in any educational institution.”

I hereby declare that I have no criminal record and that no preliminary investigations are pending against me.

Ich, Tran Thi Thuy Van, erkläre hiermit, dass die in dieser Dissertation präsentierte Arbeit von mir geleistet und ausschließlich in der Arbeitsgruppe Samenentwicklung des Leibniz-Instituts für Pflanzengenetik und Kulturpflanzenforschung (IPK) Gatersleben ausgeführt wurde. Ich habe keine anderen als die erlaubten Quellen und Hilfsmittel verwendet. Alle Quellen und Literaturangaben wurden als solche in der Arbeit kenntlich gemacht. Die vorliegende Arbeit wurde vorher noch nie zur Begutachtung eingereicht. Ich bewerbe mich damit zum ersten Mal um einen Doktorgrad.

Des Weiteren erkläre ich, dass ich weder vorbestraft bin noch dass gegen mich Ermittlungsverfahren anhängig sind.

Gatersleben, April 28th, 2016

Tran Thi Thuy Van

Appendix

Supplemental Tables

Supplemental Table S1. Oligonucleotides used for cloning of gene cDNAs and gene promoters

Primer name	Primer sequence (5' to 3')	Product size (bp)
<i>Cloning of full length VPE2a cDNA</i>		
HvVPE2a-F	CTTCCTCTAGCACTCTAGCACACGCAC	1455
HvVPE2a-R	GCATTTGCTACTGCTTCCGTGTA CTG	
<i>Cloning of VPE4 promoter</i>		
promVPE4-d1	ATCGCGCGCGTTAAATACAGCCTTTTTTATG	930
promVPE4-r1	TGCGACGACAAGACGAGGAGGAG	
<i>Cloning of VPE2a promoter</i>		
VPE2a-prom-dir1	GGGCCAGATTATCGAGACTTTCCAT	1062
VPE2a-prom-rev1	CACGCAGCCATCGCCACC	
<i>Cloning of full length MADS29 cDNA</i>		
MADS29-F	ACGTGCAGATTAATTCTTAGCAGGTCACAG	1154
MADS29-R	CTCATGCATGCATCATAAGGGTCAATCT	

Supplemental Table S2. List of primers used for qRT-PCR

Gene	Primer name	Sequence (5' to 3')	Product size (nt)
VPE2a	VPE2a_u	TGCGCTGCAGTACACGGAA	57
	VPE2a_r	TCTAGCTAGCTAGGAACCTCCG	
VPE2b	VPE2b_u	CAGCGCTTGCAACGGCTACGA	72
	VPE2b_r	TGCAAGCGGATCAGGGCTGTG	
VPE2c	VPE2c_u	GCGTCTCTGAGGCCCAAATGA	51
	VPE2c_r	TTATAACCGCCGCAAGCACTGAT	
VPE2d	VPE2d_u	GCTGCCTTTGCCATCCTG	91
	VPE2d_r	TCCCCGTTTAACTGCTCATACTT	
MADS29	MADS29_f	GGGCGGGCTGCTCAAGAAGG	114
	MADS29_r	CTGGAGGCGGGGCTGGAGTA	
actin*	Hvactin_u	GGTAGGGATGGGGCAGAAGG	415
	Hvactin_r	ACCAGCGAGATCCAAACGAAGAA	

**Hordeum vulgare actin* gene (Acc. Nr. AY145451).

Supplemental Table S3. List of primers used for preparation of genetic constructs and analysis of transgenic plants

Primer name	Primer sequence (5' to 3')*	Fragment length	Application
<i>Preparation of VPE4i construct</i>			
VPE4s-BamH1 VPE4s-Sal1	GACCACATCTTCGTCTACTACGCCGATC CAGCTGCgTCGAcGAGGAGGA	557	cloning of VPE4 sense fragment
VPE4as-Spe VPE4as-Xho	ACGGCGG <u>ACTAGT</u> GATCCTTGGGA CGTCCCCTGGTTCACTCTGG	557	cloning of VPE4 antisense fragment
VPE4prom-Stu Vpe4prom-Pst	GCGCGTTAAATACAGGCCTTTTTATGAC GCGAGCCCTGCAGAACTGCTTCTCTC	884	cloning of VPE4 promoter
<i>Preparation of VPE2i construct</i>			
VPE2a-Pst s VPE2a-Spe s rev	GATGGCTGCAGGGTGGCTTTG GCTTTTGCCGTA <u>ACTAGT</u> TGATGAAGTCG	569	cloning of VPE2a sense fragment
VPE2a-Bam2 as VPE2a-Sal2 as	TTGGATCCATGCTTTTGCCGTAACAC CTAGCACACGCACATGAAGTCGACG	569	cloning of VPE2a antisense fragment
VPE2pr-Stu-dir VPE2pr-Spe-rev	TTAGGCCTGATTATCGAGACTTTCCAT GATACTAGTTCATGTGCGTGTGCTAGAGTG	1053	cloning of VPE2a promoter
<i>Cloning of MADS29 into the pET32a vector for recombinant protein production</i>			
MADS29_BamHI-F MADS29_HindIII-R	CGGGATCCATAGCAGGCATGGGGCGCGGC CTCCACCTCAAGCTTTTGATCATCTG	759	Cloning of MADS29 into pET32a vector
Hpt-F Hpt-R	GATCGGACGATTGCGTCG TATCGGCACTTTGCATCG	707	Confirmation of transgenic plants

*Synthetic restriction site used for cloning is underlined.

Supplemental Table S4. Primers containing CARG-like boxes from Jekyll and VPE2a gene promoters and primers with modified CARG boxes

Oligonucleotide name	Oligonucleotide sequence (5' to 3')	Fragment length (bp)
<i>Oligonucleotides with CARG boxes in Jekyll gene promoter</i>		
Jekyll -109	gcgtcgctgggCTATAAATTCaggcgcccgcct*	32
Jekyll -186	tcgtgccatctaCCATTGATGGaggatccga	32
Jeky11-955	atttagattgggtttAGTTAAAAATTGtcaaaaagtgtaatg	42
<i>Oligonucleotides with modified CARG motif in Jekyll promoter</i>		
Jekyll 109-mod	gcgtcgctgggCTCTCCCTTCaggcgcccgcct**	32
Jekyl1-186-mod	tcgtgccatctaCCCGGGCTGGaggatccga	32
Jeky1-955-mod	atttagattgggtttCGTTCCCTTCtcaaaaagtgtaatg	42
<i>Oligonucleotides with CARG boxes in VPE2a gene promoter</i>		
VPE2a-77	gcggCTATAAATGaggcgttacccccacc*	31
VPE2a-186	gcattttgaagCCAAAGATGGataattgtgcag	33
VPE2a-726	ggaagaaattgaCCCAAAGTGGctctaaat	30
VPE2a-1014	catgtaaaattgaCCCAAATGGctctgggtt	32
<i>Oligonucleotides with modified CARG motif in VPE2a promoter</i>		
VPE2a-77	gcggCTCTCCCTGaggcgttacccccacc**	31
VPE2a-186	gcattttgaagCCCCGCTGGataattgtgcag	33
VPE2a-726	ggaagaaattgaCCCCCGTGGctctaaat	30
VPE2a-1014	catgtaaaattgaACCCCCTGGctctgggtt	32
<i>Control oligonucleotides</i>		
Arbitrary	TCATACTGTCGCAATGAGTCATCTGTCACAGAGTTCAG	38

*Putative CARG-box sequences are written by capital letters.

**Modified nucleotides in a CARG motif are shown in red.

Supplemental Figures

A

	10	20	30	40	50	60	70	80	90	100
CTTCCTCTAGCACTCTAGCACACGCACATGAACTCGAGGGTGGCGATGGCTGCGTGGTGGCTTTGTGGGTTCTCCCACTCCTGGCGGTGGCCGGGCGG	100									
CCGGGGAGCCGCTGATCTGGCTGCCGGGAGAAATGGGCATGCCCTGCCCTGGCCCTGAGCGCCGGCTGAAGAGTGGACGAAGTGGCCGT	200									
GCTCGTCCGGCTCCTCCGGCTACGAGAACTATCGGCACCAGGCCGATGTGTGCCACCGGTACCAGATCCTGAAGAAGGGAGGCCCAAGGATGAGAAC	300									
ATTGTGGTGTTCATGTACGATGATATCGCCAACAGCCCTGACAACCCAAAGCCCTGGAATCGTCATCAACCATCCCAAAGGCAAGATGTTTACCATGGTG	400									
TTCCCAAGGACTACACCGGTGACCAGGTCACTGCTAAGAACTTCTACGGGTTCTCTTGGGGAACAAAACCTGCGGTTACCGGAGGGAGTAGGAAGTGGT	500									
GAAACGCAAAACCAATGATCACATCTTCACTACTACACGGATCATGGGGTGTGGTTTACTTTGTATGCCCAACCCGCGCAGATGTTTATGTTGACGAC	600									
TTCATCAAAGTGTACGGCAAAAGCATGCTTCCAAAAGCTATTGAAAATGATCATATATGTTGAAGCGTGTGAAAGTGGCAGCATCTTTGAGGGTTTGA	700									
TGCCACAGGATCATAATATTTATGTTACAACGGCAGCAAATGCGCAAGAAAATAGCTGGGCAGCATACTGCCCTACTATGGAAATTCACCTCCTCTGA	800									
ATATGATACCTGTTTAGGTGATGCATACAGTGTTCATGGATGGAAGCAGTGAACCTCAAAGATCTAAAGAAGGAAAGCATCAAGCAGCAGTACGAGGTG	900									
GTTAAAGAGAGAACGGCACCCTCTCTCATGTTCATGGAGTATGGTGACAAGACATTCAAGGAGGACATGCTTTTCTCTTTCAAGGTTTCGATCCTGCAA	1000									
AGTCAAGCATCAGAAAACAGCCGCTGCCTATGCCAGCCTCAAGGGTGAATCAATCAACGAGATGCCGATATTCTTTCATGTGGAGGAAGTATGAGAA	1100									
GTTAAATCGGGATCGGAAGAGAAGCAGAGGGCTCTCAGGGAGGTCAAAGAAACCGTGTACACAGGAAGCATCTGGACAGCAGTATCGATTTCATCGGG	1200									
AAGCTTGTCTTTGGATTGCAAGGGGCCCTTCGATGCTCCAGGCTGTAGAGGCTCTGGCCAGCCATTGGTCGACGATTGGGATGTTGCTGAGGACGATGG	1300									
TGCGAGTGTTCGAGTCCAGTGGCGGCTCACTCACTCAGTACGGCATGAAGCAGTACGAGGGCGTTCGCAAACTCTGCAAAATGGCGTCTCCGAGGCCGA	1400									
GATGAAGGAGGCGAGCATCAGCCCTTGGCAGCGCTACGACATGGGGAAAGTGAACCCGCTGGTTCTAGGGCACAGCACCTGATCCGCTGCGCTGCAGTAC	1500									
ACGGAAGCAGTAGCAAATGCTCCGGAGGTTCTAGCTAGCTAGACCTCGTATATGGTGTAGATACATCACTGGTATAGATACAATCATACAAGAAACCA	1600									
CCCAACAATGGCGCCCATGTGTGTTGGTTAATCAGTAGCTTATGATCGTGGTCTGGCTTTGTAACCTAAGTTTACTGCACTCAATTGAAAGGCAAT	1700									
GATTTTTATGTAGCAAAAAAAAAAAAAAAAAAAXX	1734									

B

MYDDIANSPDMRPGIVINHPRKGDVYHGVKDYDQVTAKNFYAVLLGNKTAVTGSRKVVNSKPNDDHIFYYTDDHGAAGLLCMPNPPDVYADDFIKV	100
LRQKHASKSYSKMIIYVEACESGISIFELMPLQDHNIIYVTTAANAQENSWAAAYCPTEIIPPEYDTC LGDAYSVSWMEDSETQDLKKE SIKQQYEVVKER	200
TAPLSHVMEYGDKTFKEDMLFLFQGFDPAKSSIRNRPLPMPSLKGAINQRDADILFMWRKYEKLNAGSEKQRALREVKETVLRHRKHLDDSSIDFIGKLVF	300
GFDKGPSMLQAARSGSQPLVDDWDCRLRTHVRVFE SQCGSLTQYGMKHMRAFANICNNGVSEAEKKEASISACDGYDMGKNPLVLGHST	389

Supplemental Figure S1. Sequence of *VPE2a* cDNA (A) and its deduced protein (B).

TACTATAGGGCACGCGTGGTTCGACGGCCCGGGCTGGTATCGCCAGCTCCACCACAGCCGCGCCCCACCGCCAC
GACCACTAAGCTGATGCGTTCACGGACACTGTGGCAGCAAGGAAGAGTAGTGATGGTAGGCCGCTGCCGC
TCGAGTCCAAAGAAGACCATCACTCTTCCCTCCTGCTGAAGCTAAGCTTGGCGGGGTGAACGTCATCGACGG
ATTAGCCACCCAAACAGCACTGGCGGTGGTAGAGCTAGAGAGCGTCGATGCTAACTGGAGAAGGGCAAGGC
AAGAGACGGAGTATGAGTTCTCGGGTTCATGGCCGGACATGATGAACGGCCGCCGACAGTCATTTAGATTG
GGTTTAGTTAAAAATTGTCAAAAAGTGAATGAATTTGTTCAATTTATATAAAAAATGTTCAAAATGTAATGAT
TTTCGCTTGGCTTATACGAAAATCCGAATTGTTTGAATGAATTTGTTCCGGTTTATGCAAACTTTTTTGAATG
TATGCGGTTGCGTTGTATAGCCGGCTCTGGCGTCCCTGTTCCGGGACTAATTTCTGAGTTAATTAGCGGACAAG
AGAGAATTTCTGAGTTAGCAGTACAAAATTGGTCGATTGCGACCGTGTGTGCAGCAGTGCAGGCCGTTAACGC
CGTCACTCAGCTCATTTAGTGAACACACGCAAGCCATTTATGAGTGATCACCACCAGTCCACAACCATACTG
AAACCAGAAGCCTCTGTAAACATGCAGGTTAGATTTAGATTAGGCAGAACATTATCACCTACGCACCCATCGAT
GCGTCCAAGACATTTGTCGGTCCACCTGCTTCTAGGATACGTCTGTCCGTGTAACACCACTAAAATGTGCACT
GATCTAATACTGGCCGTTCTGAGCTGTTCTTTCAGTTACGCGTCCACTTCATGGACATTCAGAGGTTGCAGGCC
TGCCTGGTGGTGCCAAAGCTAGTAACCACGGACGCCCTGCCCTTACCAAGAAGAGCAGAATAACGGGACATCT
CGTCTACTCTGTCCCGTTTATAACAAGTAAAAGGGCATCCAACCTGAAACATTTGGTGCTAATAATCATGTACG
AATAACAAAGCTAGTGTGGCGCATCGTGCATCTACCATTGATGGAGGATCCGACGCGCACCGATCGATCAG
TACGCGAAACTGAGTGGGTGAACAGTGCGGCGTGCCTGGGCTATAAATTCAGGCGCCCGCTGCACACCCCTGC
ACATCATCCACATCCCCACCTCGGCCTCCTACCACTACCAGTAGCACTCTCCAGTCCAGTGTGACTTGAAGC
TCGATCGCGCAATG

Supplemental Figure S2. Promoter sequence of *JekyII* gene.

GGGCCAGATTATCGAGACTTCCATGTAAAATTGACCCAAAATGGCTCTGGGTTTGAATTTTTCGTTCTAACTTT
TCTTGACTTCAAAAAAGTCGTCCAACTATCGAAGATTGAATATAAGGTGGGTGTGGATTTTTGAGAAGTTTT
ACAATTTTTCTTGATTTTTTTTTGGCTCAGTCTTGACCCAAATGCCTCTGAATATGGATTTTCGTTCAAGTTTAT
GTTTTCTACTAGGCCAGATTGACAAAAAAGTGTACAACCTTCTATTTTTATTTTTGAAAAAATCTGGAAAAT
TTCAATTTTTGGGAAGAAATTGACCCAAAGTGGCTCTAAATTTATTTCTTGGTTCCACTTGGAAAAAGTTTGGAA
GACCACCTCAACAGGCACTGCCCCGTAGCTATATCAAGAAGCAGTACCGTGGGAAGACCACCTGCTACAAATT
TGGAGCCTCGCCGAGCAAGGCGTAGGCGTCCGAGCCTCTCCTTCCCCTTCCGTTGTGCCATGGATGCAGCTG
GGAGTCTGCGTAAACCACGAAGCGCTGTCGCCGGCTAATTCATGGTGCTAACCTCCATCGCCGGTGCCGAGTG
CGTCATCGTGAGTTGAGTTGATCACGCTTCTCTGTCTCCTCCTTCCAAGTTCCATCATTGCGAGAAGCTGCACA
GCGAAGAAACAATAGCGTACGAGAGGGTCTACTCTACTCTACACCCCTTCCATCTTCTTCTCTTAT
CATTGTCCGATAATTCATGACGCTAACCGCCACCGCCGGCGCCGAGTGCGACCTGCGACGTCGTGCTTGGTCCG
CCGCCAAATCACGGCACTTAGCAAGTTTTGGCGGGCATTTTGAAGGCAAAGATGGATAATTGTGCAGGCCAC
GCAAATCCCCTACGGATACTGAGGTGCCTGCGCCACGCTACGATCACACTTCAATCCCTGGCTCCCTGCACGC
CGCCGCGGCTATAAAATGAGGCGTTACCCCCACCGGAACGATCACACCTCACTACTCTCTGCCTTCTTCTCTC
TAGCACTCTAGCACACGCACATG

Supplemental Figure S3. Promoter sequence of *HvVPE2a* gene